ASTROBIOLOGICAL ANALOGS: EXPLORING THE MICROBIAL ECOLOGY OF CRYPTIC CRYOSPHERE HABITATS

A Dissertation Presented for the
Doctor of Philosophy
Degree
The University of Tennessee, Knoxville

Caleb G. Schuler
May 2023

Copyright © 2023 by Caleb G. Schuler
All rights reserved.

DEDICATION

To my family

My wife
Halle Schuler

My daughters
Amelia and Julia Schuler

and
my brothers and sisters I served with in MESD 823

ACKNOWLDEGMENTS

I am very grateful to my advisor, Dr. Jill Mikucki who took a chance bringing a nontraditional student with a blue-collar military background into her lab. Jill recognized my unique background as a strength and further enabled me to utilize this strength as I worked through graduate school. Jill fostered a network that supported me throughout my PhD. This network ranged my committee, Dr. Steven Wilhelm, Dr. Alison Buchan, Dr. Tim Sparer and Dr. Mona Papes, to collaborators Dr. Dale Winebrenner, Dr. Tim Elam, Justin Burnett, and several other great engineers at the University of Washington Applied Physics Laboratory. All of which inspired me to continue to think outside the box and hold myself to a high standard. I am further grateful for Dr. Bruce LaMattina for trusting in me and allowing me to lead and help create the SERVE (shaping experiential research for veteran education) program, in which I hoped to make an impact in sharing my joy for research with other military veteran students. I am thankful for the cohort that endured the hardships of graduate school with me as we fought though several challenges including a global pandemic. Furthermore, thank you to the Department of Microbiology and Graduate School for providing funding for my research. Finally, my wife Halle Schuler, who encouraged me to never give up, be true to myself and always stay grounded. Ten years ago, Halle talked me into going to community college, without her none of this would be possible.

ABSTRACT

Microbiology of cryosphere systems are understudied and at risk as Earth's climate continues to change. These systems are often at extreme boundaries to what microbial life can withstand and as such require adaptations that enable life to survive and thrive in some of Earth's harshest conditions. The microorganisms in these environments may play a large yet not fully understood role in the global carbon budget. In order to understand the microbiology of these systems, their bioprospecting potential, and their role in global biogeochemical cycles, it is imperative to gain access to and study these parts of the cryosphere before they are lost to global climate change.

This dissertation investigates the cryosphere from three different environments utilizing a variety of microbiological techniques, including multi-omics bioinformatic approaches, cultured based approaches, field-based measurements, and instrument development. Access to ice-covered environments remains a physical and logistical challenge, Chapter 1 of this dissertation explores mechanisms of possible contamination when melting through ice with a novel probe used for sample acquisition. The work provides the first controlled melt probe experiments to investigate particle and microbial cell movement as it relates to contamination and melt probe descent for subglacial lakes and astrobiological targets. Chapter 2 explores the life cycle of snow algae from the Pacific Northwest and the potential role that the life cycle has on snow microbial ecology and the carbon budget of snowpack. The final chapter investigates adaptations of the phototrophic inhabitants of a microbial mat near Don Juan Pond, one of the most

hypersaline liquid features on Earth, which are exposed low temperatures, elevated calcium chloride conditions, as well as both low and high light irradiances. The phototrophic genetic potential of the mat is compared to other polyextreme environments. Collectively this dissertation investigates the genetic potential, community composition, and activity in remote cryosphere locations that are in danger of being lost to climate change.

TABLE OF CONTENTS

CHAPTER ONE INTRODUCTION 1

The Cryosphere 2

Challenges to accessing cryosphere habitats 3

Microorganisms and temperature stress in the cryosphere 5

The role of salinity in cryosphere habitats and the case of Don Juan Pond 5

The role of light irradiance in cryosphere habitats 7

Cryptic habitats 8

Multi-Omic approaches 9

Conclusion 10

References 12

CHAPTER TWO MICROBIAL TRANSPORT BY A DESCENDING ICE MELTING PROBE; IMPLICATIONS FOR SUBGLACIAL AND OCEAN WORLD EXPLORATION 22

Abstract 23

Introduction 24

Methods 29

Description of the Ice Diver Melt Prove and A Laboratory-Scale Ice Block 29

A Laboratory Ice-Block with Immured Organisms and Traces in a Layer 30

Engineering Scenarios and Ice Block Experimental Sampling 31

Description of Mock Englacial Layers (MELs) 32

Exterior Cleaning and Swab Collection of the melt probe 33

Particle tracking and Meltwater Sample Collection 34
Measuring the MEL Bioload Independently of the Ice Bioload 35
Tracking Biomolecules present in both the Ice Block and MEL 37
Results 38
Pre-Melt - Probe Exterior Cleaning 38
Trends in Melt Probe Melting Scenarios 39
Targeted MEL Bioload Measurements 40
Tracking Biomolecules present in both the Ice Block and MEL 43
Discussion 45
Conclusion 49
Acknowledgments 51
Funding 51
Declaration of interest 51
References 52
Appendix I: Tables and Figures 60
CHAPTER THREE MICROBIAL ECOLOGY AND ACTIVITY OF SNOW ALGAE WITHIN A PACIFIC NORTHWEST SNOWPACK 64
Abstract 65
Introduction 66
Methods 70
Site Description and sample collection 70
Field based measurements 73

Cellular abundance 74
Carbon fixation assays 74
Snowpack CO_2 flux 76
Nucleic acid extraction 76
Microbial diversity assessment 77
Results 78
In situ measurements 78
Direct counts of algal and bacterial cells 79
Snowpack primary productivity rate and CO_2 flux 80
Snowpack microbial community composition 81
Snowpack metatranscriptomics 85
Discussion 87
Microbial ecology of Easton snowpack samples 87
Snowpack metabolic activity and carbon flux 89
Conclusion 95
Acknowledgements 96
Funding 96
Declaration of interest 96
References 97
Appendix I: Tables and Figures 110
CHAPTER FOUR DIVERSE PHOTOTROPHIC POTENTIAL AND STRESS TOLERANCES IN AN ANTARCTIC POLYEXTREME ENVIRONMENT 125

Abstract 126
Introduction 127
Methods 131
Sample Site and Sample Collection 131
Nucleic acid extraction and sequencing 132
Amplicon and metagenomic pipeline 133
Cultures and Enrichments 136
Results 138
Community Composition 138
Recovery of phototrophic classified metagenomic assembled genomes (MAGs) . 141
Light harvesting gene abundances 142
Total metagenome stress database hits 144
Phototroph enrichments 145
Discussion 147
Comparison of community composition to other studies 147
Ecologically Relevant Cultures 151
Dry Valley Conditions and Adaptations 152
Conclusion 157
Acknowledgments 159
Funding 159
Declaration of interest 159
References 160

Appendix I: Tables and Figures 182

CHAPTER FIVE CONCLUSION 199

VITA 199

LIST OF TABLES

Table 2-1. Differences in cleaning, sampling and mock englacial layers used in Scenarios 1 and 2. 60

Table 2-2. Scenario 1 concentrations 60

Table 4-1. Metagenomes used for light harvesting gene comparisons with their JGI or MG-RAST ID, extreme conditions and location 182

Table 4-5. DJPM_E1 culture conditions and growth rate measured from highest growth peak during the experiment 183

Table 4-6. DJPM_C1 culture conditions and growth rate measured from highest growth peak during the experiment 184

LIST OF FIGURES

Figure 2-1. Image of ice block constructed for Scenario 1. 61

Figure 2-2. Comparison of the cleaning protocol used for IceMole in 2013 and 2014 (Mikucki *et al*., 2022) and the Ice Diver melt probe (IDMP) 62

Figure 2-3. Measurements from both scenarios that went to background concentration or were below detectable limit by the end of the experiments. 63

Figure 3-1. Mount Baker Washington study site and images of snow conditions at each sample location. 110

Figure 3-2. Description of vertical snow pit profile sampled in 2019 111

Figure 3-3. Rates of primary productivity (µg C/g biomass C/hr) at each surface snow sample site collected in 2018. 112

Figure 3-4. CO_2 flux (µg/C/m^2/hr) at each site where primary productivity was measured in 2018. 113

Figure 3-5. Relative abundance bar plot of Family level 16S rRNA community composition for snow samples from Mount Baker, Washington. 114

Figure 3-6. Non-Metric Multidimensional Scaling plot using Bray-Curtis dissimilarity matrix on 16S rRNA gene community composition snow samples from Mount Baker, Washington 115

Figure 3-7. Relative abundance bar plot of family level 18S rRNA gene community composition for snow samples from Mount Baker Washington. 116

Figure 3-8. RDA Biplot of all 16S Amplicon Sequence Variants (ASVs) from each sample site. 118

Figure 3-9. Total Surface and Mid snowpack transcript abundances. 119
Figure 3-10. *Chloromonas* sp. transcripts from Surface and Mid snowpack samples on Mount Baker, Washington. 120
Figure 3-11. Heat map of oxidative transcripts for Surface and Mid snowpack samples. 122
Figure 3-12. Heat map of osmotic transcripts for Surface and Mid snowpack samples. Transcripts annotated by SEED subsystem level 4. More osmotic transcripts were observed at the Surface than at the Mid snowpack. 123
Figure 3-13. Heat map of antibiotic resistance transcripts for Surface and Mid snowpack samples. 124
Figure 4-0-1. Sample location for the mat adjacent to Don Juan Pond in the Upper Wright Valley of the McMurdo Dry Valleys 185
Figure 4-0-2. Variety of cultures from the mat adjacent to Don Juan Pond. 186
Figure 4-0-3. Cultures isolated from the mat adjacent to Don Juan Pond that were used for light, salt and temperature challenge experiments. 187
Figure 4-0-4. 16S rRNA ASVs relative abundances for the mat adjacent to Don Juan Pond and the sediment below the mat. 188
Figure 4-0-5. 18S rRNA ASVs relative abundances for the mat adjacent to Don Juan Pond and the sediment below the mat. 190
Figure 4-0-6. Metagenome from polyextreme environments comparing light absorbing protein gene abundances. 191

Figure 4-0-7. Statistical results of polyextreme metagenome light absorbing protein gene abundances comparisons 193
Figure 4-0-8. Stress database results grouped by phototrophic and non-phototrophic organisms of the Mat adjacent to Don Juan Pond and the sediment beneath the mat. 195
Figure 4-0-9. Growth curves of DJPM_E1 and DJPM_C1 at 20°C, cultures were isolated from the mat adjacent to Don Juan Pond. 196
Figure 4-0-10. Growth curves of DJPM_E1 and DJPM_C1 at 10°C, cultures were isolated from the mat adjacent to Don Juan Pond. 197
Figure 4-0-11. Growth curves of DJPM_E1 and DJPM_C1 at 4°C, cultures were isolated from the mat adjacent to Don Juan Pond. 198

CHAPTER ONE

INTRODUCTION

The Cryosphere

The cryosphere is generally defined as areas in which water remains frozen for at least 1 month during a year (Fountain *et al*., 2012). By this definition ~20% of Earth's surface is within the cryosphere. Systems within the cryosphere include alpine mountains, glaciers, sea ice, ice covered lakes, and polar regions including the Greenland and Antarctic ice sheets. Despite the fact that a significant portion of the Earth is considered part of the cryosphere, the microbial ecology of these features remains relatively understudied (Goordial 2021). Climate change greatly impacts these environments and the result of warming poses global problems. For example, thawing of frozen ground leads to an increase release of carbon that subsequently increases the release of harmful greenhouse gasses (Shuur *et al*., 2015), additionally, the melting of ice of glaciers and ice sheets could release harmful pathogens (Yarzábal *et al*., 2021). Due to rapid changes in these environments, studying and cataloging the organisms that are found in these environments is important, if not urgent, as these organisms potentially have unique adaptations and are untapped resources for bioprospecting (Bourquin *et al*., 2022, Margesin and Collins 2019, Yarzábal *et al*., 2021, Boetius *et al*., 2015).

The cryosphere is often composed of multiple extremes (i.e., a polyextreme system). Microorganisms in these environments must tolerate extreme cold temperatures, for example in the McMurdo Dry Valleys of Antarctica temperatures can range from 10°C to as low as -50°C (Obryk *et al*., 2020). Temperature fluctuations in the dry valleys are often coupled with other stressors such as salinity (from freshwater to brine that is

40% w/v $CaCl_2$; Harris and Cartwright 1981), nutrient availability, and extreme light (high UV and irradiance up to 1,400 μmol m^{-2} s^{-1} to zero irradiance; Chrismas *et al*., 2018). However, active microorganisms in these systems have adapted to the range of stressors present in order to survive and grow (Merino *et al*., 2019). There is currently a lack of research in polyextreme environments, and recent calls to further examine the combination of extremes, not only to expand our knowledge of the limitations of life, but also to shape the exploration for life on other planets, have been made (Carré *et al*., 2022; Goordial 2021; Cassaro *et al*., 2021; Merino *et al*., 2019; Seckbach and Rampelotto 2015). This dissertation will explore access to hard-to-reach cryosphere habitats found within and deep under ice sheets and glaciers. It will investigate the microbial ecology and extreme conditions in alpine snowpack and a polar brine system with a focus on high salinity, low temperature and varied light availability, all common stressors in cryosphere habitats.

Challenges to accessing cryosphere habitats

Access to cryosphere environments remains difficult, with each realm presenting unique challenges. Snowpack and polar lakes are surficial environments that are more easily accessible, however, much of the cryosphere is within and under ice sheets that range from 10s to 100s of meters thick. Traditionally deep ice drilling has been performed via mechanical drilling (Bulat 2016) when intact ice core collection is required, or by hot water drills (HWDs) for rapid access to the bed of the glacier (Rack 2016, Priscu *et al*., 2021). Mechanical drilling was successful in gaining access to Subglacial Lake Vostok, however the methods resulted in a contaminated borehole and

samples (Bulat 2016; Michaud *et al*., 2020). HWDs are non-coring drills that use hot water to create a borehole in ice; HWDs have been deployed successfully at Whillans and Mercer Subglacial in Antarctica. However, the drill employed for these lakes was logistically cumbersome, for example, access to Whillans Subglacial Lake needed a ~58-mile traverse that consisted of towing 26 compartments (i.e., lab spaces, berthing, camp supplies, fuel, and the drill) totaling more than 230 tons (Rack *et al*., 2014). An alternative approach involves the optimization of a previously developed tool known as a thermal melt probe (Aamot 1967; Winebrenner *et al*., 2014; 2016). Melt probes have a smaller logistical footprint and are more cost effective, their advantages all present a variety of unique challenges that HWDs do not encounter. Melt probe development has several challenges including effective steering during descent, instrument recovery, sample collection, and forward contamination induced by the process of melting a borehole. Forward contamination, defined as the inadvertent contamination of sites, is a chief concern when gaining access to remote locations. Preventing forward contamination is extremely important when accessing protected, pristine environments such as Antarctic subglacial ecosystems (NRC 2007). Currently HWDs that access pristine environments can be modified to 'clean' drilling fluid , for example the water used can be passed through submicron filters and treated with UV, high heat, and pressure to remove contaminants (Priscu *et al*., 2013), melt probes currently can only be cleaned by hand prior to deployment. Two aspects explored in this work include, 1) does the melt probe bring any contaminants with it and 2) can the probe dislodge and drag

microbes from englacial layers down to subglacial targets? These questions are explored further in Chapter 2.

Microorganisms and temperature stress in the cryosphere

Microorganisms that tolerate or thrive in low temperatures (0 to 5°C but cannot survive at temperatures ≥20°C) are known as pyschrophiles (Morita 1975; Rummel *et al*., 2014). Organisms have been found to be active in temperatures as low as -32°C, via the detection of high N_2O in 130,000-year-old ice (Miteva *et al*., 2007), but lower temperature limits are more frequently described around -20°C (Junge *et al*., 2004, Rivkina *et al*., 2000, Tuorto *et al*., 2014), however many studies that describe growth around -20°C infer activity rather than direct detection of activity (Clarke 2014). Cold adapted organisms have a variety of mechanisms to deal with temperatures, such as pigments, antifreeze proteins, and ice binding proteins (Vincent 2007; Mojib *et al*., 2013; Xiang *et al*., 2020; Vance *et al*., 2019). Some organisms, such as snow algae, spore formers, and desiccation tolerant organisms, can lie dormant until favorable conditions occur, i.e., raising of temperatures and water availability (Hoham and Duval 2001). Salinity can enable liquid water to be present at low temperatures by lowering the freezing point of water.

The role of salinity in cryosphere habitats and the case of Don Juan Pond

Salts and other solutes in sufficient concentration allow water to remain liquid at subzero temperatures. Salinity varies across the globe from freshwater systems with zero salinity to environments where the salt concentration is so high that mineral salts

precipitate. Salinity in cryosphere environments plays an important role as higher salinity depresses the freezing temperature of liquids, while also lowering the water activity (the amount of water available to organisms). Halophiles and halotolerant organisms are those that prefer, or tolerate, saline conditions. This group of organisms are represented in all three domains of life - Archaea, Bacteria and Eukaryotes and possess a range of metabolisms including phototrophy (Lui *et al*., 2019). These highly diverse organisms are classified by the amount of salt that they can tolerate (Kushner and Kamekura 1988) and have a variety of methods for tolerating salt to avoid losing water from the cell to the environment, such as the accumulation of inorganic ions intracellularly (salt-in strategy; Oren 2002), or by the accumulation of low molecular weight organic solutes (salt-out strategy; Meshba *et al*., 2008).

In this dissertation a microbial mat at the edge of one of the saltiest liquid features on Earth, Don Juan Pond (DJP; ~40% w/v $CaCl_2$; Harris and Cartwright 1981) is investigated. DJP is a closed basin pond located in the Upper Wright Valley in the McMurdo Dry Valleys of Antarctica (Dugan *et al*., 2022; Toner *et al*., 2017). Due to the high salinity of the pond, DJP has been thought to be devoid of life (Smarakin *et al.*, 2010). The high salt concentration lowers the water activity of a system causing stress to the microbial communities, though microorganisms can tolerate lower water activity by producing substances such as extracellular polymeric substances (EPS; Frösler *et al*., 2017). Adaptations like EPS production and the production of compatible solutes have helped microbes overcome the stress of salt, though there is a limit to which they can no

longer tolerate it. For example, to date no life has been found in water of DJP, this is likely due to its low water activity (aw) that ranges from 0.28aw to 0.68aw (Toner *et al*., 2017), whereas pure water is 1aw and the theoretical limit for life at 0.611aw (Hallsworth *et al*., 2017; Stevenson *et al*., 2015). However, some salt would be beneficial to microorganism around the pond. The salt could enable water to remain liquid as the temperatures at DJP can reach -10°C in the summer and -30°C in the winter (Obryk *et al*., 2009).

The role of light irradiance in cryosphere habitats

Much of the cryosphere is in polar regions that are defined as being located south of the 60° south parallel and/or north of 60° north parallel. These environments are exposed to high light irradiation, including UV, for months at a time during the summer. Conversely, polar environments also are exposed to long periods of darkness during the winter (Thomas and Dieckmann 2002). Though temperate alpine glacial systems are not exposed to long periods of light and dark, these glaciated terrains are at high elevation, and receive high levels of UV and light irradiance (Hoham and Remias 2020). Microorganisms have mechanisms to protect themselves against these high light conditions including the production of photo protectant pigments (Sajjad *et al*., 2020, Remias *et al*., 2005). Snow algae express astaxanthin when in unfavorable high light conditions (Bridigare *et al*., 1993), this acts as a shading mechanism for algae and organisms near the algae. Pigments also play an important role in light absorption which generates heat creating local areas of liquid around the algae (Dial *et al*., 2018). These pigments may also be beneficial when exposed to long periods of darkness when

absorbing as much light as possible is needed. Some phototrophs have adapted to low light conditions by using a variety of light harvesting proteins, such as far-red and low light specific photoantenna proteins, bacteriochlorophylls, and rhodopsin (Gan and Bryant 2015; Gan *et al*., 2014; Olsen *et al*., 2015; Chen *et al*., 2019; Manske *et al*., 2005). These light harvesting proteins coupled with desiccation tolerances and mixotrophy likely allows for phototroph survival in dark conditions, for extended months at a time in polar environments (Hawes *et* al., 1992; Johnsen *et al*., 2020).

Cryptic habitats

Cryptic, hidden or obscure, habitats are systems in which nutrient cycling, metabolisms or life are not observed by traditional methods. This could occur for a number of reasons, such as lack of preservation in the rock record (Having and Hamilton 2019), quick turnover of oxygen suggesting no photosynthesis is occurring (Rothschild and Giver 2002), or the inability to correctly remote sense via satellite due to physical location (Cockell *et al*., 2009). Chlorophyll a is used in remote sensing for detecting phototrophic organisms, however the detection could be limited by the depth at which the satellite detection methods can penetrate, i.e., snow surface vs at depth within snowpack (Khan *et al*., 2021). Some organisms may prefer dark environments and can migrate to lower light environments when surface light irradiances are not preferable (Gan and Bryant 2015; Becraft *et al*., 2015). This makes tracking phototrophy by only surveying surficial systems problematic. Phototrophy fuels communities by providing dissolved organic carbon, thus understanding the limits and the scale of cryptic phototrophy would

be important in accurately estimating a global carbon budget and detection of life on other planets (Cockell *et al*., 2009).

Multi-Omic approaches

Multi-omics (Zhang *et al*., 2010) is the combination of several omics'-based approaches, such as amplicon sequencing for 16S rRNA and 18S rRNA genes (for community composition), alongside metagenomics, (for identifying genetic potential), metatranscriptomics or proteomics (for measuring and tracking activity; Santiago-Rodriguez and Hollister 2021). These approaches are powerful in that they enable researchers to study a system independently of culture-based techniques, which traditionally have only captured a limited number of microorganisms (Staley and Konopka, 1985). Omics methods generate significant volumes of data, however an increase in computing power in recent years has enabled these methods to become more available, all while increasing computing time to analyze the data (Seneviratne *et al*., 2020). Independently, each omics-based approach provides a snapshot of microbial processes in natural systems (Cho 2021). However, the combination of these methods can provide a fuller picture of the system being studied (Gutleben *et al*., 2018). For example, metagenomics provides genomic potential of a community but fails to provide the abundance of community members, thus only enabling a researcher to guess at the abundance of the organisms that the genes belong to. This can leave the question as to whether the target genes are important to a community or rare. Furthermore, as metagenomics only provides genetic potential of a system or organism, metatrascriptomics can elucidate whether the genes are actively transcribed, providing

another useful tool in understanding and describing a system. Thus, the combination of these methods can enable investigations on what organisms are present in an environment and their metabolic potential as well as how they are actively responding to their environment.

Conclusion

This dissertation focuses on extremes of salinity, temperature and light irradiances in the cryosphere and the problems associated with sampling for microbiology in these remote, hard to access austere environments. Multiple strategies were used to investigate these topics, including multi-omics, culture-based experimentation, field-based measurements, and novel laboratory ice block experiments. In Chapter 2, the challenges associated with sampling deep within glacier ice using thermal melt probes are explored. Potential sources of contamination are constrained, including *in-situ* (originating with the glacier ice) contamination. In Chapter 3 the role of the snow algae life cycle on snowpack ecology and carbon budgets of alpine systems are explored using metatranscriptomics, providing the first account of multiple active snow algae life cycles within the same columns of snowpack. Lastly, the unique polyextreme system at the edge of DJP is described in Chapter 4. DJP challenges microorganisms with potential fluxes of high to no salinity, extreme shifts in temperature, and extreme diurnal cycles. Culture-based techniques were coupled with multi-omics to provide an understanding for how the phototrophs from this environment may tolerate and live under extreme conditions. In summary, this dissertation provides a framework to support future

melt probe exploration, while expanding the current knowledge of snow algae and exploring phototrophy in unique extreme conditions.

References

Aamot, H. W. (1967). The Philberth probe for investigating polar ice caps.

Becraft, E. D., Wood, J. M., Rusch, D. B., Kühl, M., Jensen, S. I., Bryant, D. A., ... & Ward, D. M. (2015). The molecular dimension of microbial species: 1. Ecological distinctions among, and homogeneity within, putative ecotypes of Synechococcus inhabiting the cyanobacterial mat of Mushroom Spring, Yellowstone National Park. *Frontiers in microbiology*, *6*, 590.

Bidigare, R. R., Ondrusek, M. E., Kennicutt, M. C., Iturriaga, R., Harvey, H. R., Hoham, R. W., & Macko, S. A. (1993). Evidence a photoprotective for secondary carotenoids of snow algae 1. *Journal of Phycology*, *29*(4), 427-434.

Boetius, A., Anesio, A. M., Deming, J. W., Mikucki, J. A., & Rapp, J. Z. (2015). Microbial ecology of the cryosphere: sea ice and glacial habitats. *Nature Reviews Microbiology*, *13*(11), 677-690.

Bourquin, M., Busi, S. B., Fodelianakis, S., Peter, H., Washburne, A., Kohler, T. J., ... & Battin, T. J. (2022). The microbiome of cryospheric ecosystems. *Nature Communications*, *13*(1), 1-9.

Bulat, S. A. (2016). Microbiology of the subglacial Lake Vostok: first results of borehole-frozen lake water analysis and prospects for searching for lake inhabitants. *Philosophical Transactions of the Royal Society A: Mathematical, Physical and Engineering Sciences*, *374*(2059), 20140292.

Carré, L., Zaccai, G., Delfosse, X., Girard, É., & Franzetti, B. (2022). Relevance of Earth-Bound Extremophiles in the Search for Extraterrestrial Life. *Astrobiology*, *22*(3), 322-367.

Cassaro, A., Pacelli, C., Aureli, L., Catanzaro, I., Leo, P., & Onofri, S. (2021). Antarctica as a reservoir of planetary analogue environments. *Extremophiles*, *25*(5), 437-458.

Chen, M., Hernandez-Prieto, M. A., Loughlin, P. C., Li, Y., & Willows, R. D. (2019). Genome and proteome of the chlorophyll f-producing cyanobacterium Halomicronema hongdechloris: Adaptative proteomic shifts under different light conditions. *BMC Genomics*, *20*(1), 207. https://doi.org/10.1186/s12864-019-5587-3

Cho, J. C. (2021). Omics-based microbiome analysis in microbial ecology: from sequences to information. Journal of Microbiology, 59(3), 229-232.

Chrismas, N. A. M., Anesio, A. M., & Sánchez-Baracaldo, P. (2015). Multiple adaptations to polar and alpine environments within cyanobacteria: A phylogenomic and Bayesian approach. Frontiers in Microbiology, 6. https://doi.org/10.3389/fmicb.2015.01070

Clarke, A. (2014). The thermal limits to life on Earth. *International Journal of Astrobiology*, *13*(2), 141-154.

Cockell, C. S., Kaltenegger, L., & Raven, J. A. (2009). Cryptic photosynthesis—extrasolar planetary oxygen without a surface biological signature. *Astrobiology*, *9*(7), 623-636.

Dial, R. J., Ganey, G. Q., & Skiles, S. M. (2018). What color should glacier algae be? An ecological role for red carbon in the cryosphere. *FEMS Microbiology Ecology*, *94*(3), fiy007.

Dugan, H.A., Doran, P.T., Grombacher, D., Auken, E., Bording, T., Foged, N., Foley, N., Mikucki, J., Virginia, R.A. and Tulaczyk, S., 2022. Brief communication: The hidden labyrinth: Deep groundwater in Wright Valley, Antarctica. The Cryosphere Discussions, pp.1-8.

Edbeib, M. F., Wahab, R. A., & Huyop, F. (2016). Halophiles: biology, adaptation, and their role in decontamination of hypersaline environments. World Journal of Microbiology and Biotechnology, 32(8), 1-23.

Fountain, A. G., Campbell, J. L., Schuur, E. A., Stammerjohn, S. E., Williams, M. W., & Ducklow, H. W. (2012). The disappearing cryosphere: impacts and ecosystem responses to rapid cryosphere loss. *BioScience*, *62*(4), 405-415.

Frösler, J., Panitz, C., Wingender, J., Flemming, H. C., & Rettberg, P. (2017). Survival of Deinococcus geothermalis in biofilms under desiccation and simulated space and martian conditions. *Astrobiology*, *17*(5), 431-447.

Gan, F., & Bryant, D. A. (2015). Adaptive and acclimative responses of cyanobacteria to far-red light. *Environmental Microbiology*, *17*(10), 3450–3465. https://doi.org/10.1111/1462-2920.12992

Gan, F., Zhang, S., Rockwell, N. C., Martin, S. S., Lagarias, J. C., & Bryant, D. A. (2014). Extensive remodeling of a cyanobacterial photosynthetic apparatus in far-red light. *Science*, *345*(6202), 1312–1317. https://doi.org/10.1126/science.1256963

Goordial, J. (2021). Cryomicrobial ecology: still much to learn about life left out in the cold. *Msystems*, *6*(5), e00852-21.

Gutleben, J., Chaib De Mares, M., Van Elsas, J. D., Smidt, H., Overmann, J., & Sipkema, D. (2018). The multi-omics promise in context: from sequence to microbial isolate. *Critical reviews in microbiology*, *44*(2), 212-229.

Hallsworth, J. E., Yakimov, M. M., Golyshin, P. N., Gillion, J. L., D'Auria, G., de Lima Alves, F., ... & McGenity, T. J. (2007). Limits of life in MgCl2-containing environments: chaotropicity defines the window. *Environmental Microbiology*, *9*(3), 801-813.

Harris, H.J.H & Cartwright k., (1981). Hydrology of the Don Juan Basin, Wright Valley Antarctica. L.D. McGinnis (Ed.), Dry Valley Drilling Project, American Geophysical Union, Washington, D. C., pp. 161-184

Havig, J. R., & Hamilton, T. L. (2019). Hypolithic photosynthesis in hydrothermal areas and implications for cryptic oxygen oases on Archean continental surfaces. *Frontiers in Earth Science*, *7*, 15.

Hawes, I., Howard-Williams, C., & Vincent, W. F. (1992). Desiccation and recovery of Antarctic cyanobacterial mats. Polar Biology, 12(6), 587-594.

Hoham, R. W., & Remias, D. (2020). Snow and glacial algae: a review1. *Journal of phycology*, *56*(2), 264-282.

Johnsen, G., Leu, E., & Gradinger, R. (2020). Marine micro-and macroalgae in the polar night. In Polar night marine ecology (pp. 67-112). Springer, Cham.

Junge, K., Eicken, H., & Deming, J. W. (2004). Bacterial activity at− 2 to− 20 C in Arctic wintertime sea ice. *Applied and Environmental Microbiology*, *70*(1), 550-557.

Khan, A. L., Dierssen, H. M., Scambos, T. A., Höfer, J., & Cordero, R. R. (2021). Spectral characterization, radiative forcing and pigment content of coastal Antarctic snow algae: approaches to spectrally discriminate red and green communities and their impact on snowmelt. *The Cryosphere*, *15*(1), 133-148.

Kushner, H., & Kamekura, M. (1988). Physiology of halophilic eubacteria, in"'Halophilic bacteria"(F. Rodrfguez-Valera, ed.)(pp. 109-140).

Liu, C., Baffoe, D. K., Zhan, Y., Zhang, M., Li, Y., & Zhang, G. (2019). Halophile, an essential platform for bioproduction. *Journal of microbiological methods*, *166*, 105704.

Manske, A. K., Glaeser, J., Kuypers, M. M., & Overmann, J. (2005). Physiology and phylogeny of green sulfur bacteria forming a monospecific phototrophic assemblage at a depth of 100 meters in the Black Sea. *Applied and environmental microbiology*, *71*(12), 8049-8060.

Margesin, R., & Collins, T. (2019). Microbial ecology of the cryosphere (glacial and permafrost habitats): current knowledge. *Applied microbiology and biotechnology*, *103*(6), 2537-2549.

Merino, N., Aronson, H. S., Bojanova, D. P., Feyhl-Buska, J., Wong, M. L., Zhang, S., & Giovannelli, D. (2019). Living at the extremes: extremophiles and the limits of life in a planetary context. *Frontiers in microbiology*, *10*, 780.

Mesbah, N. M., & Wiegel, J. (2008). Life at extreme limits: the anaerobic halophilic alkalithermophiles. Annals of the New York Academy of Sciences, 1125(1), 44-57.

Michaud, A. B., Vick-Majors, T. J., Achberger, A. M., Skidmore, M. L., Christner, B. C., Tranter, M., & Priscu, J. C. (2020). Environmentally clean access to Antarctic subglacial aquatic environments. *Antarctic Science*, *32*(5), 329-340.

Miteva, V., Sowers, T., & Brenchley, J. (2007). Production of N 2 O by ammonia oxidizing bacteria at subfreezing temperatures as a model for assessing the N 2 O anomalies in the Vostok ice core. Geomicrobiology Journal, 24(5), 451-459.

Mojib, N., Farhoomand, A., Andersen, D. T., & Bej, A. K. (2013). UV and cold tolerance of a pigment-producing Antarctic Janthinobacterium sp. Ant5-2. *Extremophiles*, *17*(3), 367-378.

Morita, R. Y. (1975). Psychrophilic bacteria. Bacteriological reviews, 39(2), 144-167.

NRC, National Research Council. (2007). Exploration of Antarctic subglacial aquatic environments: environmental and scientific stewardship. National Academies Press

Obryk, M. K., Doran, P. T., Fountain, A. G., Myers, M., & McKay, C. P. (2020). Climate from the McMurdo Dry Valleys, Antarctica, 1986–2017: surface air temperature trends and redefined summer season. Journal of Geophysical Research: Atmospheres, 125(13), e2019JD032180.

Olsen, M. T., Nowack, S., Wood, J. M., Becraft, E. D., LaButti, K., Lipzen, A., Martin, J., Schackwitz, W. S., Rusch, D. B., Cohan, F. M., Bryant, D. A., & Ward, D. M. (2015). The molecular dimension of microbial species: 3. Comparative genomics of Synechococcus strains with different light responses and in situ diel transcription

patterns of associated putative ecotypes in the Mushroom Spring microbial mat. *Frontiers in Microbiology, 6*. https://doi.org/10.3389/fmicb.2015.00604

Oren, A. (2006). Halophilic microorganisms and their environments (Vol. 5). Springer science & business media.

Priscu, J. C., Achberger, A. M., Cahoon, J. E., Christner, B. C., Edwards, R. L., Jones, W. L., ... & Vick-Majors, T. J. (2013). A microbiologically clean strategy for access to the Whillans Ice Stream subglacial environment. *Antarctic Science*, *25*(5), 637-647.

Priscu, J. C., Kalin, J., Winans, J., Campbell, T., Siegfried, M. R., Skidmore, M., ... & Elsworth, C. (2021). Scientific access into Mercer Subglacial Lake: scientific objectives, drilling operations and initial observations. *Annals of Glaciology*, *62*(85-86), 340-352.

Rack, F. R., Duling, D., Blythe, D., Burnett, J., Gibson, D., Roberts, G., ... & Fischbein, S. (2014). Developing a hot-water drill system for the WISSARD project: 1. Basic drill system components and design. *Annals of Glaciology*, *55*(68), 285-297.

Rack, F. R. (2016). Enabling clean access into Subglacial Lake Whillans: development and use of the WISSARD hot water drill system. *Philosophical Transactions of the Royal Society A: Mathematical, Physical and Engineering Sciences*, *374*(2059), 20140305.

Remias, D., Lütz-Meindl, U., & Lütz, C. (2005). Photosynthesis, pigments and ultrastructure of the alpine snow alga Chlamydomonas nivalis. *European Journal of Phycology*, *40*(3), 259-268.

Rivkina, E. M., Friedmann, E. I., McKay, C. P., & Gilichinsky, D. A. (2000). Metabolic activity of permafrost bacteria below the freezing point. Applied and environmental microbiology, 66(8), 3230-3233.

Rothschild, L. J., & Giver, L. J. (2002). Photosynthesis below the surface in a cryptic microbial mat. *International Journal of Astrobiology*, *1*(4), 295-304.

Rummel, J.D., Beaty, D.W., Jones, M.A., Bakermans, C., Barlow, N.G., Boston, P.J., Chevrier, V.F., Clark, B.C., de Vera, J.P.P., Gough, R.V. and Hallsworth, J.E., 2014. A new analysis of Mars "special regions": findings of the second MEPAG Special Regions Science Analysis Group (SR-SAG2).

Sajjad, W., Din, G., Rafiq, M., Iqbal, A., Khan, S., Zada, S., ... & Kang, S. (2020). Pigment production by cold-adapted bacteria and fungi: colorful tale of cryosphere with wide range applications. *Extremophiles*, *24*(4), 447-473.

Santiago-Rodriguez, T. M., & Hollister, E. B. (2021, October). Multi 'omic data integration: A review of concepts, considerations, and approaches. In *Seminars in Perinatology* (Vol. 45, No. 6, p. 151456). WB Saunders.

Seckbach, J., & Rampelotto, P. H. (2015). Polyextremophiles. *Microbial Evolution under Extreme Conditions; Bakermans, C., Ed.; De Gruyter Publishers: Berlin, Germany*, 153-170.

Schuur, E. A., McGuire, A. D., Schädel, C., Grosse, G., Harden, J. W., Hayes, D. J., ... & Vonk, J. E. (2015). Climate change and the permafrost carbon feedback. *Nature*, *520*(7546), 171-179.

Seneviratne, C. J., Suriyanarayanan, T., Widyarman, A. S., Lee, L. S., Lau, M., Ching, J., ... & Ramage, G. (2020). Multi-omics tools for studying microbial biofilms: current perspectives and future directions. Critical Reviews in Microbiology, 46(6), 759-778.

Staley, J. T., & Konopka, A. (1985). Measurement of in situ activities of nonphotosynthetic microorganisms in aquatic and terrestrial habitats. *Annual review of microbiology*, *39*(1), 321-346.

Stevenson, A., Cray, J. A., Williams, J. P., Santos, R., Sahay, R., Neuenkirchen, N., ... & Hallsworth, J. E. (2015). Is there a common water-activity limit for the three domains of life?. *The ISME journal*, *9*(6), 1333-1351.

Thomas, D. N., & Dieckmann, G. S. (2002). Antarctic sea ice--a habitat for extremophiles. *Science*, *295*(5555), 641-644.

Toner, J. D., Catling, D. C., & Sletten, R. S. (2017). The geochemistry of Don Juan Pond: Evidence for a deep groundwater flow system in Wright Valley, Antarctica. *Earth and Planetary Science Letters*, *474*, 190-197.

Tuorto, S. J., Darias, P., McGuinness, L. R., Panikov, N., Zhang, T., Häggblom, M. M., & Kerkhof, L. J. (2014). Bacterial genome replication at subzero temperatures in permafrost. The ISME journal, 8(1), 139-149.

Vincent, W. F. (2007). Cold tolerance in cyanobacteria and life in the cryosphere. In *Algae and cyanobacteria in extreme environments* (pp. 287-301). Springer, Dordrecht.

Vance, T. D., Bayer-Giraldi, M., Davies, P. L., & Mangiagalli, M. (2019). Ice-binding proteins and the ‘domain of unknown function’3494 family. *The FEBS journal*, *286*(5), 855-873.

Winebrenner, D. P., Elam, W. T., Carpenter, M., & Kintner III, P. (2014, December). A Thermal Melt Probe System for Extensive, Low-Cost Instrument Deployment Within and Beneath Ice Sheets. In *AGU Fall Meeting Abstracts* (Vol. 2014, pp. C53B-0314).

Winebrenner, D. P., Elam, W. T., Kintner, P. M., Tyler, S., & Selker, J. S. (2016, December). Clean, logistically light access to explore the closest places on Earth to Europa and Enceladus. In *AGU Fall Meeting Abstracts* (Vol. 2016, pp. C51E-08).

Xiang, H., Yang, X., Ke, L., & Hu, Y. (2020). The properties, biotechnologies, and applications of antifreeze proteins. *International journal of biological macromolecules*, *153*, 661-675.

Yarzábal, L. A., Salazar, L. M. B., & Batista-García, R. A. (2021). Climate change, melting cryosphere and frozen pathogens: Should we worry…?. *Environmental Sustainability*, *4*(3), 489-501.

Zhang, W., Li, F., & Nie, L. (2010). Integrating multiple ‘omics’ analysis for microbial biology: application and methodologies. *Microbiology*, *156*(2), 287-301.

CHAPTER TWO

MICROBIAL TRANSPORT BY A DESCENDING ICE MELTING PROBE; IMPLICATIONS FOR SUBGLACIAL AND OCEAN WORLD EXPLORATION

This chapter is a revised version of published work in the journal Astrobiology.

Schuler, C.G. Winebrenner, D., Elam T., Burnett J., Boles., B.W., Mikucki J. (2022) Microbial transport by a descending ice melting probe; implications for subglacial and Ocean World exploration. *Astrobiology*

Experiments and analysis were conducted by Caleb Schuler, with the help in the field from Jill Mikucki and Bruce Boles. Bruce Boles and Jill Mikucki performed ATP analysis for both ice block tests and aided in sample collection and preservation. Caleb Schuler and Jill Mikucki worked on the manuscript with collaborators from University of Washington Applied Physics Laboratory.

Abstract

Ocean Worlds beneath thick ice covers in our solar system, like subglacial lakes on Earth, may harbor biological systems. In both cases, thick ice covers (>100s of meters) present significant barriers to access. Melt probes are emerging as tools for reaching and sampling these realms due to their small logistical footprint, ability to transport payloads, and ease of cleaning in the field. On Earth, glaciers are immured with various abundances of microorganisms and debris. The potential for bioloads to accumulate around and be dragged by a probe during descent has not previously been investigated. Due to the pristine nature of these environments, minimizing and understanding the risk of forward contamination and considering the potential of melt probes to act as instrument-induced special regions is essential. Here we examined the effect that two engineering descent strategies for melt probes have on the dragging of

bioloads. We also tested the ability of a field cleaning protocol to rid a common contaminant, Bacillus. These tests were conducted in a synthetic ice block immured with bioloads using the Ice Diver melt probe. Our data suggest minimal dragging of bioloads by melt probes but conclude modifications for further minimization and use in special regions should be made.

Introduction

Subglacial lakes, such as those in Antarctica, may offer new understanding on a range of biological and geochemical questions and are relevant analogs for Ocean Worlds (Lorenz *et al*., 2011). Sediments that accumulate in lake bottoms may inform past climatic events (Siegert *et al*., 2000) and how microbial populations evolve under extreme conditions, providing insight not only into Earth's past but also potentially into life elsewhere in our solar system (Priscu and Christner 2004). However, Antarctic subglacial lakes are largely unexplored. While there are currently 773 subglacial lakes that have been identified globally (Livingstone *et al.* 2022) with 675 in Antarctica, and possibly more that have yet to be discovered (Goeller *et al*. 2016), only Subglacial Lake Whillans (i.e. Christner *et al*., 2014, Purcell *et al*. 2014, Mikucki *et al*. 2016), Mercer Subglacial Lake and the subglacial outflow of Blood Falls (Mikucki and Priscu 2007; Mikucki *et al*. 2009; Campen *et al*. 2019, Lyons *et al*., 2019; German *et al*., 2019; Mikucki *et al*., 2022) have been directly sampled for geomicrobiological analysis. There remains strong scientific interest in exploring Antarctic lakes, particularly deep lakes

such as Lake Vostok (>4 km below the surface), yet access to these lakes, given their depths, impose a significant challenge.

Melt probes offer a promising technology to meet the challenge of deep subglacial access, especially in cases where established methods such as hot-water drilling are logistically prohibitive or difficult to implement, e.g., on landed spacecraft. Logistical costs of melt probes scale relatively benignly with increasing penetration depth and decreasing ice temperature because they rely on electrical energy delivered efficiently to the point of melt (as described below). Melt probes have thus been considered for the exploration of Ocean Worlds (Horvath *et al*., 1997) and Mars (Paige 1992, Zimmerman *et al., 2001,* Kömle *et al.,* 2018 as well as subglacial targets on Earth. Moreover, such probes are inherently relatively simple to clean and require no drilling fluid which would require further microbial decimation. Thus, the prospect for melt probes to meet both Antarctic Subglacial Clean Access and planetary protection requirements increase their candidacy for terrestrial and extraterrestrial subglacial missions for astrobiological exploration.

The pristine nature of subglacial environments necessitates a careful approach to drilling and sampling in order to protect the ecosystem from being contaminated. Additionally, subglacial environments are protected under the Antarctic Treaty, which stipulates that not only does entry into these environments require the use of clean equipment, but also that amount of material dragged or deposited into a

subglacial region must contain fewer cells than the equivalent volume of ice that was passed through to reach the subglacial realm (Alekhina *et al*., 2011). Whereas hot water drills have previously been used to access Whillans and Mercer Subglacial Lakes, interest in alternative means for accessing pristine subglacial targets has grown with the increasing capabilities of melt probes. The effectiveness of a field-based cleaning protocol that follows NASA guidelines for the microbiological examination of space hardware (NASA 2010) has previously been demonstrated to meet Antarctica Code of Conduct (CoC) (Mikucki *et al*., this issue,). Although they are effective, surface-based cleaning efforts to minimize forward contamination do not take into account the potential for dragging immured bioloads of microbial cells and particles. In order to comply with Antarctic CoC, quantitative testing of immured bioloads dragged by a descending melt probe is needed. To our knowledge there have been no such studies to understand *in situ* microbial transport caused by a descending melt probe.

Glacial ice contains measurable microorganisms including viruses, bacteria, and fungal species. Cellular abundances throughout the various glacial realms, including surface snowpack, firn, meteoric ice and in basal ice materials (Anesio and Laybourn-Parry 2012), vary in cellular concentration that range up to eight orders of magnitude. Entrainment of sediments within ice from deposition of dust tend to contain higher cell numbers (Christner *et al*., 2005; Miteva *et al*., 2008). For example, Greenland ice cores contain up to $9x10^7$ cells ml^{-1} in debris rich 'silty' layers and as low as 10^3 cells ml^{-1} in clear ice (Sheridan *et al*., 2003; Miteva *et al*., 2004, 2008); englacial (subsurface)

concentrations of cells in Antarctic have been estimated to contain approximately 10^1 to 10^3 cells ml^{-1} (Boetius *et al*., 2015). Bacteria may also exist in water veins between clean solid ice crystals at higher abundances of 10^6 to 10^8 cells ml^{-1} (Mader *et al*., 2006). Furthermore, the basal layer of glaciers, the last layer between glacier and subglacial realm, contain sediment and debris laden ice that is rich with microbial life. For example, at Taylor Glacier, an outlet glacier of the East Antarctic Ice Sheet, basal ice was reported to contain ~10^4 cell g^{-1} in 'dirty ice' samples, while clean basal ice contained ~10^2 cell g^{-1} (Montross *et al*., 2014). Additionally, Prokaryotic and Eukaryotic cells have been isolated from multiple ice cores around the world, suggesting that microbial cells remain viable, despite being frozen for an extended time in glacial ice (Christner *et al*., 2000, Ma *et al*., 2005). With glacial ice having a wide range of immured bioloads, the potential of moving and dragging such bioloads to target depths must be considered as a possible mechanism for forward contamination.

As a melt probe descends, melting its way through ice, immured cells and debris will be introduced to a film of liquid water, the melt jacket, created by the melt probe. This could be considered analogous to an instrument-induced 'special region' (Rummel *et al*., 2014) that may result in the activation of dormant cells. Spore forming bacteria such as *Bacillus* have been found in glacial ice (Christner *et al*., 2000). Additionally, these spores can activate and return to life within minutes under certain conditions, such as the introduction of nutrients and chemicals (i.e., amino acids, sugars, and dipicolinic acid; Setlow 2003) or changes in the environment that result in more favorable conditions

(i.e., salt concentrations and pressure; Gould and Hurst 1969). Thus, the melt jacket created by local melting of ice has the potential not only to drag englacial cells and debris, but also to transport contaminants that survived the cleaning process. These contaminants, many of which are likely spores due to spores' ability to withstand extreme conditions (as reviewed by Nicholson *et al*., 2009), could then be activated by the introduction of nutrients from the liquid water of the melt jacket and transferred to the subglacial targets. The possibility of dragging such contaminants to pristine subglacial targets emphasizes the need to understand what happens to immured bioloads as a melt probe descends through them and to what extent they are dragged to lower glacial realms.

In this study, we performed two laboratory scenarios that tested separate engineering borehole maintenance strategies for melt probe missions and examined the impact that these strategies had on the movement of immured glacial bioloads. To mimic cells and debris found in natural glacial ice we inoculated a synthetic ice block with a mock englacial layer containing synthetic beads, Bacterial cells, and Eukaryotic algal cells. The movement of particles and cells was monitored by measuring their abundances in discrete samples as the probe descended. To test the potential of spore forming Bacteria surviving the cleaning process and being released during a melt probe descent, we inoculated the melt probe with *Bacillus subtilis*, cleaned the probe, measured spore abundance of samples before cleaning, post cleaning and during the melt probe's descent. This work will inform the extent to which microbial cells and particles are dragged

during melting operations and provide guidance for future melt probe subglacial sampling missions.

Methods

Description of the Ice Diver Melt Prove and A Laboratory-Scale Ice Block

For this study, we employed a shortened version of a Philberth ice melt probe (Philberth 1974) that was tested previously in Greenland (Winebrenner *et al*., 2016.). The basic theory operation is that the melt probe descends vertically through ice, typically at speeds of several meters per hour (Aamot 1968; Philberth 1976). Electrical energy supplied to the front of the probe (i.e., the lower end during descent) is converted to heat to warm and then melt ice, creating a channel of liquid water (the melt jacket) that typically exceeds the diameter of the probe by a few percent, depending on ice temperature and descent rate (Shreve 1962). The probe falls through the channel created by melting, with a melt jacket a few millimeters thick (in our tests), surrounding the probe barrel. Vertical travel is maintained using pendulum steering, in which the probe hangs in the melt channel by a larger-diameter flange at the top end of the device. With the center of gravity of the probe well below the flange, the probe continually orients itself toward vertical, even as additional heating of the flange widens the melt channel to permit descent (Aamot, 1967, 1970). In order to test the operation of the melt probe under various engineering scenarios, in terms of operation and sampling, laboratory-scale versions were designed (Figure 2-1; all figures and tables are located in the appendix).

Two separate laboratory-scale probe prototypes were used (experiments described further in materials and methods as Scenario 1 and 2 and referred to herein as such) with the primary difference being in probe body length from Scenario 1, which was 70 cm long with surface area of 1,318 cm^2, and Scenario 2, where the probe was 65 cm length with surface area of 1,223 cm^2. Aside from probe length, each probe was nearly identical consisting of a diameter just above the copper, paraboloid front melt head of 6.5 cm, and a rear copper flange of 8 cm diameter. Heating in the front melt head was distributed spatially so as to maintain an approximately isothermal outer surface during descent. The paraboloid shape of the front melt head permits relatively low head temperatures (compared, e.g., to a hemispherical head, at the same rate of travel), and thus limits thermal shock to the ice-immured organisms we aim to sample in meltwater. Calculations based on those of Shreve (1962) indicate that the outer surface of the melt head and water adjacent to it do not exceed 4°C for the melt probe design at a descent rate of 1 m hr^{-1}.

A Laboratory Ice-Block with Immured Organisms and Traces in a Layer

Our study was facilitated by direct, visual observations of melt-probe passage through layers of ice-immured organisms and artificial tracers, which can then be related to events in instrumental and sampling records. To this end, we constructed a visually clear ice block measuring 40 cm x 40 cm in horizontal cross section, standing 200 cm tall (Figure 2-1). Our method was derived from commercial practices in growing clear ice for ice sculptures. Specifically, we grew ice by cooling a 40 cm-square by 200 cm-long, rectangular-prism-shaped container, with the long-side kept horizontal, in a cold room

laboratory at -20°C. The container is insulated on the top and sides, so as to restrict heat flow to conduction through a metal plate at its base. After filling the container with deionized water, we circulated the water continually and also circulated air in the small headspace between the top of the container and its insulating lid. Ice grew progressively upward from the bottom of the container while progressively excluding air and other impurities. After inoculating the ice block with biological material as described below, we rotated the ice block to a vertical position for melt probe descent operations.

Engineering Scenarios and Ice Block Experimental Sampling

Each ice block scenario employed one of the two engineering strategies that would allow for sample collection and vehicle recovery in real world deployments. Scenario 1 has been illustrated as an effective approach for short distances, i.e., Blood Falls conduit (Kowalski *et al*., 2016; Mikucki *et al*. 2022). This strategy requires that the meltwater be pumped continuously to the surface during melt probe descent to keep the borehole from freezing and allowing for vehicle recovery. Scenario 2 employed a strategy that is more realistic for reaching deep targets, where pumping large volumes of liquid from kilometer scale depths to the surface is not feasible. Using this strategy, the meltwater would be maintained in the borehole, likely with an anti-freeze additive to keep the bore from freezing in. Sample collection varied under the distinct borehole maintenance strategies (Table 2-1). Briefly, meltwater from scenario 1 was pumped continuously through the melt probe nose, forward to aft, via a peristaltic pump located in an adjacent (4°C) cold room. Meltwater was collected at regular intervals, with higher resolution sampling during and after passage of the melt probe through the mock

englacial layer (MEL). In total, 31 samples were collected during descent. In Scenario 2, samples were collected from the borehole behind the melt probe as it descended through the ice block, at 10 separate depths. Autoclaved PharMed BPT Tubing was inserted behind the melt probe and meltwater was collected in acid washed (10% HCl) and autoclaved 1 L Nalgene bottle via the use of a peristaltic pump and sterile syringe. To obtain a discrete sample directly from the melt jacket surrounding the nose of the melt probe in Scenario 2 a hole was drilled through the ice block, and autoclaved PharMed BPT Tubing was inserted to drain meltwater directly from the nose and melt jacket surrounding the melt probe into an acid washed (10% HCl) and autoclaved 1 L Nalgene bottle. Since preparation of the ice block (including the water, container, and tools) used to synthesize the ice block and the cold room in which the experiments were conducted were not aseptic, we utilized distinct (traceable) organisms and synthetic beads as tracers. Thus, any potential contamination from the preparation of the ice block was considered to be background.

Description of Mock Englacial Layers (MELs)

Mock bioloads were generated to mimic layers of biomass that can develop within glacier ice. Scenario 1 contained a mixture of FITC marked 1 µm melamine resin fluorescent beads ($1.4x10^7$ beads ml^{-1}) (λ_{Ex} = 506 nm, λ_{Em} = 529 nm) (Sigma-Aldrich product no. 90305-10ML-F) and an Ampicillin resistant *E. coli*, K-12 strain ($1.7x10^8$ cells ml^{-1}). Scenario 2 was inoculated with a stock of the Eukaryotic freshwater algae, *Chlorella sp.* (NC64A), final concentration $3.78x10^5$ algal cells ml^{-1}. For each scenario, a

MEL was constructed within the synthetic ice block by drilling holes (Figure 2-1) located 40 cm from the top of the ice block. The three zones of holes extended down the ice block for a mock layer of ~ 8 cm. The holes were interspaced in such a manner to prevent gaps between the drill holes. This pattern ensured the melt probe would penetrate the mock layer to a maximum extent. Approximately 57 ml of inoculum was pipetted into each drill hole and left to freeze for ~2 hours. Drill holes were then back filled with ~18 ml of water and left to refreeze overnight.

Exterior Cleaning and Swab Collection of the melt probe

Prior to executing the ice block scenarios, the melt probe was extensively cleaned to remove potential surface contaminants using the protocol outlined in Mikucki *et al*. (2022). In Scenario 1, the melt probe was received from the engineering team and cleaned. In Scenario 2, the melt probe was first coated with *Bacillus subtilis* (ATCC 6051) to test our ability to clean recalcitrant organisms and examine their persistence during melt probe operations. *B. subtilis* was first was grown in ½ Tryptic Soy Agar (TSA), which promotes spore formation, to a final concentration of ($3.68x10^5 \pm 5.93x10^4$; n =3) Spore Colony Forming Units ($_{spore}$CFUs) ml^{-1} cm^{-2}), and then coated on the melt probe exterior with sponges soaked in the inoculant. The melt probe was then bagged in pre-sterile wrap and sat overnight at room temperature to promote additional formation of spores by limiting nutrient availability. The next day, ~12 hours later, swab samples were collected from the inoculated melt probe to determine the initial concentration.

We evaluated the effectiveness of our cleaning protocol by measuring total adenosine triphosphate (ATP) and CFU's (Scenario 1; n=3; Scenario 2 n=5) both pre- and post- cleaning in 25 cm^2 regions of the melt probe according to NASA-HDBK-6022 (NASA 2010) and Mikucki *et al*. (2022), using individually wrapped sterile CLASSIQ Swabs (COPAN part No. 164KS01). Additional CFU counts on Tryptic Soy Agar were performed for Scenario 2 both by plating the samples as collected and by heat shocking the samples at 75 °C for 15 minutes to kill non-spores (n=3). Heat shocked samples were then plated and considered representatives of colonies formed from what were previously spores. Surface samples collected from the melt probe during and after cleaning and after Scenario 2 are reported in averages of total units per the surface area swabbed ($25cm^2$).

Particle tracking and Meltwater Sample Collection

In order to evaluate the movement of components of the MELs, we collected samples for ATP, CFU's for Ampicillin resistant *E. coli* ($_{amp}$CFUs), and *B. subtilis* spores ($_{spore}$CFUs), Scenario 2 non-selective CFUs for cleaning (CFUs) and meltwater ($_{total}$CFUs), deoxyribonucleic acid (DNA), fluorescence (FITC for Scenario 1 and Chlorophyll a for Scenario 2), endotoxin (Scenario 1 only), and direct cell counts and total fluorescent bead concentrations (Scenario 1 only). Background concentrations for all measured parameters were determined in samples collected prior to the probe entering the MEL. Meltwater samples for direct cell counts, bead counts, and CFUs were collected in sterile 15 ml polypropylene tubes. Samples for ATP and endotoxin were collected in pre-combusted (450°C for 4 hours) borosilicate glass vials. Samples for direct counts

were fixed with paraformaldehyde (4% final concentration) within 2 hours of collection. Samples for DNA concentration (Scenario 1) were filtered through 0.22 µm filter and stored at -20°C. All samples, with the exception of ATP and endotoxin, which were analyzed immediately following the scenarios, were stored (4 °C for CFUs and cell counts and -20 °C for DNA) and shipped overnight to the University of Tennessee Knoxville for analysis. All meltwater samples collected during both Scenario 1 and 2 are reported as the averages of the total units per ml of meltwater collected (n= 3 for each sample).

Measuring the MEL Bioload Independently of the Ice Bioload

Selective growth of the *E. coli* strain (ampicillin resistant strain K-12) was determined by plating 100 µl aliquots of meltwater, 1-day post collection, on agar plates of Luria Broth (LB) containing Ampicillin (150 µg ml^{-1}). Plates were incubated at 37°C for 24 hours. $_{amp}$CFUs results indicate the concentration of our specific inoculant per unit of meltwater sampled (n=3 for each sample). This approach enabled us to control for interference caused by microbes in the water used to synthesize the ice block. We were unable to reestablish the *Chlorella* cells from Scenario 2 on Bolds Basal Media after being frozen in the ice block, so chlorophyll autofluorescence was used to track *Chlorella* concentration instead of viable (CFU) counts (see below). In Scenario 2, meltwater samples were plated on TSA (following the spore test protocol as described above) to test for *B. subtilis* spores in the meltwater samples (n=3 for each sample).

DNA-containing cells were visualized via epifluorescence microscopy and quantified using the nuclear counterstain, 4',6 -Diamidino-2-Pheynylindole, Dihydrochloride (DAPI). Bead abundance was determined with epifluorescence microscopy using a FITC filter. Direct counts were performed on all DNA-containing bacteria per sample in Scenario 1; in Scenario 2, only *Chlorella* cells were counted, since their size (~10 µm diameter) and shape (sphere) distinguish them from other microbes within the ice. Direct counts were performed as described by Mikucki and Priscu (2007), sample volumes were optimized to obtain between 30 and 300 cells or beads per field of view (n=3 slides per sample), and abundances were calculated according to the sample volumes used and the area of the microscope's field of view.

In Scenario 1, relative fluorescence units (RFUs) were measured on meltwater samples using the Invitrogen Qubit 3 fluorometer at 470nm for an immediate estimation of bead concentrations. Bead concentrations were based on a standard curve ($R^2 = 0.94$) developed from a serial dilution of the stock bead solution using a Guava easyCyte HT flow cytometer and confirmed with epifluorescence microscopy to determine total beads. In Scenario 2, CHLa was measured during the probe descent to track the movement of *Chlorella* and quantified using a Turner Trilogy Fluorometer with the CHLa *in vivo* module at 460nm. Relative fluorescence units of CHLa measurements were converted to µg L^{-1} of CHLa using a CHLa standard (Turner Designs part no. 10-850) with standard curve ($R^2 = 0.994$).

Tracking Biomolecules present in both the Ice Block and MEL

Total ATP was determined from 50 µl aliquots of meltwater samples via the luciferase reaction using the BioThema Intracellular ATP Kit (product no. 266-311). Light intensity of the reaction was measured with the Promega GlowMax 20/20 Luminometer. Total pmol of ATP per sample was converted into cells ml^{-1} based on an estimated ~$2.0x10^{-6}$ pmol of ATP per bacterial cell (manufacturer's manual). Endotoxin concentration was determined using the Charles River Endosafe PTS Portable Test System with Limulus Amebocyte Lysate (LAL) test cartridges (product no. PTS20F) according to the manufacturer's instructions. Nine samples (Sample numbers 1, 5, 12, 14, 16, 19, 23, 28, 31, see supplementary Table 2-1 for sample descriptions) were selected for this analysis. These samples are representative of background concentrations of pre-MEL, the observed spikes in MEL, and post MEL. Endotoxin units (Eu) were converted to cells ml^{-1} using calculations that assume 1 Eu for ~$1.05x10^{2}$ *E. coli* cells (Dawson *et al*., 1988).

For Scenario 1, aliquots (4.5 ml) of select meltwater samples were filtered through 0.22 µm filter and used for nucleic acid analysis. These samples represent background concentrations (sample 1), increased concentrations observed during MEL sampling (samples 12 and 24), and the final sample collected at the conclusion of the scenario (sample 31). The initial stock for the MEL (1 ml of cell and bead mixed) was also included in our analysis. DNA was extracted using Qiagen DNeasy PowerLyzer PowerSoil kit (product no. 12855-50), according to manufacturer's instructions. The 16S

rRNA gene was amplified using the polymerase chain reaction (PCR), with increasing PCR cycle numbers in order to constrain the detectable limit. Briefly, reactions consisted of Thermo Scientific Dreamtaq (product no. K1081) and universal 16S rRNA gene primers (27F, 5'-AGA GTTTGATCCTGGCTCAG-3' and 1492R, 5'-GGTTACTTGTTACGACTT-3') and 2.0 ng template in 25.0µl reactions performed using the following protocol; 94.0°C for 5 min, the following parameters were varied for 25, 30, 35, 40, and 45 cycles: 94.0°C for 1 minute, 55.0°C for 1.5 minutes, and 72.0°C for 3 minutes, followed by 72.0°C for 7 minutes and then stored at 4.0°C.

Results

Pre-Melt - Probe Exterior Cleaning

Scenario 1 surface swabs prior to cleaning yielded $2.71x10^{-1}$ ($\pm$ $7.90x10^{-2}$) pmol of total ATP $25cm^{-2}$ from the probe's surface. Post cleaning, $1.33x10^{-2}$ ($\pm 6.94x10^{-2}$) pmol of total ATP $25cm^{-2}$ was recovered. Air swab controls contained $7.86x10^{-2}$ ($3.63\pm x10^{-3}$) pmol of total ATP $25cm^{-2}$. Attempted CFU measurements for Scenario 1 yielded no growth, both pre and post cleaning for $_{amp}$CFU and non-ampicilin CFU plates. In Scenario 2, pre and post cleaning ATP measurements after the probe was inoculated with *Bacillus* spores had similar concentrations, prior to cleaning the *B. subtilis,* $3.06x10^{-2}$ ($\pm 8.01x10^{-3}$) pmol of total ATP $25cm^{-2}$ and after cleaning *B. subtilis*, $3.31x10^{-2}$ ($\pm 1.27x10^{-2}$) pmol of total ATP $25cm^{-2}$.This was likely due to the low ATP production of the *Bacillus* being in a spore state (Chollet and Ribault 2012). Our cleaning efforts prior to *Bacillus* inoculation in Scenario 2, as well as in Scenario 1, were comparable to a previous study (Mikucki *et al*., 2022) that used the same protocol (Figure 2-2), the

cleaning met the proposed ATP cleanliness standard of 0.023 Total ATP $pmol^{-1}$ $25cm^{-2}$ (Benardini and Venkateswaran 2016). In Scenario 2, $_{spore}$CFUs showed a significant decrease from *Bacillus* spores on the melt probe pre-cleaning $9.73x10^{2}$ ($\pm 3.06x10^{2}$) $_{spore}$CFUs $25cm^{-2}$ to the concentration on the cleaned melt probe $9.26x10^{-1}$ ($\pm 9.26x10^{-3}$) $_{spore}$CFUs $25cm^{-2}$ (p value = $9.2x10^{-3}$). The non-heat shocked treatments measured a similar decline in CFUs $25cm^{-2}$ with the *Bacillus* spore inoculant that was left on the melt probes surface sterile bagging overnight, $4.05x10^{6}$ ($\pm 9.17x10^{5}$) CFUs $25cm^{-2}$ to post cleaning $8.33x10^{-1}$ ($\pm 8.33x10^{-1}$) CFUs $25cm^{-2}$ (p-value = $8.6x10^{-4}$).

Trends in Melt Probe Melting Scenarios

Seven independent measurements were made in Scenario 1 to track the concentration of microbial cells and FITC labeled beads frozen in the ice block during melting. Two distinct spikes, in both total bead and cell concentrations (Table 2-2), were observed. The first spike occurred as the melt probe nose penetrated the MEL (~39.0 cm) and the second spike as the tail penetrated at nose depth ~106 cm. At ~49 cm the melt probe nose exited the MEL and a corresponding reduction in bioload concentration was observed in all assays. Likewise, a decrease in all measured metrics was observed following the exit of the tail flange from the MEL (Table 2-2). With the exception of total bead concentrations, all samples returned to background levels when the probe exited the MEL entirely (nose depth ~125.0 cm; Figure 2-3).

Despite applying a different sampling scheme in Scenario 2, where borehole water was not evacuated and was instead collected for analysis from behind the probe, a bioload dragging trend similar to Scenario 1 was observed (Figure 2-3). Because meltwater was collected from the bulk mixture of borehole water at discrete time points in Scenario 2, results are described based on the relation of the melt probe to the MEL, rather than exact depths. As in Scenario 1, distinct spikes in all bioload metrics were observed as the nose of the melt probe entered the MEL followed by a decline in the metrics measures. A second spike was observed as the tail of the melt probe entered the MEL followed by a decline to background levels. A single *Chlorella* cell was detected in a 5 ml sample of meltwater at the end of the experiment (Appendix table no. 1).

Targeted MEL Bioload Measurements

Scenario 1 CFU measurements were designed to target only the ampicillin resistant *E. coli* we inoculated into the MEL, and no colonies were observed on $_{amp}$CFU plates from samples collected prior to the melt probe head entering the MEL. Colonies were first observed on plates collected from ~40cm (nose depth) when the probe penetrated the MEL. The maximum number of colonies ($8.07x10^6 \pm 2.53x10^6$ $_{amp}$CFUs ml^{-1}) was observed when the tip of the probe nose exited the MEL and the body penetrated the MEL (nose depth ~50 cm). A second, smaller peak in $_{amp}$CFUs ($4.18x10^6 \pm 3.20x10^6$ $_{amp}$CFUs ml^{-1}) occurred in samples collected from the widest part of the probe's tail flange (1.59 cm greater than the nose) as it penetrated the MEL, at nose depth ~113 cm. $_{amp}$CFUs tapered as the tail of the probe began to exit the MEL at ~117 cm

($1.14x10^6 \pm 1.47x10^5$ $_{amp}$CFUs ml^{-1}). No further $_{amp}$CFUs were observed in any of the samples following the sample at ~117 cm.

$_{total}$CFUs collected from the non-heat shocked meltwater samples followed a similar trend as other bioload measurements from Scenario 2 including *Chlorella* direct counts, chlorophyll concentrations and ATP measurements. While no bacterial cells were added to the MELs, the *Chlorella* culture stock was non-axenic, thus we hypothesize heterotrophs in the *Chlorella* culture contributed to the total $_{total}$CFU. *B. subtilis* spores were not detected in any of the meltwater samples from Scenario 2 subjected to the spore-former assay (heat shock). This suggests that the heat shock method eliminated both non spores and any vegetative cells from the meltwater samples prior to plating. Non-heat shocked $_{total}$CFUs ranged from $1.99x10^2$ to $2.87x10^3$ $_{total}$CFUs ml^{-1} and no colonies were detected on the heat shocked meltwater samples. Colonies were detected in both heat shocked swab samples (9.0 ± 1.25 $_{spore}$CFUs $25cm^{-2}$) and non-heat shocked ($1.59x10^2 \pm 1.31x10^2$ CFUs $25cm^{-2}$) swab samples collected from the melt probe surface following its recovery from the ice block.

FITC beads were not detected in meltwater collected prior to entry into the MEL by direct microscopy counts. The detection limit of flow cytometry is $10^2 – 10^3$, thus direct microscopy counts were required to accurately detect the absence of beads (Gruden *et al*., 2004). A maximum concentration ($1.73x10^7$ beads ml^{-1}) was observed at nose depth ~113 cm, when the tail flange was within the MEL. The first spike in bead

concentrations ($1.41x10^7$ beads ml^{-1}) was observed at nose depth ~55 cm, when the nose of the probe was in the MEL. Bead concentrations did not return to background levels, although they did decrease by three orders of magnitude (from 10^7 to 10^4 cell ml^{-1}) by the end of the experiment (nose depth ~ 156 cm). Direct counts, as well as flow cytometry, showed similar trends once the melt probe entered the MEL. The FITC beads used in this experiment were often observed clustered in small groups when viewed under the microscope and may provide an example of aggregated debris. Similar melamine resin-based beads have previously been described as aggregating (Jakobsson *et al*., 2014; Lv *et al*., 2015).

Direct microscopy counts of algal cells from Scenario 2 followed the same trends described in Scenario 1 (Table 2-3, Figure 2-3). No algal cells were observed in the meltwater samples before the MEL, thus we report background as 0 cells per ml. Further, no algal cells were detected until the melt probe nose began to penetrate the MEL. The spike in algal cells recovered in samples occurred when the full nose of the probe was in the MEL ($8.71x10^3$ algal cells ml^{-1}). A decline in algal cell concentration was then observed again until the tail flange of the probe entered the MEL ($4.61x10^2$ algal cells ml^{-1}). Once the tail exited the MEL, algal cells continued to decrease in concentration until the end of the experiment, however samples collected directly from the nose of the probe at the end of the scenario contained algal cells (1 cell per 1.6 ml) as did the meltwater that surrounded the probe (1 algal cell per 5 ml).

Tracking Biomolecules present in both the Ice Block and MEL

Background concentrations of DNA-containing cells in the ice block was determined on samples collected before the probe entered MEL and ranged from 10^5 to 10^6 cells ml^{-1}. During Scenario 1, the first peak in cell concentration, $4.87x10^7$ cell ml^{-1}, was observed as the probe penetrated the MEL (nose depth of ~50 cm). This first spike in concentration was followed by a second comparable spike, $2.69x10^7$ cell ml^{-1}, as the tail flange hit the MEL at nose depth of ~113 cm. A background cell concentration of $4.53x10^6$ cell ml^{-1} was observed before the tail entered the MEL. The lowest cell concentrations, $3.46x10^4$ cell ml^{-1}, was observed at the nose depth of ~121 cm when the probe's tail flange exited the MEL. This result is consistent with $_{amp}$CFU concentrations suggesting background levels were obtained by the end of the experiment.

Endotoxin analysis followed the same trend as cell enumerations, CFU and ATP measurements; conversion of Endotoxin units to cells per ml further confirms this trend (Table 2-3). Endotoxin analysis was only performed in Scenario 1 and background levels observed before the nose of the probe entered the MEL was $7.4x10^{-2}$ Eu. The highest concentration of endotoxin ($1.61x10^4$ Eu), was observed at the nose depth of ~53 cm when the nose of the probe was within the MEL. The second spike in endotoxin concentration was observed when the tail flange of the probe was within the mock englacial layer, ($8.04x10^3$ Eu; nose depth ~110 cm). At nose depth ~156cm, an endotoxin low of $1.35x10^{-1}$ Eu was observed.

Concentrations of total ATP followed a trend similar to that observed in all assays for both scenarios (Figure 2-3). For Scenario 1, background Total ATP before entering the MEL, at a nose depth of ~40 cm, was 8.45×10^{-4} pmol of ATP. The highest ATP concentrations were measured at a depth of ~55 cm when the nose was immersed in the MEL (4.07 pmol ATP) and again when the tail flange of the probe passed through the last of the MEL (7.18×10^{-1} pmol ATP, nose depth ~113 cm). At nose depth ~135.0 cm ATP returned to background levels (5.63×10^{-4} pmol ATP) and maintained background level concentrations to the end of the experiment.

The same trends were observed in both scenarios. ATP (Table 2-3) spiked when the nose of the melt probe was within the MEL (1.45×10^{-2} pmol ATP). ATP then decreased until the tail of the probe was in the MEL (5.73×10^{-3} pmol ATP). However, meltwater collected from the nose (1.92×10^{-4} pmol ATP) and from the water surrounding the probe (2.67×10^{-4} pmol ATP) were comparable to background measurements of the ice and lower than the original concentration of ATP detected on the probe post cleaning prior to Scenario 2.

PCR is more sensitive than viable or direct counts as it can detect single copies of DNA. Thus, we attempted to amplify 16S rRNA genes from meltwater samples at selected depths (30.0 cm, 53.1 cm, 109.5 cm, and 156.4 cm; Table 2-2). Concentrations of extracted DNA followed the same trend as direct cell counts and $_{amp}$CFU; low levels followed by a spike, decline, second spike and decline. These samples were also positive

for amplification of the 16S rRNA gene. No PCR product was obtained from pre- MEL samples, or the last sample collected, until 45 amplification cycles were performed. Thus, we concluded these results as being inconclusive. Each cycle increases the sensitivity of the test, however there is an increase in PCR artifacts and chimeras when 40+ cycles are conducted (Kanagawa 2003). Using more volume of or other methods for these samples may have resulted in more PCR product, however we were limited by sample volumes. PCR product at nose depths of 53 cm (nose in MEL) and ~113 cm (tail in MEL) were detected and amplified at 25 cycles.

Discussion

Laboratory-based ice block experiments enable the testing of distinct engineering scenarios for subglacial environment exploration and can reveal the potential effects of melting on the dragging of microbial bioloads with a probe. In our experiments we prepared ice blocks that contained a maximum number of cells relative to those likely to be found in natural glacier ice. The MEL cell and particle abundances are comparable to the highest concentrations reported for glacier surfaces (108 cells ml-1; Boetius *et al*., 2015) and the algal abundances used are within the reported range of chlorophyll containing particles (102 to 103 cells ml-1) found in Antarctic ice cores (Price and Bay 2012). Comparison between our two ice block scenarios suggests that pumping meltwater to the surface during the probe's descent may be useful in removing in situ cells and particles. The higher concentrations of cells behind the probe compared to the nose of the probe in Scenario 2, suggests that the meltwater jacket around the probe may transport

cells and particles from the nose to behind the tail during descent. As per the Antarctic CoC (NRC 2007), our results suggest that either engineering strategy for borehole maintenance (retaining or removing meltwater) is sufficient in preventing forward contamination of immured bioloads to target depths.

Microbially rich basal ice presents a scenario in which there is minimal distance travelled from glacier to subglacial realm, potentially allowing for microbial dragging to affect the subglacial zone. While few measurements of such ice have been made, these layers visually contain a high sediment load and have been shown to contain cells (i.e., 102-104 cell g^{-1}) (Montross *et al*., 2014). The introduction of cellular debris, organic matter and nutrients located in the basal layer (Skidmore *et al*., 2000; Wadham *et al*., 2004, 2008; Tung *et al*., 2005; Yde *et al*., 2010; Doyle 2014) could inadvertently influence the subglacial realm, changing the microbial ecology and geochemical parameters. This type of forward contamination is addressed in the Antarctic CoC, which states that "drilling in conjunction with sampling procedures will inevitably introduce microorganisms into the subglacial aquatic environments. The number of microbial cells contained in or on the volume of any material or instrument added to or placed in these environments should not exceed the minimum concentration of microbes in the basal glacial ice being passed through" (NRC 2007). To determine the extent that bioload materials from upper layers of ice were dragged, we calculated Decimal reduction values (D-Values) for the tracers that were present at the end of our experiments (FITC beads and Chlorella cells). D-values were modified to incorporate the distance travelled by the

melt probe, rather than time of bioburden decimation that is typically used in D-value calculations. The second spike in bioload concentrations of FITC beads and Chlorella cells followed by samples collected through the end of the scenarios were used to determine D-values that would determine the distance that the melt probe would have had to travel to rid itself of 90% of the MEL bioload. Based on this calculation, we found that the melt probe had to travel 12.3 to 15.5 cm past the MEL to reduce the dragged bioload by 90%. However, our experiments continued ~35 cm past the 90% reduction mark. Calculations of percent reduction from the melt probe tail exiting the MEL to the end of experiment suggests that the final bioload at the end of the scenarios was reduced > 99.9% with a log reduction of 7.27 for Chlorella cells and a log reduction of 2.87 for FITC beads (as determine from direct microscopy counts). This data suggests that both scenarios would be compliant with the Antarctic CoC.

The melt probe approaches we investigated here are informative for terrestrial subglacial lake explorations. We show that the dragging of materials by melt probes is minimal and within Antarctic CoC considerations. Previous work for in situ bioload reduction has been suggested but not yet implemented on a melt probe. Possibilities include the use of an on-vehicle UV collar (Winebrenner *et al*., 2021) or flushing probe systems with H_2O_2 (Kowalski *et al*., 2016). Both possibilities have promise but do have caveats. UV treatment would not eliminate all particles that could act as contaminants to subice systems, and pumping H_2O_2 from the surface down to the probe and flushing that

H_2O_2 out may be challenging at depths. However, in situ forward contamination may be more important than in situ bioload reduction for astrobiological targets.

We also tested the ability to clean spore-forming bacteria from a melt probe using a previously established field-based cleaning protocol (Mikucki *et al*., 2022). We calculated the probability that a spore would survive our cleaning protocol and be dislodged during the melt probe descent. We showed a 99.9% reduction (3.19 log reduction) of *B. subtilis*, with 9.26×10^{-1} ($\pm 9.26 \times 10^{-3}$) sporeCFUs $25cm^{-2}$ remaining on the melt probe post cleaning (prior to Scenario 2 descent). No *B. subtilis* spores were detected in the meltwater of Scenario 2, suggesting that the melt probe did not contaminate the meltwater by dislodging any *B. subtilis*. However, *B. subtilis* spores were detected on the surface of the melt probe after the Scenario 2 descent, at a concentration of 9.0 ± 1.25 sporeCFUs $25cm^{-2}$ (ratio from pre-cleaning to post-Scenario 2 9.25×10^{-3}). The NASA bioburden reduction standards (ratio of final concentration to starting concentration) for hardy-organisms, i.e., spores, is $\leq 10^{-3}$ with a total risk of contamination for a mission being $\leq 10^{-4}$ (NASA 2011, Kminek *et al*., 2017). If the ice block scenario were considered a mission, the bioburden reduction from our field-based cleaning of the probe would be compliant with a ratio 9.52×10^{-4} for spores and 2.06×10^{-7} for non-spores, however spores detected on the melt probe after the experiment suggests further improvements can be made, specifically in cleaning the joints and seams of the melt probe. Due to the increase in sporeCFUs on the melt probe surface after Scenario 2, compared to after cleaning prior to the descent in Scenario 2, we hypothesize that the act

of melting may have dislodged spores from the joints and seams of the melt probe. This increase resulted in a ratio of 9.72 for post-melt-run sporeCFUs to post-cleaning sporeCFUs. Though the probability of contamination would be quite low without inoculating the melt probe with spores, we found that there is a chance that spores could hitch a ride on the melt probe during descent and contaminate the melt water a within the bore hole and possibly the subglacial target. With the localized heating of water around the probe, there is a possibility that a 'special region' may be created (Rummel *et al*., 2014). Several microorganisms have been shown to produce spores or cysts when under stress in order to survive extreme conditions, including species of *Bacillus* and *Actinomycetes* immured in ice (Christner *et al*., 2000) as well as snow algae, *Chlamydomonas nivalis* and *Chloromonas nivalis*, when exposed at the snow surface (as reviewed in Anesio *et al*., 2017). These organisms could potentially be 'activated' upon changing conditions, such as thawing and the addition of liquid (Ganey *et al*., 2017) which could be induced by melt probes. Further understanding of how the melt jacket may activate bioloads on realistic drilling timescales and descents (i.e., greater than our experimental Scenarios) should be explored to constrain 'special region' risks of contamination for melt probes.

Conclusion

In this study we acquired and analyzed quantitative data on two key elements of microbial transport by a descending ice melt probe, namely prevention of the introduction of exogenous organisms to glacial environments (i.e., forward contamination), and transport of microbes from one depth to another in ice (i.e., dragging) by probes.

Dragging of particles and cells by the Ice Diver was observed in both ice block scenarios, however we determined it to be minimal. We conclude that instances where the traveling distance from ice to subglacial target may not be long enough for the melt jacket to flush cells behind a probe or when targets are at depths too deep to pump meltwater to the surface, additional germicidal methods may need to be employed to rid a melt probe of an englacial bioburden. Furthermore, to differentiate microbial samples of englacial and subglacial habitats, multiple samples at varying depths should also be considered as part of melt probe sampling protocols.

With respect to forward contamination, we have shown by probe-inoculation with identifiable organisms (not found in the background in our experiments) that adapting previously developed cleaning methods reduces contamination to levels that meet standards for (a) access into to pristine subglacial lakes on Earth (Mikucki *et al*. 2022); and (b) can test the implementation of NASA-based planetary protection procedures for spacecraft and payload in analog settings. With respect to dragging, our initial data on decimeter scales, comparable to the probe length in our experiments and using two different meltwater sampling methods, indicate that the abundance of dragged microbes and their proxies decline to background levels within a few decimeters of probe descent below a Mock Englacial Layer.

While these initial data do not address all questions and scenarios for either forward contamination or dragging, they provide important information to formulate additional questions and motivate further studies. We note in particular the need to confirm and extend dragging studies over longer length scales of at least meters to tens of meters. Emerging technical means such as UVC irradiation of ice just prior to melting and of melt water around a probe (Winebrenner *et al*., in prep., 2022) may enable increasingly stringent controls on both forms of potential contamination. We believe the prospect of clean melt probe access to englacial and subglacial environments, on Earth and elsewhere, at relatively low costs (and therefore in more instances), provides strong motivation for continued work in these directions.

Acknowledgments

Funding

This work was supported by NASA COLDTech Grant # NNX17AF68G. We would also like to thank Keith Magness, Nick Wogan, Karen Junge, Shelly Carpenter, APL shared wet lab personnel and the APL shipping department.

Declaration of interest

The authors declare no conflict of interest.

References

Aamot, H.W. C. (1967). Pendulum Steering for Thermal Probes in Glaciers. *Journal of Glaciology*, *6*(48), 935–938.

Aamot, H. W. (1968). Self-contained thermal probes for remote measurements within an ice sheet. In *International Symposium on Antarctic Glaciological Exploration (ISAGE), Hanover, NH* (pp. 63-68).Aamot, H. W. C. (1970). Development of a Vertically Stabilized Thermal Probe for Studies in and Below Ice Sheets. *Journal of Engineering for Industry*, *92*(2), 263–268.

Alekhina, I., Doran, P., Naganuma, T., di Prisco, G., Storey, B., Vincent, W., ... & Walton, D. (2011, June). Code of conduct for the exploration and research of subglacial aquatic environments. In *XXXIV Antarctic Treaty Consultative Meeting, Buenos Aires* (Vol. 20).

Anesio, A. M., & Laybourn-Parry, J. (2012). Glaciers and ice sheets as a biome. *Trends in Ecology & Evolution*, *27*(4), 219–225.

Anesio, A. M., Lutz, S., Chrismas, N. A. M., & Benning, L. G. (2017). The microbiome of glaciers and ice sheets. *Npj Biofilms and Microbiomes*, *3*(1), 10.

Benardini, J. N., & Venkateswaran, K. (2016). Application of the ATP assay to rapidly assess cleanliness of spacecraft surfaces: a path to set a standard for future missions. *AMB Express*, *6*(1), 113

Boetius, A., Anesio, A. M., Deming, J. W., Mikucki, J. A., & Rapp, J. Z. (2015). Microbial ecology of the cryosphere: sea ice and glacial habitats. *Nature Reviews Microbiology*, *13*(11), 677–690.

Campen, R., Kowalski, J., Lyons, W. B., Tulaczyk, S., Dachwald, B., Pettit, E., ... & Mikucki, J. A. (2019). Microbial diversity of an Antarctic subglacial community and high-resolution replicate sampling inform hydrological connectivity in a polar desert. *Environmental microbiology*.

Christner, B. C., Mosley-Thompson, E., Thompson, L. G., Zagorodnov, V., Sandman, K., & Reeve, J. N. (2000). Recovery and identification of viable bacteria immured in glacial ice. *Icarus*, *144*(2), 479-485.

Christner, B. C., Mikucki, J. A., Foreman, C. M., Denson, J., & Priscu, J. C. (2005). Glacial ice cores: A model system for developing extraterrestrial decontamination protocols. *Icarus*, *174*(2), 572–584.

Christner, B. C., Priscu, J. C., Achberger, A. M., Barbante, C., Carter, S. P., Christianson, K., ... & Vick-Majors, T. J. (2014). A microbial ecosystem beneath the West Antarctic ice sheet. *Nature*, *512*(7514), 310.

Dawson, M. E., Novitsky, T. J., & Gould, M. J. (1988). Microbes, endotoxins and water. *Pharm. Engineering*, *8*(2), 145-148.

Doyle, S. (2014). Diversity and Activity of Bacteria in Basal Ice Environments.

Ganey, G. Q., Loso, M. G., Burgess, A. B., & Dial, R. J. (2017). The role of microbes in snowmelt and radiative forcing on an Alaskan icefield. *Nature Geoscience*, *10*(10), 754–759.

German, L., Mikucki, J. A., Welch, S. A., Kathleen A, W., Lutton, A., Dachwald, B., ... & Espe, C. (2019). Validation of sampling antarctic subglacial hypersaline waters

with an electrothermal ice melting probe (IceMole) for environmental analytical geochemistry. *International Journal of Environmental Analytical Chemistry*, 1-14.

Goeller, S., Steinhage, D., Thoma, M., & Grosfeld, K. (2016). Assessing the subglacial lake coverage of Antarctica. *Annals of Glaciology*, *57*(72), 109-117.

Gould, G. W., & Hurst, A. (1969). The bacterial spore. *The Bacterial Spore.*

Gruden, C., Skerlos, S., & Adriaens, P. (2004). Flow cytometry for microbial sensing in environmental sustainability applications: current status and future prospects. *FEMS Microbiology Ecology*, *49*(1), 37–49.

Horvath, J. C., Carsey, F. D., Cutts, J. A., Jones, J. A., Johnson, E. D., Landry, B. M., … Bradley, A. (1997). Searching for ice and ocean biogenic activity on Europa and Earth. In *Instruments, Methods, and Missions for the Investigation of Extraterrestrial Microorganisms* (Vol. 3111, pp. 490–501). International Society for Optics and Photonics.

Jakobsson, O., Grenvall, C., Nordin, M., Evander, M., & Laurell, T. (2014). Acoustic actuated fluorescence activated sorting of microparticles. *Lab Chip*, *14*(11), 1943–1950.

Kminek, G., Conley, C., Hipkin, V., and Yano, H. (2017) COSPAR's planetary protection policy. Space Res Today 200:12–25.

Kömle, N. I., Tiefenbacher, P., Weiss, P., & Bendiukova, A. (2018). Melting probes revisited–Ice penetration experiments under Mars surface pressure conditions. *Icarus*, *308*, 117-127.

Kowalski, J., Linder, P., Zierke, S., von Wulfen, B., Clemens, J., Konstantinidis, K., … Helbing, K. (2016). Navigation technology for exploration of glacier ice with maneuverable melting probes. *Cold Regions Science and Technology*, *123*, 53–70.

Livingstone, S.J., Li, Y., Rutishauser, A., Sanderson, R.J., Winter, K., Mikucki, J.A., Björnsson, H., Bowling, J.S., Chu, W., Dow, C.F. and Fricker, H.A., 2022. Subglacial lakes and their changing role in a warming climate. *Nature Reviews Earth & Environment*, pp.1-19.

Lorenz, R. D., Gleeson, D., Prieto-Ballesteros, O., Gomez, F., Hand, K., & Bulat, S. (2011). Analog environments for a Europa lander mission. *Advances in Space Research*, *48*(4), 689–696.

Lv, T., Yan, H., Cao, J., & Liang, S. (2015). Hydrophilic Molecularly Imprinted Resorcinol–Formaldehyde–Melamine Resin Prepared in Water with Excellent Molecular Recognition in Aqueous Matrices. *Analytical Chemistry*, *87*(21), 11084–11091.

Lyons, W. B., Mikucki, J. A., German, L. A., Welch, K. A., Welch, S. A., Gardner, C. B., ... & Dachwald, B. (2019). The geochemistry of englacial brine from Taylor Glacier, Antarctica. *Journal of Geophysical Research: Biogeosciences*, *124*(3), 633-648.

Ma, L.-J., Catranis, C. M., Starmer, W. T., and Rogers, S. O., 2005: The significance and implications of the discovery of filamentous fungi in glacial ice. *In* Castello, J. D. and Rogers, S. O. (eds.), *Life in Ancient Ice*. Princeton and Oxford: Princeton University Press, 159-180.

Mader, H. M., Pettitt, M. E., Wadham, J. L., Wolff, E. W., & Parkes, R. J. (2006). Subsurface ice as a microbial habitat. *Geology*, *34*(3), 169–172.

Mikucki, J. A., & Priscu, J. C. (2007). Bacterial Diversity Associated with Blood Falls, a Subglacial Outflow from the Taylor Glacier, Antarctica. *Applied and Environmental Microbiology*, *73*(12), 4029–4039.

Mikucki, J. A., Pearson, A., Johnston, D. T., Turchyn, A. V., Farquhar, J., Schrag, D. P., ... & Lee, P. A. (2009). A contemporary microbially maintained subglacial ferrous" ocean". *Science*, *324*(5925), 397-400.

Mikucki, J. A., Lee, P. A., Ghosh, D., Purcell, A. M., Mitchell, A. C., Mankoff, K. D., ... & Fricker, H. A. (2016). Subglacial Lake Whillans microbial biogeochemistry: a synthesis of current knowledge. *Philosophical Transactions of the Royal Society A: Mathematical, Physical and Engineering Sciences*, *374*(2059), 20140290.

Mikucki J.A., Schuler C.G., Digel I., j. Kowalski J., Tuttle M.J., Chua M., Davis R., a. Purcell A., Ghosh D., Francke G., Feldmann M., Espe C., Heinen D., Dachwald B., Joachim Clemens, Lyons W.B., Tulaczyk S., and the midge science team. (2022) Field-based planetary protection operations for melt probes: validation of clean access into the Blood Falls, Antarctica englacial ecosystem. *Astrobiology*

Miteva, V. I., Sheridan, P. P., & Brenchley, J. E. (2004). Phylogenetic and Physiological Diversity of Microorganisms Isolated from a Deep Greenland Glacier Ice Core. *Appl. Environ. Microbiol.*, *70*(1), 202–213.

Miteva, V. (2008). Bacteria in Snow and Glacier Ice. In R. Margesin, F. Schinner, J.-C. Marx, & C. Gerday (Eds.), *Psychrophiles: From Biodiversity to Biotechnology* (pp. 31–50).

Montross, S., Skidmore, M., Christner, B., Samyn, D., Tison, J.-L., Lorrain, R., … Fitzsimons, S. (2014). Debris-Rich Basal Ice as a Microbial Habitat, Taylor Glacier, Antarctica.

NRC, National Research Council. (2007). Exploration of Antarctic subglacial aquatic environments: environmental and scientific stewardship. National Academies Press

NASA. (2010). Handbook for the Microbiological Examination of Space Hardware, NASA-HDBK-6022.

NASA. (2011). Planetary protection provisions for robotic extraterrestrial missions. *NPR 8020.12D*.

Nicholson, W. L., Schuerger, A. C., & Race, M. S. (2009). Migrating microbes and planetary protection. *Trends in Microbiology, 17*(9), 389–392.

Paige, D. A. (1992). The Mars polar pathfinder/proposal for a discovery mission. In *Discovery Program Workshop, Concept* (Vol. 83).

Philberth, K. (1974). The thermal probe deep-drilling method by EGIG in 1968 at Station Jarl-Joset, central Greenland. In *Ice-core Drilling. Proceedings of the Symposium at University of Nebraska* (pp. 28-30).

Priscu, J. C., & Christner, B. C. (2004). Earth's Icy Biosphere. *Microbial Diversity and Bioprospecting*, 130–145.

Price, P. B., & Bay, R. C. (2012). Marine bacteria in deep Arctic and Antarctic ice cores: a proxy for evolution in oceans over 300 million generations. *Biogeosciences Discussions*, *9*(6).

Purcell, A. M., Mikucki, J. A., Achberger, A. M., Alekhina, I. A., Barbante, C., Christner, B. C., ... & Scherer, R. (2014). Microbial sulfur transformations in sediments from Subglacial Lake Whillans. *Frontiers in microbiology*, *5*, 594.

Rack, F. R. (2016). Enabling clean access into Subglacial Lake Whillans: development and use of the WISSARD hot water drill system. *Philosophical Transactions of the Royal Society A: Mathematical, Physical and Engineering Sciences*, *374*(2059), 20140305.

Rummel, J. D., Beaty, D. W., Jones, M. A., Bakermans, C., Barlow, N. G., Boston, P. J., ... & Hallsworth, J. E. (2014). A new analysis of Mars "special regions": findings of the second MEPAG Special Regions Science Analysis Group (SR-SAG2).

Sheridan, P. P., Miteva, V. I., & Brenchley, J. E. (2003). Phylogenetic Analysis of Anaerobic Psychrophilic Enrichment Cultures Obtained from a Greenland Glacier Ice Core. *Applied and Environmental Microbiology*, *69*(4), 2153–2160.

Shreve, R. L. (1962). Theory of performance of isothermal solid-nose hotpoints boring in temperate ice. *Journal of Glaciology*, *4*(32), 151-160.

Siegert, M. J. (2000). Antarctic subglacial lakes. *Earth-Science Reviews*, *50*(1), 29–50.

Skidmore, M. L., Foght, J. M., & Sharp, M. J. (2000). Microbial Life beneath a High Arctic Glacier. *Applied and Environmental Microbiology*, *66*(8), 3214–3220.

Setlow, P. (2003). Spore germination. *Current Opinion in Microbiology*, *6*(6), 550–556.

Tung, H. C., Bramall, N. E., & Price, P. B. (2005). Microbial origin of excess methane in glacial ice and implications for life on Mars. *Proceedings of the National Academy of Sciences of the United States of America*, *102*(51), 18292–18296.

Wadham, J. L., Bottrell, S., Tranter, M., & Raiswell, R. (2004). Stable isotope evidence for microbial sulphate reduction at the bed of a polythermal high Arctic glacier. *Earth and Planetary Science Letters*, *219*(3), 341–355.

Wadham, J. L., Tranter, M., Tulaczyk, S., & Sharp, M. (2008). Subglacial methanogenesis: A potential climatic amplifier?: METHANE PRODUCTION UNDER ICE. *Global Biogeochemical Cycles*, *22*(2)

Winebrenner, D. P., Elam, W. T., Kintner, P. M., Tyler, S., & Selker, J. S. (2016, December). Clean, logistically light access to explore the closest places on Earth to Europa and Enceladus. In *AGU Fall Meeting Abstracts* (Vol. 2016, pp. C51E-08).

Winebrenner, D.P., S. Carpenter, W.T. Elam, M. Karpack, S. Larson, R. Wicks, and K. Junge, "Ultraviolet susceptibilities of cold-adapted microbes in water and water ice", in preparation for submission to *Astrobiology*, 2021.)

Yde, J. C., Finster, K. W., Raiswell, R., Steffensen, J. P., Heinemeier, J., Olsen, J., … Nielsen, O. B. (2010). Basal ice microbiology at the margin of the Greenland ice sheet. *Annals of Glaciology*, *51*(56), 71–79.

Zimmerman, W., Bonitz, R., & Feldman, J. (2001, March). Cryobot: an ice penetrating robotic vehicle for Mars and Europa. In *2001 IEEE Aerospace Conference Proceedings (Cat. No. 01TH8542)* (Vol. 1, pp. 1-311). IEEE.

Appendix I: Tables and Figures

Table 2-1. Differences in cleaning, sampling and MELs used in Scenarios 1 and 2.

	Scenario 1	**Scenario 2**
Cleaning	Cleaned after handled by team.	Inoculated with *B. subtilis* spores prior to cleaning.
Sampling Method	Samples collected by pumping from nose of the probe, pumping borehole dry	Borehole was maintained, samples collect behind the melt probe, and 1 sample at the nose of the probe
MEL	*E. coli* and FITC beads	*Chlorella sp.*

Table 2-2. Scenario 1 concentrations. With maximum concentrations, probe nose in MEL (1st spike), probe tail in MEL (2nd spike), and the end of experiment concentrations. *Below detection limit.

	ATP (pmol ATP ml^{-1})	**CHLa** (µg/L)	**Chlorella cells** (cells ml^{-1})
Stock	$1.8x10^{1}$	$3.93x10^{3}$	$3.78x10^{5}$
Background	$4.5x10^{-4}$	BDL*	BDL*
Spike 1	$1.45x10^{-2}$	$1.58x10^{1}$	$8.71x10^{3}$
Spike 2	$5.73x10^{-3}$	5.85	$4.61x10^{2}$
End of test – Melt jacket sample	$2.67x10^{-4}$	BDL*	$2.00x10^{-1}$

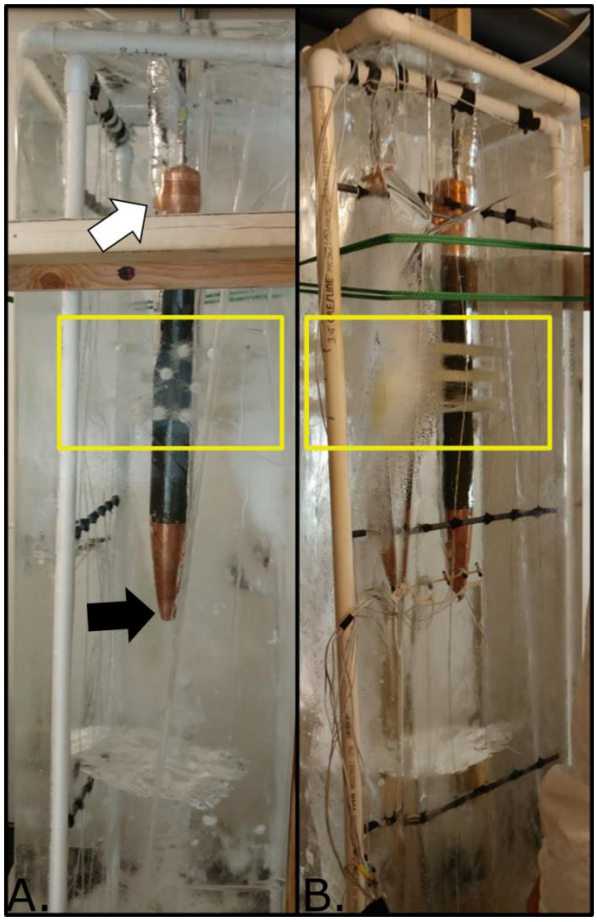


Figure 2-1. Image of ice block constructed for Scenario 1. Scenario 2 used the same inoculating and ice building protocol. Dimensions of ice block are 2.00m x 0.38m x 0.40m. melt probe is 73.75 cm in length from tip to tail. A) View of ice block with the melt probe (used in scenario 1) descending through MEL, highlighted in yellow box. B) Side view angle of ice block with the melt probe melt probe descending through MEL highlighted by yellow box. White arrow indicates the size difference in tail flange which leads to a secondary spike and dragging of materials. Black arrow indicates the nose of the probe in which samples were collected through as the probe descended in scenario 1.

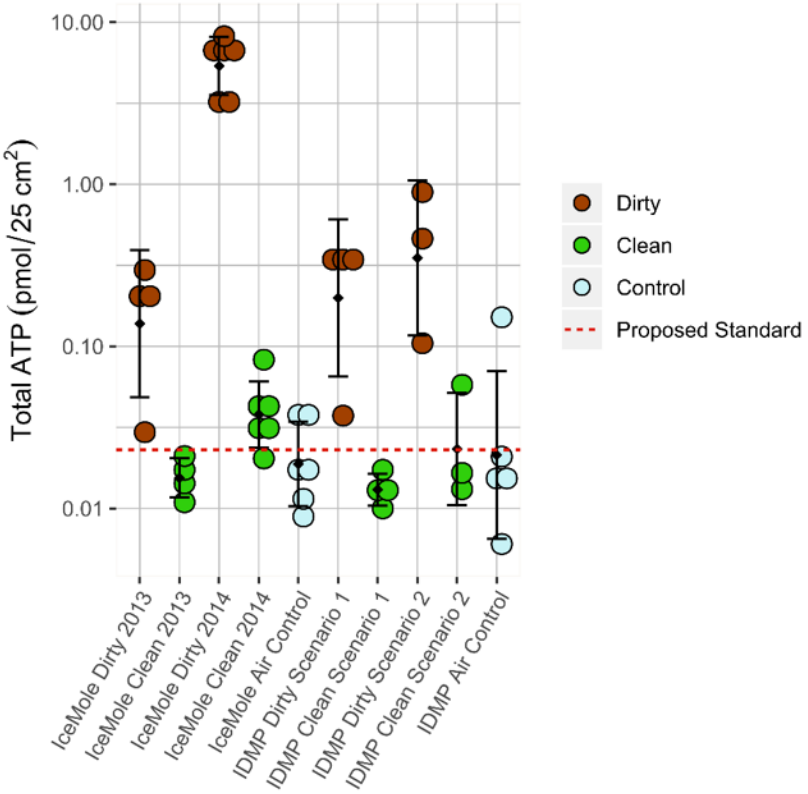


Figure 2-2. Comparison of the cleaning protocol used for IceMole in 2013 and 2014 (Mikucki *et al.*, 2022) and the Ice Diver melt probe (IDMP). Measurements of Total ATP ($pmol^{-1}$ $25cm^{-2}$) are reported in comparison to the suggested NASA standard for clean spacecraft surfaces, red horizontal line at 0.023 Total ATP ($pmol^{-1}$ $25cm^{-2}$; Benardini and Venkateswaran 2016).

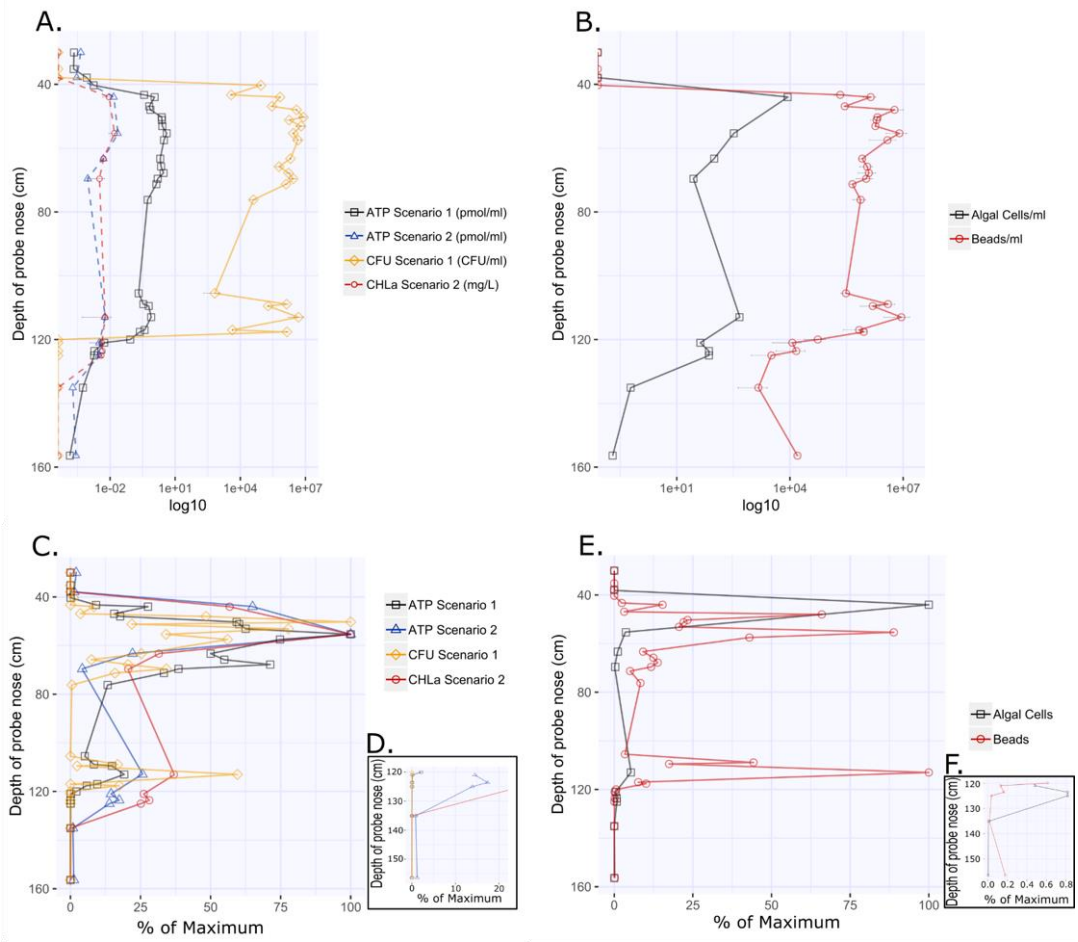


Figure 2-3. Measurements from both scenarios that went to background concentration or were below detectable limit by the end of the experiments. (A, C, D) measurements that went to background concentration by the end of the experiment. Measurements that did not go back to background concentrations and were detected at the end of the experiment, beads reduced from 10^7 beads ml^{-1} to 10^4 beads ml^{-1} and algal cells from 10^5 cells ml^{-1} to 10^{-1} cells ml^{-1} (B, E, F). A and B concentrations are on log scale illustrating the exact concentration changes, while C – F measurements are in percent maximum from highest concentration sampled during the melt probe's descent.

CHAPTER THREE

MICROBIAL ECOLOGY AND ACTIVITY OF SNOW ALGAE WITHIN A PACIFIC NORTHWEST SNOWPACK

This chapter is a revised version of work submitted to the journal; Artic, Antarctic, and Alpine Research.

Experiments and analysis were conducted by Caleb Schuler and Jill Mikucki. Jill Mikucki performed ATP analysis and helped collect and preserve snow samples. In 2019 Jill Mikucki collected snow pit samples and analyzed ATP and chlorophyll in the field. Caleb Schuler and Jill Mikucki wrote the manuscript.

Abstract

Snow algae blooms are common occurrences in alpine systems and contribute to increasing snow and glacial ice melt rates. Despite the cosmopolitan distribution of snow algae, little is known about the role their life cycle plays in community composition and activity in snowpack. Mount Baker Washington, USA is a rapidly changing alpine ecosystem. Here we present estimates of cellular biomass, microbial community composition and primary productivity measurements associated with surficial snow algae blooms and a vertical profile within a snow pit in order to characterize the microbial ecology of this snowpack system. Chloromonas was the most abundant algae detected in our samples. Sphingobacteriaceae were the most dominant bacteria in samples where fungi were the most abundant Eukaryote, whereas Chitinophagaceae dominated when Chlorophyceae where the most abundant Eukaryote. In a snow pit vertical profile we observed more algae in the green-pigmented, flagellated life cycle stage at depth (~30 cm below the surface), than at the surface where the astaxanthin-rich, aplanospore life cycle stage dominated. Higher resolution analyses revealed Chloromonas associated photosynthesis transcripts to be more abundant at depth than at the surface of the

snowpack. These results suggest there is a photosynthetic niche within alpine snowpack that has unknown impacts on the carbon budget and provides potentially undetected primary productivity resulting in a 'cryptic' photosynthetic system.

Introduction

Snow algae are thought to be key drivers of biogeochemical cycles in alpine snowpacks (Hotaling *et al*., 2017). Previous studies have shown that blooms of highly pigmented algae play a role in amplifying glacier and snowpack melt (Thomas and Duval 1995, Stibal *et al*., 2012) by decreasing surface albedo by 20% to 40% causing a cascade of ecological implications (Ganey *et al*., 2017, Lutz *et al*., 2015a, 2016). Lowering of surface albedo due to microorganisms leads to increased light absorption which enhances melt of ice and snow (Musilova *et al*., 2016, Cook *et al*., 2017). Accelerated snow melt mobilizes nutrients within the snowpack that subsequently stimulates additional algal growth (Ganey *et al*., 2017). Blooms often cover large areas of snow that can be quantified and tracked via satellite imagery (Huovinen *et al*., 2018; Ganey *et al*., 2017; Takeuchi *et al*., 2006). However, the distinctive red pigmented blooms observed on snow surfaces represent only one stage of the active snow algae life cycle and therefore surface surveys may underestimate their total ecological role.

Most snow algal blooms appear to be dominated by *Chloromonas* and *Sanguina* genera (Remias *et al*., 2005, 2013; Procházková *et al*., 2019, Engstrom *et al*., 2020). Studies in the Pacific Northwest have shown that *Sanguina* (formerly assigned to *Chlamydomonas*), *Chlainomonas* and *Chloromonas* are the dominant snow algae taxa

(Havig and Hamilton 2019; Hamilton and Havig 2020; Hoham and Remias 2020, Hoham 1974a; Hoham 1974b, Engstrom *et al*., 2020). Microbial communities associated with algal blooms vary, with some studies suggesting co-occurrence of algae with members of the Betaproteobacteria and Bacteroidetes (Krug *et al*., 2020; Hoham and Remias 2020), however these correlations do not appear to be specific across different algae taxa (Yakimovich *et al*., 2020). Fungal groups, including Basidiomycota, Ascomycete and occasionally Chytridiomycota have also been found to co-occur with snow algae (Brown and Jumpponen 2019; Brown *et al*., 2015).

The proposed life cycle of snow algae begins on the soil surface following snowmelt in the summer, in a 'spore-like' resting state known as an aplanospore (Kawecka 1981, 1986). These 'spores' are then covered by snow, where it is hypothesized that they lie dormant until the start of snow melt in early spring (Jones *et al*., 2001; Hoham and Duval 2001; Hoham *et al*. 2006). Once liquid water reaches the algae at the snow/soil interface, the aplanospores germinate and flagellate vertically through the snowpack within water veins that form between snow crystals (Remias 2012). The algae navigate via these water veins to a depth with optimal light irradiance, ~100 to 900 µmol m^{-2} s^{-1} (Remias *et al*., 2005). As the season progresses and snowpack continues to melt, algae that were previously protected by overlying snow become exposed to higher levels of irradiance that, depending on elevation and cloud cover, can reach up to >3,000 µmol m^{-2} s^{-1} (Gorton *et al*., 2001). Laboratory studies have found that high irradiances and UV cause snow algae to lose their flagella and form aplanospores

(Hoham and Remias 2020). This resting stage is characterized by asexual cells that synthesize copious amounts of the red photo-protectant pigment, astaxanthin (Badania 1986, Jones *et al*., 2001, Stibal *et al*., 2007). Astaxanthin aids the algae in reducing light irradiance at the snow's surface by 50% (Gorton et al., 2001). However, astaxanthin also decreases photosynthetic energy transfer (Zhang *et al*., 2017). When not producing astaxanthin, high UV light exposure inhibits photosynthesis in snow algae by 85%, during the production of astaxanthin a 25% reduction of photosynthetic activity has been observed (Thomas and Duval 1995). As snow continues to melt through the spring and summer, algae accumulate in melt channels (Hoham and Ling 2000). For this reason, snowpacks in alpine systems that are not subjected to steep vertical gradients, where algae can accumulate during melt, may be ideal locations to study *in-situ* snow algae life cycle dynamics.

The reduction of UV stress makes the interior of snowpack an ideal niche for algae, where they may be more productive despite the decrease in photosynthetic active radiation (PAR). Different snow algae life-cycle stages can co-exist in snowpack, with astaxanthin producing cysts abundant on the surface and vegetative algal stages at depth (Gorton and Vogelmann 2003). Irradiance conditions rapidly change in the first few cm of the snowpack, with UV radiation dropping by 50% within the first 2 cm of snow down to non-detectable levels at 8 cm beneath the snow surface (Gorton and Vogelmann 2003). At least 1% of PAR can be detected as far as 50 cm within the snowpack (Thomas and Duval 1995), with some data suggesting light can penetrate as deep as 110 cm (Hoham

and Mullet 1977). Thus, previous studies measuring snowpack primary production and carbon flux in surficial samples alone may miss activity at depth within the snowpack (Hamilton and Havig 2017; Stibal *et al*., 2007; Williams *et al*., 2003) where conditions for photosynthesis may be more ideal.

Mount Baker is an active volcano located in the North Cascade Mountain range, Washington State, USA. The Easton Glacier resides on Mount Baker's southern slope and has been monitored since 1912. This long-term data indicates the glacier has since receded ~1.95 km (Whelan and Bach 2017) with the regional climate experiencing warming of 0.2°C per decade since 1970 (Abatzoglou *et al*. 2014). Easton Glacier is part of the 396 glaciers that feed Puget Sound's largest watershed, the Skagit watershed. This watershed has seen a net decrease in glacial discharge of 24% ± 9% from 1969 to 2009, yet glacier outflow and melt still comprises 6-12% of Skagit River stream flow (Riedel and Larrabee 2016). Decrease in glacial discharge is expected to continue, resulting in changes of biodiversity (Jacobsen et al., 2012; Wilhelm et al., 2013). Alpine and glacial ecosystems are affected by a multitude of factors including precipitation, temperature, and anthropogenic effects (Harper 1993; Hansen and Nazarenko 2003; McCabe and Fountain 2013; Ming et al., 2009), to which snow algae are intrinsically tied. As these factors continue to influence alpine ecosystems, the impact on the snow and glacier microbiome remains unknown.

A baseline understanding of the core microbiomes and their ecological function in snowpack systems is critical for understanding the impacts that climatic change has on these microbial communities (Stibal *et al*., 2020). We aimed to characterize the microbial ecology of the Mount Baker snowpack associated with the Easton Glacier valley. Prokaryotic and eukaryotic microbial diversity was assessed on select snow samples along an elevational gradient and at depth within alpine snowpack. Photosynthetic activity of the Mount Baker snowpack community was measured using primary productivity assays and metatranscriptomic analyses, which revealed gene expression patterns. Collectively these data shed light on *Chloromonas* abundance and activity in Pacific Northwest snowpack.

Methods

Site Description and sample collection

Samples were collected along a southwest transect of Mount Baker, WA, USA off the Park Butte Trail (N48.7012, W121.8054) leading up towards Easton Glacier (Figure 3-1, Appendix table no. 2) from 1,025 to 1,491 m.a.s.l. during June 2018 and May 2019. This area is predominantly home to mountain hemlock, Douglas fir, and pacific silver fir trees (Rosa 2016). While the plants within the low meadow area of Mount Baker are typically arctic lupine, mountain-heather, huckleberry and dwarf bilberry (Hagedorn and Flower 2021). During January through May the average median snow depth, from 2010 to 2023, was 2.2 meters at the Schreibers Meadow (N48.7, W121.82) snow course/aerial marker station and the average median snow water equivalent was 0.86 meters, in the same time period (Natural Resources Conservation Service 2013).

Snow and meltwater samples were collected along an elevation gradient in 2018 (Table 1). On 6 June 2018, materials were collected from sites designated as 'Meadow' and 'Upper Clearing.' The Meadow sample site was collected in an open clearing with no surrounding trees; Upper Clearing was collected in a small clearing with trees interspaced. Both sample sites were collected midday, under partly cloudy skies with an air temperature of ~24°C. On 7 June 2018, 'Trailhead' was sampled in a small clearing surrounded by trees at midday. Skies were partly cloudy and ambient air temperatures during sampling was ~25°C. During this time, snow algae was only visible at lower elevations around the tree line (≤ 1,463 m.a.s.l.), and not on or near the tongue of Easton Glacier (N48.73, W121.83, ~ 1,768 m.a.s.l.) Surfaces snowpack samples were collected from the Easton Glacier tongue, however we were not able to extract sufficient DNA for microbial analysis, thus these samples are not discussed further. All samples in this study were selected based on presence or absence of visible snow algae communities. Trailhead samples contained patches of red snow, the snow from the Meadow site was white with limited debris and no visible snow algae, Upper Clearing were patches of mixed (brown/red) snow.

All snow samples were collected with individually wrapped sterile spatulas or scopes (Sterileware). Snow for primary productivity assays was placed into non-vented and non-treated tissue culture flasks (Corning) until snow filled the flask and melted down to ~20 ml per incubation. Snow for nucleic acid analyses was collected in sterile

whirl-pak (Nasco) bags, melted at ambient temperatures, and passed through a 0.22 μm pore size Sterivex filter (MilliporeSigma) on site via 60 ml individually wrapped sterile syringes. Sterivex filters were then stored and shipped to UTK frozen at -20°C. Aliquots for cell enumeration were transferred into 50 ml polypropylene tubes and fixed with paraformaldehyde (PFA; 4% final concentration) and stored at 4°C until filtered and enumerated.

In 2019, a single snow pit was dug at an elevation near to our 2018 Trailhead sample (N48.7039, W121.8156) for a vertical profile. The (Figure 3-2) profile was collected by first digging a pit to the ground surface with an ethanol cleaned shovel. The snow along the pit column was then scrapped away using sterile spatulas (Sterileware) to ensure any snow touched by the shovel was removed. Snow was then collected at depth using a new sterile scoop for each sample; this snow was then placed in sterile whirl-pak bags and shipped frozen (at -20°C). Snow samples for each depth were also collected in sterile whirl-pak bags, as described above, and melted for various biogeochemical analyses described below. Samples for cell enumeration were collected in the same manner as described for the 2018 samples. Sample selection throughout the snowpack was based on visible density (to the naked eye) of algae. Surface snowpack (0-2 cm depth) had visible red snow, while the Mid snowpack (at ~27.9 cm depth) had visible dense green snow, and the Base snowpack (at ~69.9 cm) was the snow directly overlaying the soil and contained now visible pigmentation.

Field based measurements

Light intensity was measured using a REED Instruments Light Meter SD-1128 in lumens per square meter (lux). Lux measurements were collected every 30 seconds during primary productivity assays and converted to the average lux per hour at each site. The light meter was placed at the surface of snowpack next to where incubations were conducted. Measurements of lux are not equivalent to photosynthetic active radiation and as such we use these data to provide a comparison of the relative amount of incoming illumination at each site during sampling. Electrical conductivity measurements were collected on freshly melted samples in the field using the sympHony SP80PC (VWR) meter with a sympHony conductivity probe. Colored dissolved organic matter (CDOM) and Chlorophyll A (CHLa) were measured on melted samples using a Turner Trilogy Fluorometer with the CHLa *in vivo* module at 460 nm for CHLa. Relative fluorescence units of CHLa measurements were converted to µg L^{-1} of CHLa using a CHLa standard (Turner Designs) with a standard curve ($R^2 = 0.994$). CDOM was measured with the CDOM/FDOM module (Turner) at 365nm. Relative fluorescence units of CDOM were converted to µg ml^{-1} using IHSS Suwannee River Fulvic Acid Standard II (www.humic-substances.org) via standard curve ($R^2 = 0.939$). Snow for Chlorophyll measurements were collected via sterile scoops into acid washed amber Nalgene bottles, hiked back to camp, thawed at 4°C and measured immediately after thawing (~6-8 hours after collection).

Cellular abundance

DNA-containing cells were counted by staining aliquots of 4% PFA-fixed samples with the nuclear counterstain, 4',6 -Diamidino-2-Pheynylindole, Dihydrochloride (DAPI), and then filtering onto 0.2 μm black polycarbonate filters for visualizing and quantifying with an epifluorescence microscopy (Zeiss Axio Image M2) using methods described in Mikucki and Priscu (2007). Sample volumes used for each slide were optimized so each field of view would have between 30 and 300 cells. The same filters and slides from each site were used to count algal cells and bacteria cells. Algal cells were counted first using brightfield to differentiate green and red algal cells as to not overexpose the algae to light when counting the bacteria cells. Algal cells that were red-pigment under brightfield were counted as astaxanthin-containing cells; green-pigmented cells were counted as not producing the astaxanthin pigment Bacteria was counted at 100X magnification, and algal cells were counted at 10X and 20X depending on the abundance per slide.

Carbon fixation assays

Inorganic carbon uptake was measured via microcosm incubations by amending samples with ^{13}C-labeled $NaHCO_3$ using the method of Hamilton and Having (2017). Briefly, 100 μM $NaH^{13}CO_3$ was incubated in 15 ml volumes of snowmelt in triplicate for ~60 min at ambient temperature and solar exposure. Controls at each site included triplicate incubations with no added substrate and labeled samples in culture flasks wrapped in electrical tape and placed inside white bag (dark controls). Incubation times varied, however all were performed around midday. Data were normalized to incubation

time by dividing carbon uptake by the total incubation time for each site. For example, Trailhead B incubations were terminated after 2 hours due to logistical constraints, whereas other locales were incubated for ~1 hour. $NaH^{13}CO_3$ (Cambridge Isotope Laboratories, Inc., Andover MA) was prepared with 18.2 MΩ/cm deionized water and added to each microcosm via sterile pipet tips. Experiments were terminated by filtering samples through pre-combusted (450°C for 4 hours) 0.2 µm glass fiber filters. Filters were then wrapped individually in pre-combusted aluminum foil (450°C for 4 hours) via flame sterilized tweezers and stored and shipped frozen to UTK (-20°C) for processing.

At UTK, each filter was thawed, washed with HCl (1M) to remove any residual $NaH^{13}CO_3$, briefly rinsed with 18.2 MΩ/cm deionized water, and dried at 60°C for three days. One quarter of each filter was then scraped into tin boats and sealed to be loaded and analyzed via a Costech Instruments Elemental Analyzer (EA; ECS 4010) connected to a Thermo Scientific Isotope Ratio Mass Spectrometer (IR-MS) at the Stable Isotope Lab at the University of Tennessee, Knoxville. Linearity corrections, standards and calculations were made as described in Schuler *et al*. (2017). Reported values of ^{13}C uptake (carbon fixation rates) were calculated using the difference in absolute $^{13}C/^{12}C$ ratios between labeled incubations and non-amended controls. Results are presented in units relating to the mass of organic carbon in the material used for the incubations, accounting for the sample biomass added to the filter and scrapped off for EA-IRMS analysis. Results are reported as micrograms of carbon incorporated (µg C) per gram of carbon in the incubation material (g Biomass C) per hour to provide a direct comparison

to other carbon uptake in snow algae experiments. The amount of $\delta^{13}C$ for each incubation were compared to non $\delta^{13}C$ amended samples to confirm uptake occurred. Both light dependent (light treatment) and light independent (dark treatment) uptake over time was assessed for each of the 2018 surface snow samples to determine primary productivity rates (PPR; Figure 3-3). Results were interpreted statistically via a Tukey honestly significant difference (HSD) test.

Snowpack CO_2 flux

CO_2 flux measurements were collected using an a portable force diffusion infrared CO_2 flux detector (Eosense eosFD). At each site the eosFD sensor was placed near the incubations and programmed to take a measurement every 5 minutes, with a minimum of 4 measurements per site. Results provided by the instrument are given in CO_2 ppm/m^2/s. Flux measurements for each site were averaged and converted to μg C/m/hr for comparison to carbon uptake microcosm experiments. Difference in flux data between sites was evaluated using a paired, unequal variance T-test.

Nucleic acid extraction

Methods adapted from Jacobs *et al.*, 2009 and Cruaud *et al*., 2017 were used to remove the internal filters from the Sterivex plastic housing. Briefly, pliers were used to break open the back end of the Sterivex casing (non luer-lok end), releasing the filter and filter holder. Filter and holder were then pulled out of the casing and the filter was cut at the edges using a flame sterilized scalpel, then peeled away with flame sterilized tweezers. Filters were cut with flame sterilized scissors into small pieces and placed into

bead beating tubes with flame sterilized tweezers. DNA was extracted from 0.22 µm pore sized Sterivex (2018 samples) or 47mm (Pall Supor) filters (2019 samples) utilizing Qiagen's DNAeasy extraction kit per the manufacturer's instructions with slight modifications. MP Bio bead-beating lysing matrix E tubes were substituted for those supplied with kit. Filters were divided into two extraction tubes. Our bead beating step included 45 seconds beating at 6.6 m/s followed by 30 seconds rest and 45 seconds at 6.6 m/s in a 10°C cold room using MBio fastprep24 bead beater. RNA was extracted from the 2019 snow pit samples for transcriptomics using TriZol (Invitrogen) according to the manufacturer protocols with an additional bead beating step (6.5 m/s for 45 seconds followed by 30 seconds rest and then another 45 seconds at 6.5 m/s). All sample processing was performed in a class 100 biological safety cabinet.

Microbial diversity assessment

Amplicon sequencing that targeted the V4 region of the 16S rRNA gene (515F - GTGCCAGCMGCCGCGGTAA, 806R - GGACTACHVGGGTWTCTAAT) and the V9 region of the 18S rRNA gene (1380F – CCCTGCCHTTTGTACACAC, 1510R - CCTTCYGCAGGTTCACCTAC) was performed by Novogene Corporation Inc. (Sacramento CA) on DNA extracts using NovaSeq 6000 (Illumina) resulting in PE250 bp amplicon data. Amplicon sequence variants (ASVs) for both 16S and 18S data (Callahan *et al.*, 2017) were generated using the DADA2 pipeline v1.16 (Callahan *et al*., 2016) following default parameters. Taxonomy was classified using the SILVA reference database v138 (Quast *et al*., 2012). Statistical and Shannon diversity analysis was performed using phyloseq v1.22.3, via 'plot_richness' command (McMurdie and Holmes

2013), and figures were made with GGPlot2 v3.3.2 (Wickham, 2016) using R (v4.0.3). The top 10 fungal ASVs designated as 'NA_Fungi' (Appendix Table no. 3), and 'Uncultured Chloromonas' (Appendix Table no. 4) by the DADA2 pipeline from each sample site were identified using Basic Local Alignment Search Tool (BLAST; Altschul *et al*., 1990).

RNA libraries were constructed following Oxford Nanopore Direct cDNA Native Barcoding Protocol (SQK-DCS109 with EXP-NBD104 and EXP-NBD114; Version DCB_9091_v109_revF_04Feb209) using kit SQK-DCS109 and were sequenced on Oxford nanopore MinIon using Flowcell FAL0048. The RNA library was not polyadenylated in an attempt to sequence only Eukaryotic RNA, and rRNA was not depleted from the libraries before sequencing. Post processing was completed via Guppy (V3.4.4) with rRNA sequences removed by SortmeRNA (V2.1). Metatranscriptomic data from Surface and Mid snowpack samples were compared by normalizing the datasets via transcripts (annotated genes) per 1 million genes (transcript/total transcripts x 1,000,000), as well as comparing relative abundance of transcripts utilizing SEED Subsystem categories (Overbeek et al., 2014), following the SAMSA2 pipeline (Westreich et al., 2018). All sequences were also annotated using Diamond (Buchfink et al., 2015) against NCBI's non-redundant database (Pruitt et al., 2007).

Results

In situ measurements

Conductivity varied little between sites on sampling days whereas lux varied by an order of magnitude. Conductivity ranged from 2.32 to 7.14 µS/cm across 2018 surface sites and lux ranged from $2.4x10^4$ (Meadow) to $2.5x10^5$ (Upper Clearing and Trailhead) average lux/hr (Table 1); in 2019 the average lux was $2.5\ x10^4$ lux/hr at the surface where the snow pit was established (Table 1). In 2018 CDOM ranged from $1.2x10^1$ (Meadow) to $1.9x10^3$ CDOM ug/ml (Upper Clearing), with Trailhead at $2.1x10^1$ CDOM ug/ml. CDOM was not collected for the snowpack samples 2019. CHLa varied across all sites, from as low as 5.16 CHLa µg/ml at Base snowpack to 29.52 CHLa µg/ml at Meadow site, with the highest value of $2.0x10^3$ CHLa µg/ml at Upper Clearing. CHLa concentrations were noticeably lower in sites where astaxanthin pigmented algae (red algae samples) were more abundant than non-astaxanthin pigmented algae (algae that were green), such as Trailhead ($3.2x10^1$CHLa µg/ml) and Surface snowpack ($2.5\ x10^1$ CHLa µg/ml) vs Upper Clearing $1.9\ x10^3$ CHLa µg/ml and Mid snowpack $1.2\ x10^3$CHLa µg/ml).

Direct counts of algal and bacterial cells

Green and red pigmented algal cells were observed microscopically in all sample sites (Table 1). In 2018, total algal cells ranged from to $9.7x10^4$ cells/ml (at Trailhead) to $6.4x10^2$ cells/ml (at Meadow), with Upper Clearing having $4.2x10^4$ cell/ml. Each of these sites had more non astaxanthin containing algae (green cells) than astaxanthin-pigmented (red cells) with an average ratio of red to green pigmented algae of $2.6x10^{-1}$. Bacterial cell counts (cell counts excluding algae) for these sites also varied; Upper Clearing had the highest number of cells at $3.9x10^6$ cells/ml, followed by Trailhead $2.5x10^6$ cells/ml,

and Meadow having the lowest cells/ml ($2.0x10^5$ cells/ml). Microscopic observations of the 2019 snowpack samples showed more green-pigmented algal cells than cells that produced astaxanthin (red) at ~30 cm depth (Mid snowpack), with the inverse true for the Surface snowpack sample. Mid snowpack had $3.86x10^4$ green- pigmented algal cells/ml and $3.3x10^2$ astaxanthin-pigmented (red) algal cells/ml with a ratio of red to green of $8.2x10^{-3}$. Conversely, the Surface snowpack had more red pigmented cells green algal cells ($7.9x10^3$ green cells/ml and $1.4x10^4$ red algal cell/ml with a ratio of red to green of 1.7). The Base snowpack had $1.0x10^3$ green-pigmented algal cells/ml and 5 astaxanthin pigmented algal cells/ml. Total algal count thus ranged from $3.8x10^4$ algal cells/ml (Mid snowpack) to $1.1x10^3$ algal cells/ml (Base snowpack) with Surface having $2.1x10^4$ algal cells/ml. Bacterial counts were only conducted for Surface snowpack ($1.4x10^4$ cells/ml) and Mid snowpack ($1.1x10^5$ cells/ml).

Snowpack primary productivity rate and CO_2 flux

Trailhead had the highest percent C (15.55%) and percent N (1.28%) with the lowest C:N ratio (13.64) out of the 3 surface samples from 2018 (Table 1). Upper Clearing had the second highest percent C (4.98%) and N (0.28%) with a C:N of 17.56. Meadow had the lowest percent C (3.98%), and N (0.14%) with the highest C:N ratio (28.56). The natural abundance of $\delta^{13}C$ was -28.4‰ for Trailhead, Upper Clearing was -28.38‰ and Meadow was -27.64‰. $\delta^{15}N$ ranged from -4.89‰ (Trailhead), -5.59‰ (Upper Clearing) and -6.57‰ at Meadow.

Primary productivity rates (PPR) were measurable at each of the 2018 sites (Figure 3-3), however statistical significance was only found between Light vs Dark treatments in both Trailhead Sites A ($p = 5.5x10^{-5}$) and B ($p = 2.6x10^{-5}$). No significance was found between Meadow (Dark vs Light) or Upper Clearing (Dark vs Light). Trailhead B had the highest PPR (89.5 +/- 8.4 μg C uptake/g biomass C/hr), followed by Trailhead A (81.3 +/- 10.05 μg C uptake/g biomass C/hr), Upper Clearing (32.4 +/- 21.4 μg C uptake/g biomass C/hr), and Meadow (5.9 +/- 2.8 μg C uptake/g biomass C/hr). Furthermore, Trailhead sites were both significantly different from Meadow, (Light, Trailhead A $p = 1.2x10^{-4}$ and Trailhead B $p = 2.78x10^{-5}$) as well as from Upper Clearing (Light, A $p = 0.017$ and B $p = 0.003$). No statistically significant differences were observed between any of the dark treatments across sites.

CO_2 flux followed a similar trend as PPR (Figure 3-4) in that the sites with visibly pigmented algae, and higher PPR, had negative CO_2 flux. Upper Clearing and Trailhead had negative flux indicating drawdown of CO_2 into the snowpack ($-3.57x10^{-3}$ +/- $2.89x10^{-3}$ μg/C/hr and $-1.82x10^{-3}$ +/- $1.06x10^{-3}$ μg/C/hr, respectively). Meadow, which had the lowest measured PPR rates, had a positive CO_2 flux of $9.86x10^{-3}$ +/- $2.84x10^{-3}$ μg/C/hr. Statistically significant difference were found between Trailhead and Meadow ($p = 0.019$), and Upper Clearing and Meadow ($p = 0.031$).

Snowpack microbial community composition

Quality filtering for clean reads of 16S rRNA genes (16S) resulted in an average of 138,620 merged, non-chimeric 16S sequences per sample and a total of 2,302 unique

16S ASVs across all samples (106 Meadow, 124 Trailhead, 917 Upper Clearing, 154 Surface snowpack, 747 Mid snowpack, 89 Base snowpack). Quality filtering for 18S rRNA genes (18S) averaged 80,679 merged, non-chimeric 18S sequences per sample and resulted in a total of 1,251 unique 18S ASVs across all samples (111 Meadow, 174 Trailhead, 236 Upper Clearing, 192 Surface snowpack, 261 Mid snowpack, 277 Base snowpack).

Dominant ASVs varied across our samples with Chitinophagaceae, Comamonadaceae, Sphingobacteraceae and Oxalobacteraceae as the most abundant bacteria families. The most abundant 16S ASV in our dataset belonged to the Chitinophagacea family (16S-ASV1) and comprised 3.58% of Meadow, 52.4% of Trailhead, 48.71% of Upper Clearing, 30.95% of Surface snowpack, 11.14% of Mid snowpack and 2.02% of Base snowpack ASVs (Figure 3-5). 16S-ASV1 was unclasssified at the genus level by the DADA2 workflow, and was further identified via BLAST as an uncultured bacterium from glacial systems associated with ice worms (99.2% sequence identity; Murakmi *et al*., 2015). The majority of ASVs from the Sphingobacteraceae family belonged to the *Solitalea* genus. In the Meadow sample, *Solitalea* comprised 93.08% of all ASVs and 99.7% of the Sphingobacteraceae ASVs. Furthermore *Solitalea* comprised 6.06% of all ASVs and 73.4% of Sphingobacteraceae at the Trailhead site; 10.45% of all ASVs and 98.6% of Sphingobacteraceae ASVs at the Upper Clearing site. This trend was also observed in the 2019 snow pit samples with 23.86% of all ASVs and 99.8% of Sphingobacteraceae ASVs in the Surface snowpack and 15.58% of all ASVs

and 94.3% of Sphingobacteraceae ASVs in Mid snowpacksampels. The base sample was the only exception, where only 0.03% of all Base snowpack ASVs and 0.3% of the Sphingobacteraceae ASVs were *Solitalea*. For the Base sample, rather than *Solitalea* being the most abundant Sphingobacteraceae ASV, *Mucilaginibacter sp.* was the most abundant (48.35% of Sphingobacteraceae Base snowpackASVs and 7.01% of all Base snowpack ASVs). ASVs from the Oxalobacteraceae family were the most abundant ASV in the Mid snowpack site and were dominated by a single ASV (16S-ASV6 which was 86.2% of Oxalobacteraceae ASVs in the Mid snowpack). This sequence was unclasssified at the genus level by the DADA2 workflow, and identified via BLAST as a *Massilia sp.* (100% sequence identity) originally sequenced from leaf colinization and cold adapted arctic bacteria studies (Assession # MN989074). The Rhodanobacteraceae family ASV (16S-ASV5) that dominated the Base snowpack (29.8% of all Base snowpack ASVs) was identified as belonging to the *Rhodanobacter* genus by the DADA2 workflow. No Archaeal sequences were detected by our work flow.

Sites with higher abundances of algae sequences compared to fungi had similar bacterial communities and were distinct from sites that had higher abundance of fungi, with the exception of the Mid snowpack (Figure 3-6). Chitinophagaceae and Comamonadaceae were more abundant in sites that algae made up the majority of 18S ASVs (Upper Clearing, Surface snowpack and Mid snowpack), whereas Sphingobacteraceae were more abundant in the sites in which fungi ASVs made up the majority of 18S ASVs (Meadow, Trailhead). In Mid snowpack Oxalobacteraceae were

the most abundant family (23.8% of all ASVs) and in the Base snowpack where Rhodanobacteraceae, was the most abundant (29.8% of all ASVs; Figure 3-5).

Eukaryotic community composition was similar across all sites (Figure 3-7), however, relative abundance of algae and fungal ASVs varied. *Chloromonas* were the most abundant 18S ASVs in Upper Clearing (43.8%), Surface snowpack (71.6%), and Mid snowpack sites (48.%), whereas Meadow and Trailhead sites were dominated by a group of fungi that could not be assigned by the DADA2 workflow (NA-Fungi). NA-Fungi comprised 78.1% of Meadow fungal groups and 59.6% in Trailhead. The majority of Base snowpack ASVs belonged to NA-Charophyta (44.9%). Further characterization of these 'NA' sequences using BLAST identified the top "NA-Fungi" ASV from the Trailhead site (18S-ASV4) as sharing sequence identity (95.9%) with a *Paranamyces uniporus*, originally isolated from non-saline mud/soil (Simmons *et al*., 2020; Letcher *et al*., 2015). The top "NA-Fungi" (18S-ASV6) from the Meadow site shared sequence identity (97.7%) with an uncultured Basidiomycete, originally sequenced from indoor building mold (Pitkaranta *et al*., 2008). The "NA-Charophyta" ASVs were identified as Charophyta but were not assigned at any higher taxonomic level, the top ASV from this group (18S-ASV5) shared sequence identity (99.4%) with *Symphoricarpos occidentalis* of the honeysuckle plant family (NCBI non-redundant database, GenBank: MT610964.1). There was no overlap between 18S ASVs across samples, each site had a unique set of ASVs.

Alpha diversity of 16S ASVs between sites identified Meadow as the least diverse site (1.03), followed by Trailhead (2.13), Surface snowpack (2.21), and Upper Clearing (2.84). Mid snowpack (3.62) and Base snowpack (4.02) was the most diverse site. Bacterial differences between samples were driven by 3 ASVs, an uncultured Chitinophagacea genus (16S-ASV1), *Solitalea* (16S-ASV2), and *Rhodanobacter* (16S-ASV5; Figure 3-8). Analyses with NMDS (Bray-Curtis dissimilarity) indicate Meadow and Base snowpack were the most dissimilar across sites; Upper Clearing and Trailhead cluster together while Surface and Mid snowpack cluster. Alpha diversity of 18S ASVs followed a similar trend as the 16S diversity. Trailhead was the least diverse site (3.68) followed by Meadow (3.72), then Surface snowpack (3.82), while Base snowpack (4.31), Mid Snowpack (4.43),and Upper Clearing (4.48) were the most diverse of the sites. There was no overlap in 18S ASVs from site to site, thus RDA resulted in the most abundant 18S ASV from each site driving the observed differences between sites. However, NMDS (Bray-Curtis dissimilarity) resulted in snowpack samples (Surface, Mid and Base) being most different from each other and Upper Clearing, Meadow and Trailhead clustering together.

Snowpack metatranscriptomics

Active communities within the snowpack were assessed utilizing long read metatranscriptomics on samples from the Surface and ~ 30 cm below the surface (Mid) of a snow pit (Figure 3-2). Sequencing resulted in 600,119,229 bases in 889,046 clean sequences for Surface snowpack and 493,649,225 bases in 889,046 clean sequences for Mid snowpack. Because we were limited to a single sample from each depth, data were

normalized by transcripts (annotated genes) per 1 million genes (transcript/total transcripts x 1,000,000); we avoid making statistical conclusions given our limited sample size. Transcripts for photosynthesis and respiration were observed in both snow pit samples, with a greater number of transcripts associated with photophosphorylation (133,174 vs 44,496 annotated genes/million transcripts), CO_2 fixation (21,349 vs 8,322 annotated genes/million transcripts), and respiration (20,416 vs 11,140 annotated genes/million transcripts) in the sample at ~30 cm depth (Mid snowpack Supplemental; Figure 3-8). Transcripts specifically associated with *Chloromonas* were also more abundant in our Mid snowpack sample (62,103 total annotated *Chloromonas* genes/million transcripts) compared to Surface snow (35,859 total annotated *Chloromonas* genes/million transcripts). Furthermore, we observed more ribosomal gene transcripts in the Mid snowpack compared to the Surface snowpack (12,996 annotated ribosomal genes/million transcripts and 7,337 annotated ribosomal genes/million transcripts respectively; Figure 3-9).

Conversely, a higher abundance of transcripts associated with stress responses were detected in the Surface snowpack compared to Mid snowpack including oxidative stress (14,303 vs 7,067 annotated genes/million transcripts respectively) and osmotic stress (3,054 vs 2,281 annotated genes/million transcripts respectively; Figures 3-11and 3-12). Transcripts associated with oxidative stress included phytochrome, two-component sensor histidine kinase, manganese superoxide dismutase, organic hydroperoxide resistance protein, gamma-glutamyltranspeptidase as well as several other transcripts.

Transcripts associated with osmotic stress included outer membrane protein A precursor, cyclic beta-1,2-glucan synthase, choline dehydrogenase and other transcripts at low abundances. Also of note, the complete pathway for astaxanthin production was expressed in the Surface snowpack dataset whereas only the transcripts for the synthesis of phytoene to lycopene were detected at depth (Mid snowpack). Transcripts associated with antibiotic resistance genes including multidrug efflux pumps, cobalt-zinc-cadmium resistance, acriflavine resistance, arsenic resistance, and beta-lactamase, as well as others at low abundance, were also present at both depths, though they were more prevalent in the Surface sample (25,581 annotated genes/million transcripts) compared to the Mid snowpack (8,792 annotated genes/million transcripts; Figure 3-13).

Discussion

Microbial ecology of Easton snowpack samples

Mount Baker alpine snowpack contains visibly red patches of snow formed by abundant *Chloromonas* algal cells. This finding as well as the observed bacterial diversity associated with our pigmented snow samples is consistent with previous studies of other Pacific Northwest patches of red and orange-pigmented snowpack (Hamilton and Havig 2017; 2020; Havig and Hamilton 2019; Yakimovich *et al*., 2020). However, the dominant algae in other snow-covered environments have also been described as *Sanguina* and *Chlainomonas* (Ji *et al*., 2021; Davey *et al*., 2019; Soto *et al*., 2020). Our Mid snowpack sample, which was collected at ~30 cm below an observed red snow patch, contained the most non-astaxanthin containing (green-pigmented) algal cells. The bacterial community associated with these algae cells detected at depth were distinct from other reports in that

the most abundant ASVs belonged to Oxalobactereacea (30% relative abundance). Other studies have found Flavobacteriaceae, Sphingobacteriaceae, Sphingomonadaceae to be the most abundant bacterial taxa associated with snow algal blooms (Davey *et al*., 2019; Krug *et al*., 2020). Some Oxalobactereacea have been shown to produce auxin, a plant growth promoting hormone, that has also been shown to promote growth in algae (Lin *et al*., 2022). A recent study by Krug *et al*. (2020) demonstrated that auxin producing bacteria increased biomass of *Chloromonas* in microcosms. Thus, the Oxalobacteracea may support growth of *Chloromonas* while in their non-astaxanthin pigmented stage, however investigating bacteria transcripts for auxin production was not possible due to our RNA-cDNA libraries not being polyadenylated. Auxin promoting transcripts produced by algae were not detected in our samples. The high abundance of Sphingobacteriaceae and Chitinophagaceae in our surface snow samples suggests a potential relationship with the red-pigmented algae and fungi in which the bacteria may degrade high molecular weight compounds produced by the algae (Fernández-Gómez *et al*., 2013; Gómez-Pereira *et al*., 2012; Krug *et al*., 2020; Zhu *et al*., 2020) and chitin produced by the fungi (Rosenberg 2014; Abo Elsoud and El Kady 2019). *Chloromonas* and Basidiomycete fungi have been widely identified in association with snow algae communities across the globe (Hoham and Remias 2020; Brown and Jumpponen 2019).

Our results add evidence to the proposed snow algae life cycle in that we observed *Chloromonas* as the primary 18S ASVs in both the Surface (majority red pigmented algae) and at the Mid snowpack (majority green-pigmented algae; Kawecka

1981; 1986; Jones *et al*., 2001; Hoham and Duval 2001; Hoham *et al*. 2006). Furthermore, we observed a change in alpha diversity, and the 16S rRNA and 18s rRNA community composition throughout the same snowpack. The bottom or Base sample had low algal cell abundances yet was the most diverse among the snow pit samples(4.02, 16S rRNA Shannon index), while our Mid sample had high algal cell abundances of which the majority were non-astaxanthin producing and was less diverse (3.62, 16S rRNA Shannon index) compared to the Base snowpack.. Whereas in the surface sample, the majority of the algal cells were astaxanthin pigmented and was the least diverse sample among the snow pit samples (2.21, 16S rRNA Shannon index). This suggests that the life cycle of snow algae may play a role in shaping the bacterial community.

Snowpack metabolic activity and carbon flux

Productivity associated with snow algal communities are of interest due to their abundant presence across snow and glacier systems (Ganey *et al*., 2017). Previous studies of snow algal metabolic activity suggest the algae play an important role in biogeochemical processes (Hodson *et al*., 2017). The productivity of these microbial communities impact the carbon budget by either sequestering carbon via photosynthesis or releasing carbon via respiration; their acquisition of growth factors can further influence glacier nutrient budgets. Understanding the carbon budget of these systems on a global and local scale is becoming increasingly important as alpine glaciers and snowpack are rapidly receding (Wilson *et al*., 2021; Williams *et al*., 2003).

The Mount Baker snowpack contained diverse, active microbial communities both on the snowpack surface and at depth as measured by stable isotope incorporation assays and transcriptomics. Primary production in Mount Baker samples showed similar carbon uptake compared to other snowpack primary production studies in the Pacific Northwest (Hamilton and Havig 2017, 2020; Havig and Hamilton 2019). Our data further supports active microbially-mediated carbon cycling based on observed CO_2 flux measurements, which followed the same trend as our PPR measurements. The recovery of rRNA belonging to snow algae at the snow-air interface, and at 30 cm depth within the snowpack, along with the expression of transcripts necessary for photosynthesis and respiration, further supports the hypothesis of an active photosynthesizing community at multiple depths within the snowpack.

The Trailhead site had similar PPR to other studies that measured the activity of dense snow algae blooms, although our Trailhead sample had a higher average PPR. Samples from Meadow were similar to other snow sites with little to no visible algal blooms. Our Upper Clearing site was most similar to mixed snow samples described by Hamilton and Havig (2017). The higher PPR measured at Trailhead compared to other reported rates for pigmented alpine snowpack studies could be explained by differences in elevation and available nutrients. Hamilton and Havig (2017; 2020) collected snow from higher elevation (>2000 m.a.s.l.), while our study was within the tree line where there was less light irradiance and nutrients accumulate and support metabolic activity. For example, the nitrogen content of the Mount Baker snowpack (0.57% N average

across all sites) was higher than in supraglacial snow described by Hamilton and Havig (2017), which observed 0.18% average across sites. Observed C:N ratios were similar to other snow algae sites in the arctic (Spijkerman et al., 2012; Lutz et al., 2015; 2016) and alpine mountains (Hamilton and Having 2017). Furthermore, a single sample collected above the tree line on Easton Glacier in 2018 contained 2.53 ug/ml CDOM, which was 10 to 1,000 times less the CDOM observed at the 2018 surface sites, suggesting more organic matter at lower elevations which may support metabolic activity.

CO_2 drawdown was greater at sites with higher PPR, however Trailhead and Upper Clearing sites drew down less CO_2 into the snowpack than Meadow released. Meadow, which had low activity rates (5.9 +/- 2.8 μg C uptake/g biomass C/hr) and no visible red patches, was the only site where positive CO_2 flux from the snowpack was measured ($9.86x10^{-3}$ +/- $2.84x10^{-3}$ μg/C/hr). This could be due to a higher abundance of heterotrophic bacteria in relation to the algae within this sample site, compared to our other sites. Trailhead, which had the highest PPR, and the second lowest CO_2 draw down ($-1.82x10^{-3}$ +/- $1.06x10^{-3}$ μg/C/hr), received an order of magnitude less light ($2.4x10^4$ lux) than the other sites during our PPR incubations. Trailhead was located between a small opening of trees, which likely shaded the amount of light penetrating to the snow surface. Lower light intensities may be beneficial for snow algae activity, as light has previously been discussed as a major factor in the life cycle and activity of snow algae (Remias *et al.*, 2005). Collectively, our PPR data suggests that even patches of snow without visible pigments (such as the Meadow site) contain active snow algae. Still, these communities

may be contributing to carbon sequestration. Tools with higher resolution than the naked eye, such as field mobile spectral radiometers, can better inform site selection for algal assessment studies. While a broader study (both temporally and spatially) would better inform the net rates of activity in Mount Baker snowpack, the range of patches we sampled suggest carbon fixation is slower than CO_2 release from the snowpack. However, surface surveys do not necessarily account for the potential productivity at depth within the snow.

The life cycle of snow algae is complex, with stages occurring throughout the snowpack, rather than just at the surface. This presents challenges for an accurate assessment of snowpack carbon budgets. Our limited study shows a range of primary productivity rates and CO_2 fluxes with variations depending on whether the snow contains visible pigmented algae. Specifically, we detected transcripts and rRNA that belong to snow algae at the snow air interface and at depth within the snowpack. Previous work has suggested that algae communities are found from the surface to within 10 to 25 cm snow depth (Gorton and Vogelmann 2003; Fogg 1967). These studies found that light irradiance was also a factor that influenced the vertical position of the algae within the snowpack, i.e., high irradiances may cause snow algae to migrate 10-15 cm deeper within the snowpack (Grinde 1983) to a depth where the algae are protected from light saturation (Stibal *et al*., 2007). Thomas (1972) performed a transplant experiment in which activity was measured on a surface algae bloom placed 50 cm below the surface. However, activity was not observed naturally *in situ* or in samples collected at depth. In

our study, we found that photosynthesis and respiration were occurring 30 cm beneath the snow air interface. We also observed a higher chlorophyll concentration in the Mid snowpack compared to the Surface sample, however disparities in chlorophyll concentrations between samples could be due to astaxanthin pigment masking the chlorophyll during analysis (Bidigare et al., 1993; Lang 1968; Hoham and Remias 2020), or the breakdown of chlorophyll to phaecophytin by UV (Edwards et al., 2004). These data, along with microscopic observations, and rRNA sequences within the snowpack, indicates that algal communities are actively transforming carbon at tens of cm below the surface and suggests that snow algae can be active during multiple life stages within the snowpack at the same time, including both the red aplanospore stage and the green flagellated stage.

Surface snow microbial communities are exposed to many stressors such as high light irradiances and UV (Leya *et al*., 2013). Additional stressors for snow algal communities can include osmotic stress (Holzinger *et al*., 2016) and interactions with other microorganism (Bergk *et al*., 2019) such as exposure to antibiotics expressed in active communities as mediators of competition (Cornforth and Foster 2013). We observed relatively higher levels of stress and antibiotic response transcripts in the Surface snowpack metatranscriptome compared to that of the Mid snowpack. Additionally, the full pathway for astaxanthin production was only observed in the Surface snowpack data. Reduction of photosynthesis at the snow surface due to astaxanthin production (Zhang *et al*., 2017) may be occurring. Both UV and visible light

decrease exponentially with depth (Thomas and Duval 1995; Gorton and Vogelmann 2003), however, we observed more transcripts for genes involved in CO_2 fixation and photosynthesis in the Mid snowpack samples relative to the Surface. This finding suggests that photosynthesizing at depth within the snowpack, where cells are protected from the most intense UV, could be more advantageous for algae even if less light is available. In addition to the higher abundance of transcripts belonging to the *Chloromonas* genus, direct counts of algal cells were also more abundant in the Mid snowpack site. Though additional replication would be required to statistically conclude the Mid snowpack was more photosynthetically active than the surface, our data suggests that at minimum, there is activity at depth in snowpack.

It has been hypothesized that snow algae play an important role in the global carbon budget (Williams *et al*., 2003), however recent research does not include seasonal nor depth of snow algae which, as a result, may miss a large portion of snowpack carbon fixation and respiration. As evidence, we observed activity at depth within the snowpack and on the snow surface where no visible algae blooms were occurring (Meadow site). Previous remote sensing studies of snow algal blooms focused on albedo and algae biogeography (Ganey *et al*., 2017, Huovinin *et al*. 2018, Hisakawa *et al*., 2015, Takeuchi *et al*., 2006) and may have missed activity occurring at depth or within non-pigmented surface snow patches. Thus, future work to determine if airborne, or even surface, spectral radiometers can detect snow algae within snowpack should be performed. Further research in quantifying primary production and gene transcript differences within

snowpack and across varying levels of blooms will inform how the snow algae life cycle contributes to the snowpack carbon budget and nutrient cycling.

Conclusion

Understanding changes to the biodiversity and metabolic activity of snowpack systems is paramount in a warming world, however studies that survey alpine snowpacks remain limited (Stibal *et al.,* 2020). Here we present a first survey of the microbial (prokaryotic and eukaryotic) diversity associated with snowpack on Mount Baker. We found higher primary production rates and increased CO_2 draw down associated with sample sites that contained a higher proportion of algal cells, however even snow that appeared white to the naked eye had low abundance of snow algae and low, but measurable, rates of productivity. We further observed multiple life cycles of the snow algae, classified as *Chloromonas*, throughout a vertical snowpack profile. Red-pigmented, astaxanthin producing snow algae dominated the surface of the snowpack, whereas dense green-pigmented algae dominated the snow at ~30 cm beneath the surface, and few algal cells were detected at the base of the snowpack, ~70 cm beneath the surface at the snow/soil interface. The middle of the snowpack had a higher algal cell abundance than the surface, as well as higher expression of genes for photosynthesis, including CO_2 fixation and respiration. Our study suggests that snowpack has the potential to be a larger carbon sink than previously described, specifically at depth within the snowpack. We further observed shifts in microbial community composition in samples associated with different snow algae life cycle stages and whether algae or fungi were the most abundant eukaryotic organisms within the samples.

Seasonal studies of snowpack microbial communities may inform snow algal life cycle dynamics, which currently has unknown impacts on snow ecology and the carbon budget. Current tools for tracking snow algae, i.e., remote sensing, should take the seasonality of the life cycle into account and address activity at depth. In addition, many factors contribute to snowpack carbon dynamics and influence the activity of microbes that mediate these transformations, including sunlight, nutrients, snow depth and microbial interactions. Further work should be conducted to elucidate how cryptic photosynthesis in snowpack impacts local ecosystems, the snowpack microbiome, and global carbon budgets.

Acknowledgements

Funding

This work was supported by NASA Astrobiology Early Career Collaboration Award to CGS; NASA Coldtech (16-CLDTCH16_2-0020 -UWSC9720) to JAM; and the UTK Office of Research, Innovation and Economic Development.

We are grateful to Abigail Jarratt, Justin Burnett, Oliva Husted, Nick Wogan, Keith Magness, David Shean and the Northwest Glacier Cruisers snowmobile club for their assistance in the field.

We would also like to thank Jake Shaffer for laboratory assistance and Anthony Faiia at the UTK stable isotopes lab for assistance in running the EA IR-MS. With additional support from UW APL shipping department and Dale Winebrenner.

Declaration of interest

The authors declare no conflict of interest.

References

Abatzoglou, J. T., Rupp, D. E., & Mote, P. W. (2014). Seasonal climate variability and change in the Pacific Northwest of the United States. Journal of Climate, 27(5), 2125-2142.

Abo Elsoud, M. M., & El Kady, E. M. (2019). Current trends in fungal biosynthesis of chitin and chitosan. Bulletin of the National Research Centre, 43(1), 1-12.

Altschul, S. F., Gish, W., Miller, W., Myers, E. W., & Lipman, D. J. (1990). Basic local alignment search tool. *Journal of molecular biology*, *215*(3), 403-410.

Badania, P. (1986). Ecology of snow algae 2. *General characteristics of snow algae*, *3*, 407-415.

Bergk Pinto, B., Maccario, L., Dommergue, A., Vogel, T. M., & Larose, C. (2019). Do organic substrates drive microbial community interactions in Arctic snow?. *Frontiers in microbiology*, 2492.

Bidigare, R. R., Ondrusek, M. E., Kennicutt, M. C., Iturriaga, R., Harvey, H. R., Hoham, R. W., & Macko, S. A. (1993). Evidence a photoprotective for secondary carotenoids of snow algae 1. Journal of Phycology, 29(4), 427-434.

Brown, S. P., & Jumpponen, A. (2019). Microbial ecology of snow reveals taxa-specific biogeographical structure. *Microbial ecology*, *77*(4), 946-958.

Brown, S. P., Olson, B. J., & Jumpponen, A. (2015). Fungi and algae co-occur in snow: an issue of shared habitat or algal facilitation of heterotrophs?. *Arctic, Antarctic, and Alpine Research*, *47*(4), 729-749.

Buchfink, B., Xie, C., & Huson, D. H. (2015). Fast and sensitive protein alignment using DIAMOND. Nature Methods, 12(1), 59–60. https://doi.org/10.1038/nmeth.3176

Callahan, B. J., McMurdie, P. J., Rosen, M. J., Han, A. W., Johnson, A. J. A., & Holmes, S. P. (2016). DADA2: High-resolution sample inference from Illumina amplicon data. *Nature methods*, *13*(7), 581-583.

Callahan, B. J., McMurdie, P. J., & Holmes, S. P. (2017). Exact sequence variants should replace operational taxonomic units in marker-gene data analysis. The ISME journal, 11(12), 2639-2643.

Cook, J. M., Hodson, A. J., Gardner, A. S., Flanner, M., Tedstone, A. J., Williamson, C., ... & Tranter, M. (2017). Quantifying bioalbedo: a new physically based model and discussion of empirical methods for characterising biological influence on ice and snow albedo. *The Cryosphere*, *11*(6), 2611-2632.

Cornforth, D. M., & Foster, K. R. (2013). Competition sensing: the social side of bacterial stress responses. *Nature Reviews Microbiology*, *11*(4), 285-293.

Cruaud, P., Vigneron, A., Fradette, M. S., Charette, S. J., Rodriguez, M. J., Dorea, C. C., & Culley, A. I. (2017). Open the SterivexTM casing: An easy and effective way to improve DNA extraction yields. Limnology and Oceanography: Methods, 15(12), 1015-1020.

Davey, M. P., Norman, L., Sterk, P., Huete-Ortega, M., Bunbury, F., Loh, B. K. W., ... & Smith, A. G. (2019). Snow algae communities in Antarctica: metabolic and taxonomic composition. *New Phytologist*, *222*(3), 1242-1255.

Edwards, H. G., De Oliveira, L. F., Cockell, C. S., Ellis-Evans, J. C., & Wynn-Williams, D. D. (2004). Raman spectroscopy of senescing snow algae: Pigmentation changes in an Antarctic cold desert extremophile. International Journal of Astrobiology, 3(2), 125-129.

Engstrom, C. B., Yakimovich, K. M., & Quarmby, L. M. (2020). Variation in snow algae blooms in the Coast Range of British Columbia. *Frontiers in Microbiology*, *11*, 569.

Fernández-Gomez, B., Richter, M., Schüler, M., Pinhassi, J., Acinas, S. G., González, J. M., & Pedros-Alio, C. (2013). Ecology of marine Bacteroidetes: a comparative genomics approach. The ISME journal, 7(5), 1026-1037.

Fogg, G. E. (1967). Observations on the snow algae of the South Orkney Islands. Philosophical Transactions of the Royal Society of London. Series B, Biological Sciences, 252(777), 279-287.

Ganey, G. Q., Loso, M. G., Burgess, A. B., & Dial, R. J. (2017). The role of microbes in snowmelt and radiative forcing on an Alaskan icefield. *Nature Geoscience*, *10*(10), 754-759.

Gómez-Pereira, P. R., Schüler, M., Fuchs, B. M., Bennke, C., Teeling, H., Waldmann, J., ... & Amann, R. (2012). Genomic content of uncultured Bacteroidetes from contrasting oceanic provinces in the North Atlantic Ocean. Environmental Microbiology, 14(1), 52-66.

Gorton, H. L., Williams, W. E., & Vogelmann, T. C. (2001). The Light Environment and Cellular Optics of the Snow Alga Chlamydomonas nivalis (Bauer) Wille†¶. *Photochemistry and Photobiology*, *73*(6), 611-620.

Gorton, H. L., & Vogelmann, T. C. (2003). Ultraviolet Radiation and the Snow Alga Chlamydomonas nivalis (Bauer) Wille¶. *Photochemistry and Photobiology*, *77*(6), 608-615.

Grinde, B. (1983). Vertical distribution of the snow alga Chlamydomonas nivalis (Chlorophyta, Volvocales). Polar biology, 2(3), 159-162.

Hagedorn, B., & Flower, A. (2021). Conifer Establishment and Encroachment on Subalpine Meadows around Mt. Baker, WA, USA. Forests, 12(10), 1390.

Havig, J. R., & Hamilton, T. L. (2019). Snow algae drive productivity and weathering at volcanic rock-hosted glaciers. *Geochimica et Cosmochimica Acta*, *247*, 220-242.

Hamilton, T. L., & Havig, J. (2017). Primary productivity of snow algae communities on stratovolcanoes of the Pacific Northwest. *Geobiology*, *15*(2), 280-295.

Hamilton, T. L., & Havig, J. R. (2020). Inorganic carbon addition stimulates snow algae primary productivity. *The ISME journal*, *14*(3), 857-860.

Hansen, J., & Nazarenko, L. (2004). Soot climate forcing via snow and ice albedos. *Proceedings of the National Academy of Sciences*, *101*(2), 423–428.

Harper, J. T. (1993). Glacier Terminus Fluctuations on Mount Baker, Washington, U.S.A., 1940–1990, and Climatic Variations. *Arctic and Alpine Research*, *25*(4), 332–340.

Hisakawa, N., Quistad, S. D., Hester, E. R., Martynova, D., Maughan, H., Sala, E., ... & Rohwer, F. (2015). Metagenomic and satellite analyses of red snow in the Russian Arctic. *PeerJ*, *3*, e1491.

Hodson, A. J., Nowak, A., Cook, J., Sabacka, M., Wharfe, E. S., Pearce, D. A., ... & Vieira, G. (2017). Microbes influence the biogeochemical and optical properties of maritime Antarctic snow. *Journal of Geophysical Research: Biogeosciences*, *122*(6), 1456-1470.

Hoham, R. W. (1974a). CHLAINOMONAS KOLII (HARDY ET CURL) COMB. NOV.(CHLOROPHYTA, VOLVOCALES), A REVISION OF THE SNOW ALGA, TRACHELOMONAS KOLII HARDY ET CURL (EUGLENOPHYTA, EUGLENALES) 1, 2. Journal of Phycology, 10(4), 392-396.

Hoham, R. W. (1974b). New findings in the life history of the snow alga, Chlainomonas rubra (Stein et Brook) comb. nov. (Chlorophyta, Volvocales). Syesis 7:239–47.

Hoham, R. W., & Mullet, J. E. (1977). The life history and ecology of the snow alga Chloromonas cryophila sp. nov.(Chlorophyta, Volvocales). *Phycologia*, *16*(1), 53-68.

Hoham, R. W., & Ling, H. U. (2000). Snow algae: the effects of chemical and physical factors on their life cycles and populations. In *Journey to diverse microbial worlds* (pp. 131-145). Springer, Dordrecht.

Hoham, R. W. & Duval, B. 2001. Microbial ecology of snow and freshwater ice with emphasis on snow algae. *In* Jones, H. G., Pomeroy, J. W., Walker, D. A. & Hoham, R. W. [Eds.] *Snow Ecology. An Interdisciplinary Examination of Snow-Covered Ecosystems*. Cambridge University Press, Cambridge, pp. 168–228.

Hoham, R. W., Berman, J. D., Rogers, H. S., Felio, J. H., Ryba, J. B., & Miller, P. R. (2006). Two new species of green snow algae from Upstate New York, Chloromonas chenangoensis sp. nov. and Chloromonas tughillensis sp. nov.(Volvocales,

Chlorophyceae) and the effects of light on their life cycle development. *Phycologia*, *45*(3), 319-330.

Hoham, R. W., & Remias, D. (2020). Snow and glacial algae: a review1. *Journal of phycology*, *56*(2), 264-282.

Holzinger, A., Allen, M. C., & Deheyn, D. D. (2016). Hyperspectral imaging of snow algae and green algae from aeroterrestrial habitats. *Journal of Photochemistry and Photobiology B: Biology*, *162*, 412-420.

Hotaling, S., Hood, E., & Hamilton, T. L. (2017). Microbial ecology of mountain glacier ecosystems: biodiversity, ecological connections and implications of a warming climate. *Environmental microbiology*, *19*(8), 2935-2948.

Huovinen, P., Ramírez, J., & Gómez, I. (2018). Remote sensing of albedo-reducing snow algae and impurities in the Maritime Antarctica. *ISPRS Journal of Photogrammetry and Remote Sensing*, *146*, 507-517.

Jacobs, J., Rhodes, M., Sturgis, B., & Wood, B. (2009). Influence of environmental gradients on the abundance and distribution of Mycobacterium spp. in a coastal lagoon estuary. Applied and Environmental Microbiology, 75(23), 7378-7384.

Jacobsen, D., Milner, A. M., Brown, L. E., & Dangles, O. (2012). Biodiversity under threat in glacier-fed river systems. *Nature Climate Change*, *2*(5), 361–364.

Ji, M., Kong, W., Jia, H., Ding, C., Anesio, A. M., Wang, Y., & Zhu, Y. G. (2022). Similar heterotrophic communities but distinct interactions supported by red and green-snow algae in the Antarctic Peninsula. *New Phytologist*, *233*(3), 1358-1368.

Jones, H. G., Pomeroy, J. W., Walker, D. A., & Hoham, R. W. (Eds.). (2001). *Snow ecology: an interdisciplinary examination of snow-covered ecosystems*. Cambridge University Press.

Kawecka, B. (1981). Biology and ecology of snow algae. *Acta Hydrobiol*, *23*, 211-215.

Kawecka, B. (1986). Ecology of snow algae. *Polish polar research*, *7*(4).

Krug, L., Erlacher, A., Markut, K., Berg, G., & Cernava, T. (2020). The microbiome of alpine snow algae shows a specific inter-kingdom connectivity and algae-bacteria interactions with supportive capacities. *The ISME journal*, *14*(9), 2197-2210.

Lang, N. J. (1968). ELECTRON MICROSCOPIC STUDIES OF EXTRAPLASTIDIC ASTAXANTHIN IN HAEMATOCOCCUS 1 2. Journal of Phycology, 4(1), 12-19.

Lin, Hanzhi, Yantao Li, and Russell T. Hill. "Microalgal and bacterial auxin biosynthesis: implications for algal biotechnology." *Current Opinion in Biotechnology* 73 (2022): 300-307.

Letcher, P. M., Powell, M. J., & Davis, W. J. (2015). A new family and four new genera in Rhizophydiales (Chytridiomycota). Mycologia, 107(4), 808-830.

Leya, T. (2013). Snow algae: adaptation strategies to survive on snow and ice. In *Polyextremophiles* (pp. 401-423). Springer, Dordrecht.

Lutz, S., Anesio, A. M., Field, K., & Benning, L. G. (2015). Integrated ‘omics’, targeted metabolite and single-cell analyses of Arctic snow algae functionality and adaptability. *Frontiers in microbiology*, *6*, 1323.

Lutz, S., Anesio, A. M., Edwards, A., & Benning, L. G. (2015a). Microbial diversity on Icelandic glaciers and ice caps. *Frontiers in microbiology*, *6*, 307.

Lutz, S., Anesio, A. M., Raiswell, R., Edwards, A., Newton, R. J., Gill, F., & Benning, L. G. (2016b). The biogeography of red snow microbiomes and their role in melting arctic glaciers. *Nature communications*, *7*(1), 1-9.

Lutz, S., Anesio, A. M., Edwards, A., & Benning, L. G. (2017). Linking microbial diversity and functionality of arctic glacial surface habitats. *Environmental microbiology*, *19*(2), 551-565.

McCabe, G. J., & Fountain, A. G. (2013). Glacier variability in the conterminous United States during the twentieth century. *Climatic Change*, *116*(3), 565–577

McMurdie, P. J., & Holmes, S. (2013). phyloseq: an R package for reproducible interactive analysis and graphics of microbiome census data. *PloS one*, *8*(4), e61217.

Mikucki, J. A., & Priscu, J. C. (2007). Bacterial diversity associated with Blood Falls, a subglacial outflow from the Taylor Glacier, Antarctica. *Applied and environmental microbiology*, *73*(12), 4029-4039.

Ming, J., Xiao, C., Cachier, H., Qin, D., Qin, X., Li, Z., & Pu, J. (2009). Black Carbon (BC) in the snow of glaciers in west China and its potential effects on albedos. *Atmospheric Research*, *92*(1), 114–123.

Murakami, T., Segawa, T., Bodington, D., Dial, R., Takeuchi, N., Kohshima, S., & Hongoh, Y. (2015). Census of bacterial microbiota associated with the glacier ice worm Mesenchytraeus solifugus. *FEMS microbiology ecology*, *91*(3).

Musilova, M., Tranter, M., Bamber, J. L., Takeuchi, N., & Anesio, A. M. (2016). Experimental evidence that microbial activity lowers the albedo of glaciers. *Geochem. Perspect. Lett*, *2*, 106-116.

Natural Resources Conservation Service, 2023. NWCC Report Generator, Schreibers Meadow station 21A10. National Water and Climate Center. Retrieved January 3, 2023, from https://wcc.sc.egov.usda.gov/reportGenerator/view/customSingleStationReport,metric/monthly/start_of_period/21A10:WA:SNOW%7Cid=%22%22%7Cname/2010-01-01,2023-01-03/WTEQ::collectionDate,WTEQ::value,WTEQ::median_1991,WTEQ::pctOfMedian_1991,SNWD::value,SNWD::median_1991,SNWD::pctOfMedian_1991?fitToScreen=false

Overbeek, R., Olson, R., Pusch, G. D., Olsen, G. J., Davis, J. J., Disz, T., ... & Stevens, R. (2014). The SEED and the Rapid Annotation of microbial genomes using Subsystems Technology (RAST). Nucleic acids research, 42(D1), D206-D214.

Pitkaranta, M., Meklin, T., Hyvarinen, A., Paulin, L., Auvinen, P., Nevalainen, A., & Rintala, H. (2008). Analysis of fungal flora in indoor dust by ribosomal DNA sequence analysis, quantitative PCR, and culture. *Applied and environmental microbiology*, *74*(1), 233-244.

Procházková, L., Leya, T., Křížková, H., & Nedbalová, L. (2019). Sanguina nivaloides and Sanguina aurantia gen. et spp. nov.(Chlorophyta): the taxonomy, phylogeny, biogeography and ecology of two newly recognised algae causing red and orange snow. *FEMS microbiology ecology*, *95*(6), fiz064.

Pruitt, K. D., Tatusova, T., & Maglott, D. R. (2007). NCBI reference sequences (RefSeq): a curated non-redundant sequence database of genomes, transcripts and proteins. Nucleic acids research, 35(suppl_1), D61-D65.

Quast, C., Pruesse, E., Yilmaz, P., Gerken, J., Schweer, T., Yarza, P., ... & Glöckner, F. O. (2012). The SILVA ribosomal RNA gene database project: improved data processing and web-based tools. *Nucleic acids research*, *41*(D1), D590-D596.

Remias, D., Lütz-Meindl, U., & Lütz, C. (2005). Photosynthesis, pigments and ultrastructure of the alpine snow alga Chlamydomonas nivalis. *European Journal of Phycology*, *40*(3), 259-268.

Remias, D. (2012). Cell structure and physiology of alpine snow and ice algae. In *Plants in alpine regions* (pp. 175-185). Springer, Vienna.

Remias, D., Wastian, H., Lütz, C., & Leya, T. (2013). Insights into the biology and phylogeny of Chloromonas polyptera (Chlorophyta), an alga causing orange snow in Maritime Antarctica. *Antarctic Science*, *25*(5), 648-656.

Riedel, J. L., & Larrabee, M. A. (2016). Impact of Recent Glacial Recession on Summer Streamflow in the Skagit River. *Northwest Science*, *90*(1), 5–22.

Rosa, K. A. (2016). One Hundred Years of Vegetation Succession in the Easton Glacial Foreland, Mount Baker, Washington. WWU Graduate School Collection. 506. https://cedar.wwu.edu/wwuet/506

Rosenberg, E. (2014). “The family Chitinophagaceae” in The prokaryotes. eds. E. Rosenberg, E. F. DeLong, S. Lory, E. Stackebrandt, and F. Thompson (Heidelberg, Germany: Springer), 493–495.

Schuler, C. G., Havig, J. R., & Hamilton, T. L. (2017). Hot spring microbial community composition, morphology, and carbon fixation: implications for interpreting the ancient rock record. *Frontiers in Earth Science*, 97.

Simmons, D. R., Bonds, A. E., Castillo, B. T., Clemons, R. A., Glasco, A. D., Myers, J. M., ... & James, T. Y. (2020). The Collection of Zoosporic Eufungi at the University of Michigan (CZEUM): introducing a new repository of barcoded Chytridiomyceta and Blastocladiomycota cultures. *IMA fungus*, *11*(1), 1-22.

Soto, D. F., Fuentes, R., Huovinen, P., & Gómez, I. (2020). Microbial composition and photosynthesis in Antarctic snow algae communities: integrating metabarcoding and pulse amplitude modulation fluorometry. *Algal Research*, *45*, 101738.

Spijkerman, E., Wacker, A., Weithoff, G., & Leya, T. (2012). Elemental and fatty acid composition of snow algae in Arctic habitats. *Frontiers in microbiology*, *3*, 380.

Stibal, M., Elster, J., Šabacká, M., & Kaštovská, K. (2007). Seasonal and diel changes in photosynthetic activity of the snow alga Chlamydomonas nivalis (Chlorophyceae) from Svalbard determined by pulse amplitude modulation fluorometry. *FEMS Microbiology Ecology*, *59*(2), 265-273.

Stibal, M., Šabacká, M., & Žárský, J. (2012). Biological processes on glacier and ice sheet surfaces. *Nature Geoscience*, *5*(11), 771-774.

Stibal, M., Bradley, J.A., Edwards, A., Hotaling, S., Zawierucha, K., Rosvold, J., Lutz, S., Cameron, K.A., Mikucki, J.A., Kohler, T.J. and Šabacká, M., 2020. Glacial ecosystems are essential to understanding biodiversity responses to glacier retreat. *Nature Ecology & Evolution*, *4*(5), pp.686-687.

Takeuchi, N., Dial, R., Kohshima, S., Segawa, T., & Uetake, J. (2006). Spatial distribution and abundance of red snow algae on the Harding Icefield, Alaska derived from a satellite image. *Geophysical research letters*, *33*(21).

Thomas, W. H. (1972). OBSERVATIONS ON SNOW ALGAE IN CALIFORNIA 1, 2. *Journal of phycology*, *8*(1), 1-9.

Thomas, W. H., & Duval, B. (1995). Sierra Nevada, California, USA, snow algae: snow albedo changes, algal-bacterial interrelationships, and ultraviolet radiation effects. *Arctic and alpine research*, *27*(4), 389-399.

Westreich, S.T., Treiber, M.L., Mills, D.A. et al. SAMSA2: a standalone metatranscriptome analysis pipeline. BMC Bioinformatics 19, 175 (2018) doi:10.1186/s12859-018-2189-z

Whelan, P., & Bach, A. J. (2017). Retreating Glaciers, Incipient Soils, Emerging Forests: 100 Years of Landscape Change on Mount Baker, Washington, USA. *Annals of the American Association of Geographers*, *107*(2), 336–349.

Wickham, H., Chang, W., & Wickham, M. H. (2016). Package 'ggplot2'. *Create elegant data visualisations using the grammar of graphics. Version*, *2*(1), 1-189.

Wilhelm, L., Singer, G. A., Fasching, C., Battin, T. J., & Besemer, K. (2013). Microbial biodiversity in glacier-fed streams. *The ISME Journal*, *7*(8), 1651–1660.

Williams, W. E., Gorton, H. L., & Vogelmann, T. C. (2003). Surface gas-exchange processes of snow algae. *Proceedings of the National Academy of Sciences*, *100*(2), 562-566.

Wilson, A. C., Nolin, A. W., & Bladon, K. D. (2021). Assessing the Role of Snow Cover for Post-Wildfire Revegetation Across the Pacific Northwest. *Journal of Geophysical Research: Biogeosciences*, *126*(11), e2021JG006465.

Yakimovich, K. M., Engstrom, C. B., & Quarmby, L. M. (2020). Alpine snow algae microbiome diversity in the coast range of British Columbia. *Frontiers in microbiology*, 1721.

Zhang, L., Su, F., Zhang, C., Gong, F., & Liu, J. (2017). Changes of photosynthetic behaviors and photoprotection during cell transformation and astaxanthin accumulation in Haematococcus pluvialis grown outdoors in tubular photobioreactors. *International journal of molecular sciences*, *18*(1), 33.

Zhu, C., Miller, M., Lusskin, N., Bergk Pinto, B., Maccario, L., Häggblom, M., ... & Bromberg, Y. (2020). Snow microbiome functional analyses reveal novel aspects of microbial metabolism of complex organic compounds. *Microbiologyopen*, *9*(9), e1100.

Appendix I: Tables and Figures



Figure 3-1. Mount Baker Washington study site and images of snow conditions at each sample location. (a) Map of Mount Baker, dashed line represents estimated extent of snowpack on the mountain during sampling. Sample sites (b) Upper Clearing (mixed – brown/red snow), (c) Meadow (white snow), (d) Snowpack / Snow pit (layered snowpack sampling) and (e) Trailhead (red snow). Culture flasks in pictures are containers used for primary productivity rate incubation experiments. Easton Snowpack point on map is the sample site where snowpack on Easton glacier was collected. Satellite image retrieved from Google Earth.

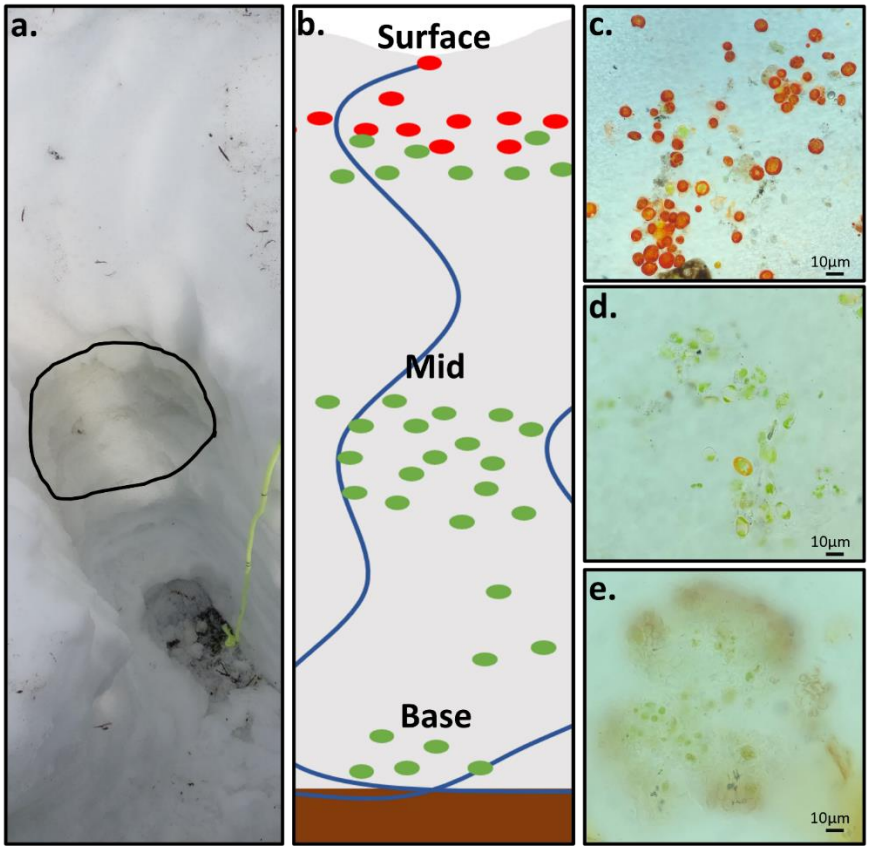


Figure 3-2. Description of vertical snow pit profile sampled in 2019. (a) Photo of snowpack after surface sample collection. Green rope marked distance between sample sites (i.e., Surface – 0 cm depth, Mid – 29.9 cm depth and Base – 69.9 cm depth), black outline shows the extent of the green patch of snow (Mid sample) . (b) Cartoon illustration of the vertical profile of the snow pit with labels describing sample location and red/green 'cells' to illustrate the type of algal cells (astaxanthin-containing (red) and non-astaxanthin pigmented (green) not to scale. Brightfield microscope images (c – e) of samples from the snow pit with 10 µm scale bar. (c) is the Surface, (d) is the Mid, and (e) is the Base snowpack.

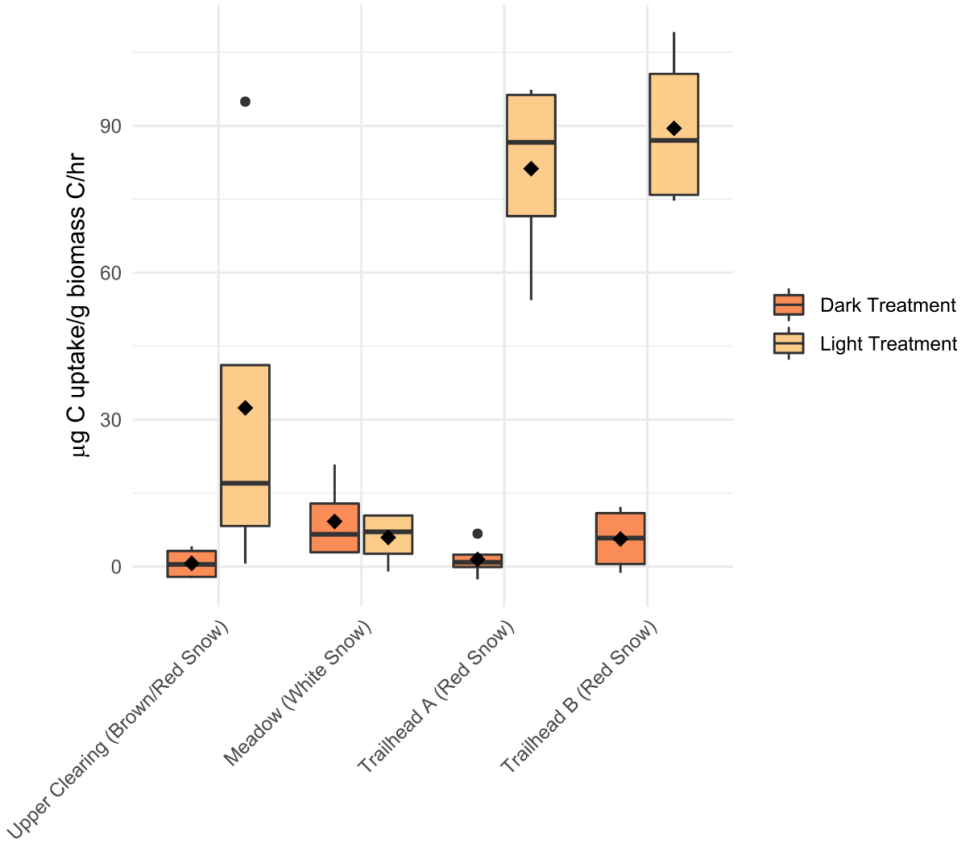


Figure 3-3. **Rates of primary productivity (µg C/g biomass C/hr) at each surface snow sample site collected in 2018.** Statistical significance between Light vs Dark treatments in both Trailhead Sites A ($p = 5.5x10^{-5}$) and B ($p = 2.6x10^{-5}$). No significance was found between Meadow (Dark vs Light) or Upper Clearing (Dark vs Light). Both Trailhead sites were significantly different from Meadow, (Light, Trailhead A $p = 1.2x10^{-4}$ and Trailhead B $p = 2.78x10^{-5}$) as well as from Upper Clearing (Light, A $p = 0.017$ and B $p = 0.003$).

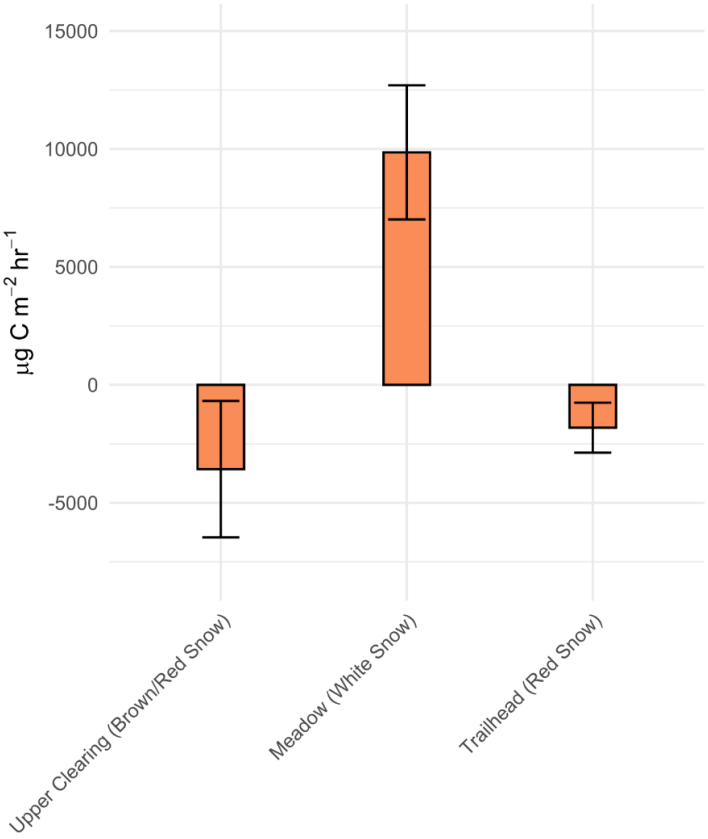


Figure 3-4. **CO_2 flux (µg/C/m^2/hr) at each site where primary productivity was measured in 2018.** CO_2 draw down (negative value) occurred in sites with higher algae abundance (Upper Clearing and Trailhead). CO_2 release (positive value) occurred at sites with little to no algae (Meadow). Algal abundance based on microscopy counts.

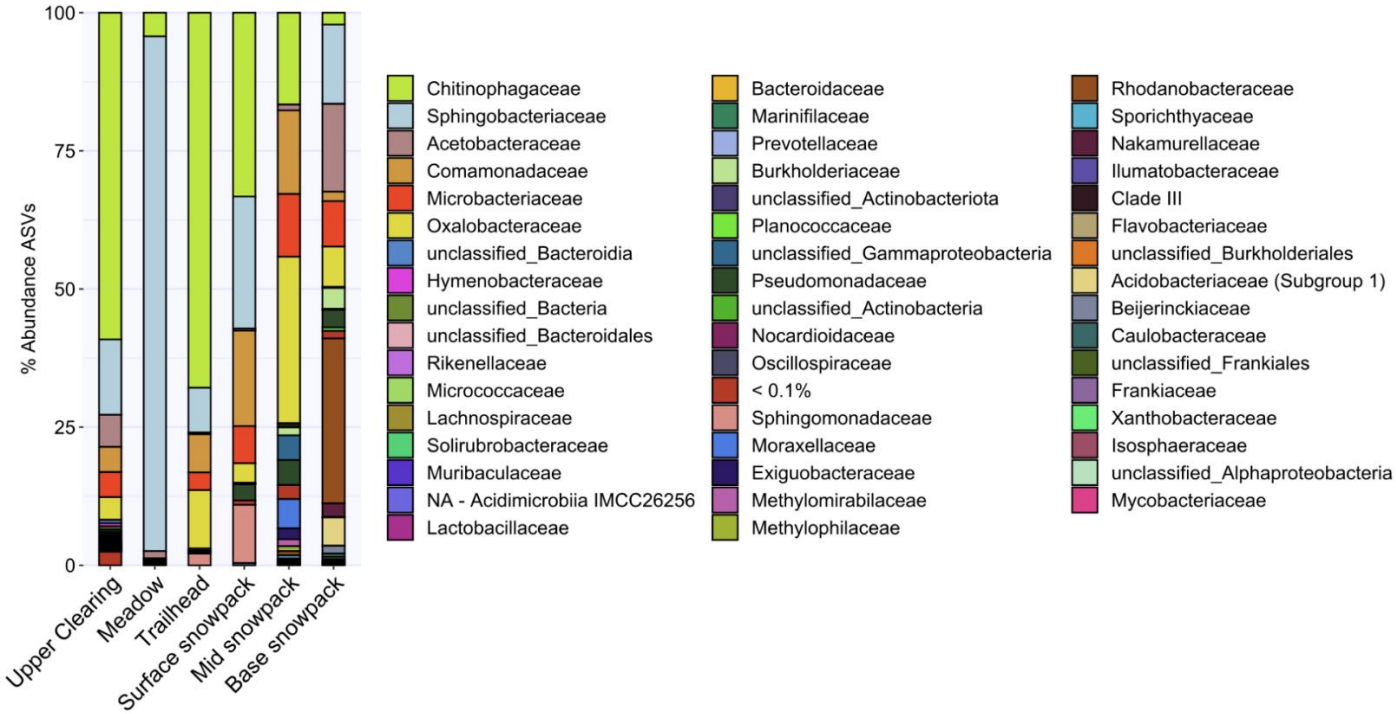


Figure 3-5. Relative abundance bar plot of Family level 16S rRNA community composition for snow samples from Mount Baker, Washington. Community structures varied across sample sites. Surface sites that had red patches of snow were Upper Clearing, Trailhead, Surface snowpack. Whereas Meadow had no visible algae on the surface snowpack, Mid snowpack was observed to have mostly green-pigmented algae, and Base snowpack had low abundances of algae that were also mostly green-pigmented.

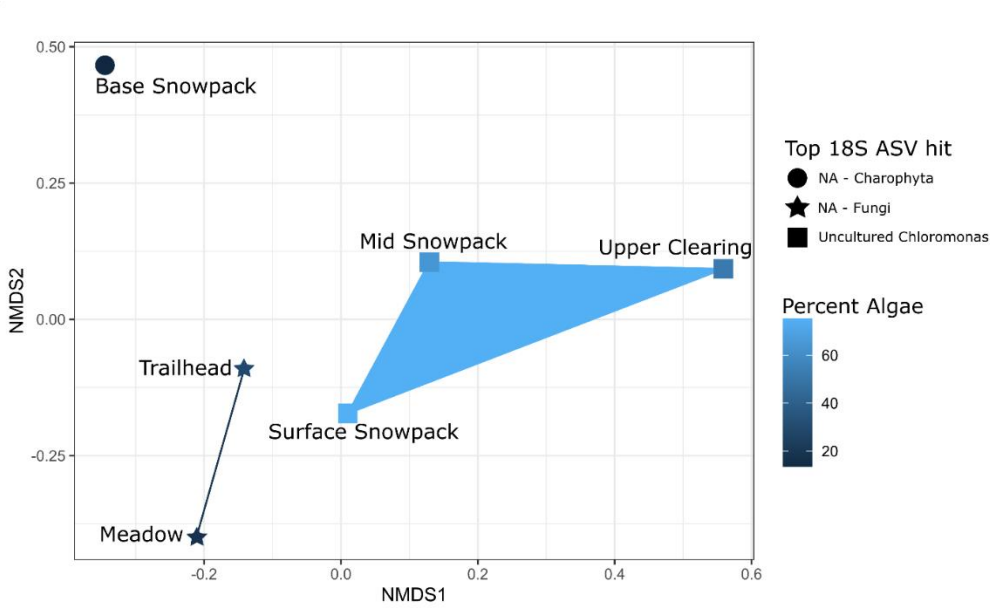
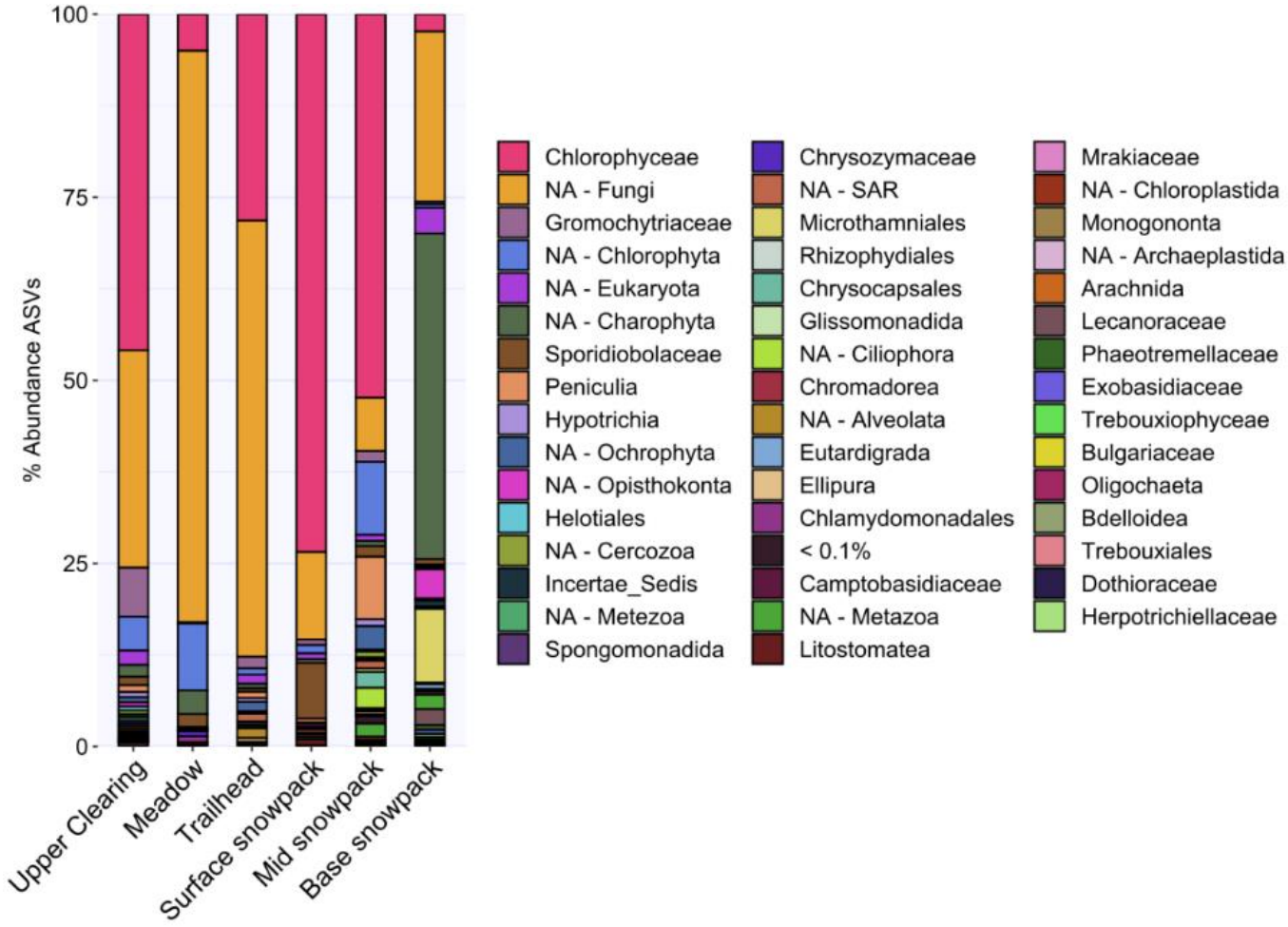


Figure 3-6. Non-Metric Multidimensional Scaling plot using Bray-Curtis dissimilarity matrix on 16S rRNA gene community composition snow samples from Mount Baker, Washington. The dissimilarity between 16S rRNA gene community composition with the relative percent of algae from the 18S rRNA community composition a variable, dark blue (low percent algae) to light blue (high percent algae). Each sample site shape represents the most abundant 18S rRNA gene Amplicon Sequence Variant (ASV). Sites with higher percentage of algae relative to fungi group together (Mid snowpack, Surface snowpack and Upper Clearing) and sites with lower percentage algae, with higher percentage of fungi, group together (Meadow and Trailhead). Base snowpack is an outlier as the top ASV was a Charophyta associated with the honeysuckle plant.

Figure 3-7. Relative abundance bar plot of family level 18S rRNA gene community composition for snow samples from Mount Baker Washington. 18S rRNA gene community composition across sample sites were similar with Chlorophyceae and Fungi as the dominant members. Base snowpack variation was due to the high abundance of Charophyta. *Chloromonas* was the most abundant genus of the Chlorophyceae family at each site. 'NA' categories are ASVs that the DADA2 workflow using the SILVA datbase could not classify and were grouped together at the lowest taxonimcal rank provided by our workflow. Supplemental table 1 provides top two BLAST hits for the top 10 fungal ASVs classified here as 'NA-Fungi' for each sample site. Supplemental table 2 provides the top two BLAST hits for the top 10 *Chloromonas* ASVs for each sample site.


100
75
50
25
0
% Abundance ASVs
Upper Clearing
Meadow
Trailhead
Surface snowpack
Mid snowpack
Base snowpack
Chlorophyceae
NA - Fungi
Gromochytriaceae
NA - Chlorophyta
NA - Eukaryota
NA - Charophyta
Sporidiobolaceae
Peniculia
Hypotrichia
NA - Ochrophyta
NA - Opisthokonta
Helotiales
NA - Cercozoa
Incertae_Sedis
NA - Metezoa
Spongomonadida
Chrysozymaceae
NA - SAR
Microthamniales
Rhizophydiales
Chrysocapsales
Glissomonadida
NA - Ciliophora
Chromadorea
NA - Alveolata
Eutardigrada
Ellipura
Chlamydomonadales
< 0.1%
Camptobasidiaceae
NA - Metazoa
Litostomatea
Mrakiaceae
NA - Chloroplastida
Monogononta
NA - Archaeplastida
Arachnida
Lecanoraceae
Phaeotremellaceae
Exobasidiaceae
Trebouxiophyceae
Bulgariaceae
Oligochaeta
Bdelloidea
Trebouxiales
Dothioraceae
Herpotrichiellaceae

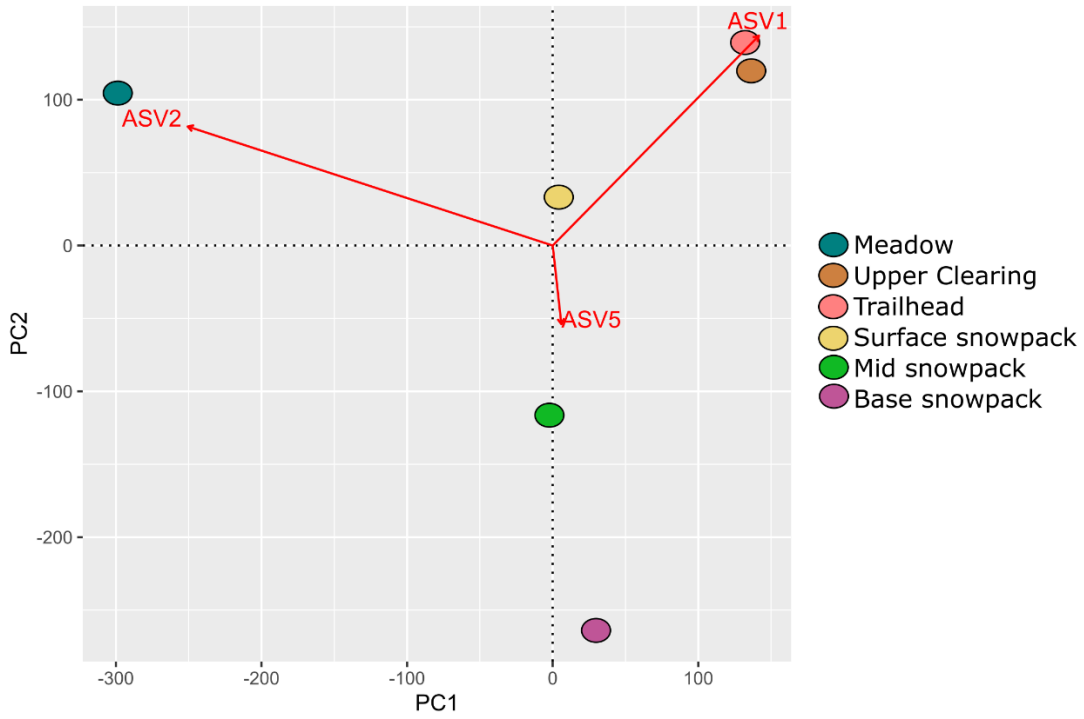


Figure 3-8. RDA Biplot of all 16S Amplicon Sequence Variants (ASVs) from each sample site. Single ASVs drove the community composition difference between sample sites. All ASVs, except for the 16S-ASV1, 16-ASV2, and 16S-ASV5, were clustered in the center of the plot and were removed from the figure. 16S-ASV2 (identified as *Solitalea*) is more present in Meadow than other sites. Whereas 16S-ASV5 (identified as *Rhodanobacter*) drove community differences in Mid and Base snowpack. 16S-ASV1 (uncultured Chitinophagacea genus) drove observed difference between Upper Clearing and Trailhead.

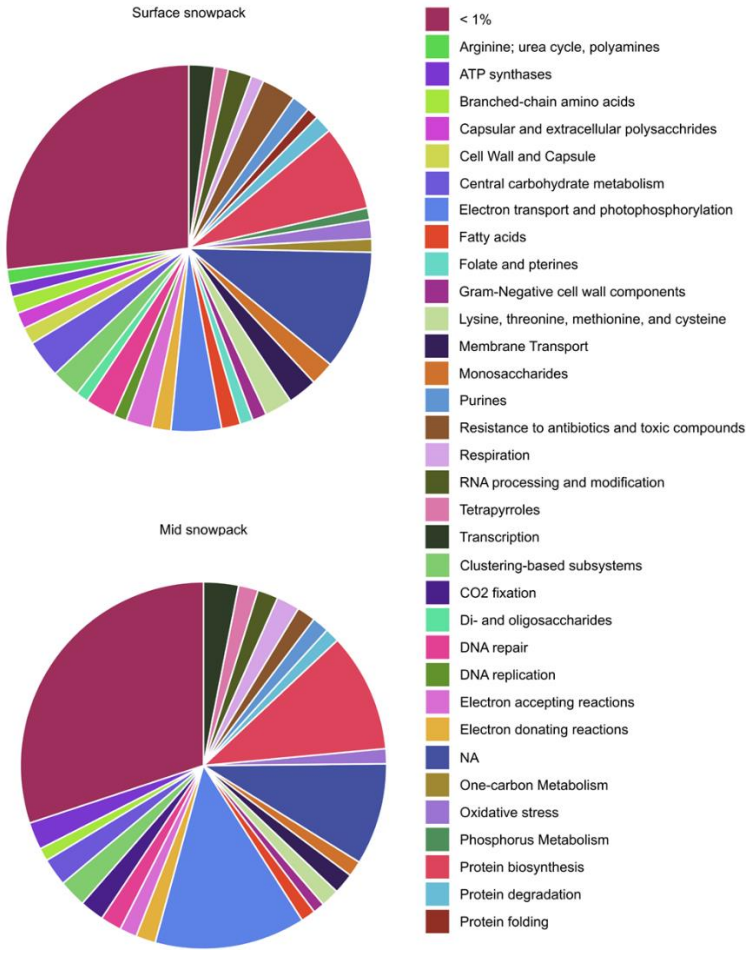
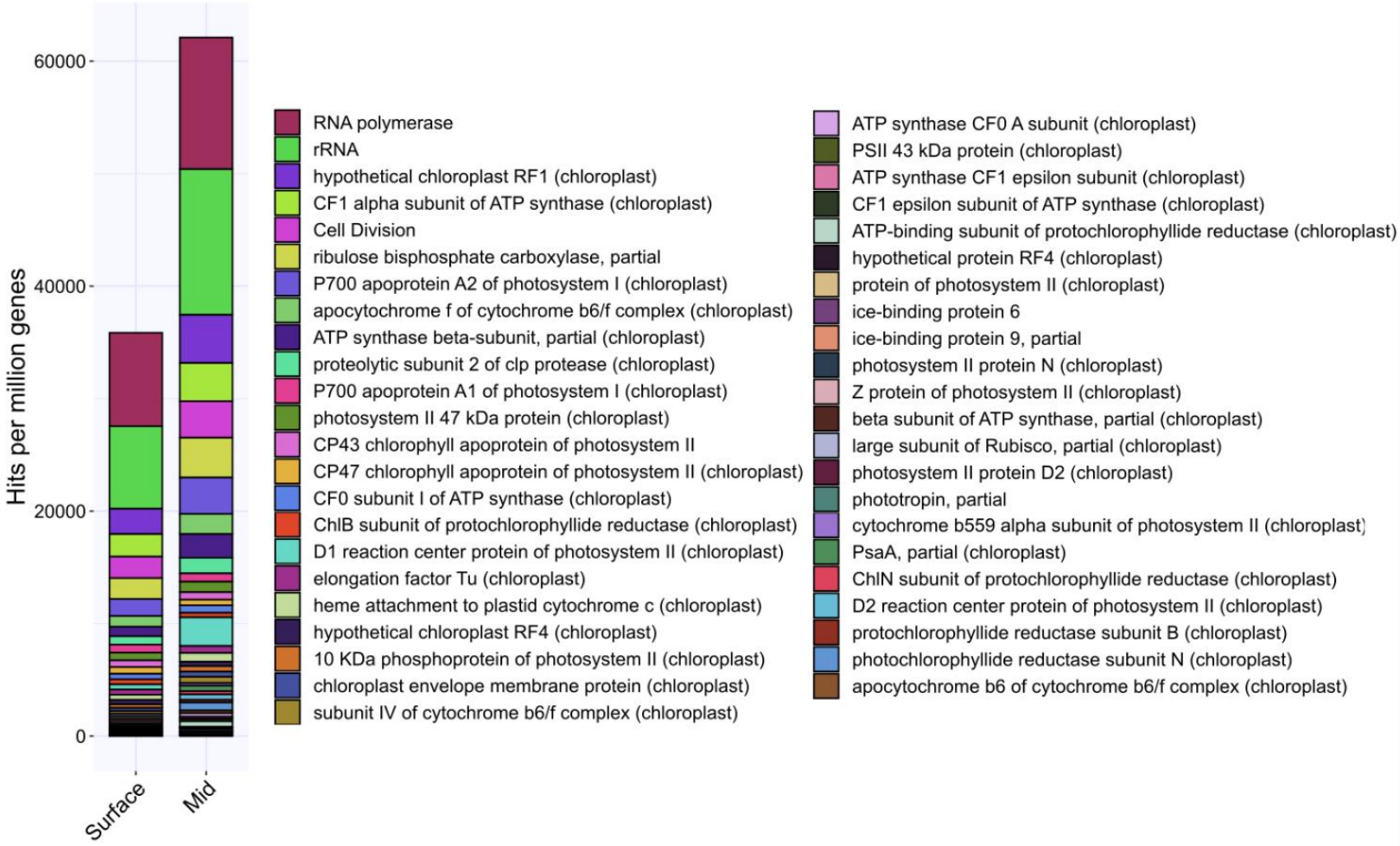


Figure 3-9. Total Surface and Mid snowpack transcript abundances. All transcripts of Surface and Mid snowpack annotated via subsystem at level 1 classification. Electron transport and photophosphorylation transcripts were more abundant in the Mid snowpack compared to the Surface snowpack. <1% transcripts are comprised of all transcript groups that individually make up <1% of the total abundance of transcripts from each site. Number of hits were normalized to account for difference in library size of each sample by dividing transcripts hits of interest by total transcripts in the library multiplied by 1 million (hits per million genes).

Figure 3-10. *Chloromonas* sp. transcripts from Surface and Mid snowpack samples on Mount Baker, Washington.

Transcripts were run against the NCBI non-redundant database, hits were sorted to Chloromonas sp. transcripts with > 40% similarity to the annotation are shown. Number of hits were normalized to account for difference in library size of each sample by dividing transcripts hits of interest by total genes transcribed in the library, multiplied by 1 million (hits per million genes). Mid snowpack had 62,103 hits per million genes for Chloromonas sp., whereas the surface had 26,244 hits per million genes less with a total of 35,859 hits per million genes. 1,998 of the total hits per million genes from the Surface belong to cytochrome b6f complex transcripts, typically associated with respiration, compared to 3,561 hits per million genes of the Mid sample. The other photosynthesis transcripts resulted in 16,302 hits per million genes in the Surface sample compared to 30,662 hits per million genes from the Mid sample.


Hits per million genes
60000
40000
20000
0
Surface
Mid
RNA polymerase
rRNA
hypothetical chloroplast RF1 (chloroplast)
CF1 alpha subunit of ATP synthase (chloroplast)
Cell Division
ribulose bisphosphate carboxylase, partial
P700 apoprotein A2 of photosystem I (chloroplast)
apocytochrome f of cytochrome b6/f complex (chloroplast)
ATP synthase beta-subunit, partial (chloroplast)
proteolytic subunit 2 of clp protease (chloroplast)
P700 apoprotein A1 of photosystem I (chloroplast)
photosystem II 47 kDa protein (chloroplast)
CP43 chlorophyll apoprotein of photosystem II
CP47 chlorophyll apoprotein of photosystem II (chloroplast)
CF0 subunit I of ATP synthase (chloroplast)
ChlB subunit of protochlorophyllide reductase (chloroplast)
D1 reaction center protein of photosystem II (chloroplast)
elongation factor Tu (chloroplast)
heme attachment to plastid cytochrome c (chloroplast)
hypothetical chloroplast RF4 (chloroplast)
10 KDa phosphoprotein of photosystem II (chloroplast)
chloroplast envelope membrane protein (chloroplast)
subunit IV of cytochrome b6/f complex (chloroplast)
ATP synthase CF0 A subunit (chloroplast)
PSII 43 kDa protein (chloroplast)
ATP synthase CF1 epsilon subunit (chloroplast)
CF1 epsilon subunit of ATP synthase (chloroplast)
ATP-binding subunit of protochlorophyllide reductase (chloroplast)
hypothetical protein RF4 (chloroplast)
protein of photosystem II (chloroplast)
ice-binding protein 6
ice-binding protein 9, partial
photosystem II protein N (chloroplast)
Z protein of photosystem II (chloroplast)
beta subunit of ATP synthase, partial (chloroplast)
large subunit of Rubisco, partial (chloroplast)
photosystem II protein D2 (chloroplast)
phototropin, partial
cytochrome b559 alpha subunit of photosystem II (chloroplast)
PsaA, partial (chloroplast)
ChlN subunit of protochlorophyllide reductase (chloroplast)
D2 reaction center protein of photosystem II (chloroplast)
protochlorophyllide reductase subunit B (chloroplast)
photochlorophyllide reductase subunit N (chloroplast)
apocytochrome b6 of cytochrome b6/f complex (chloroplast)

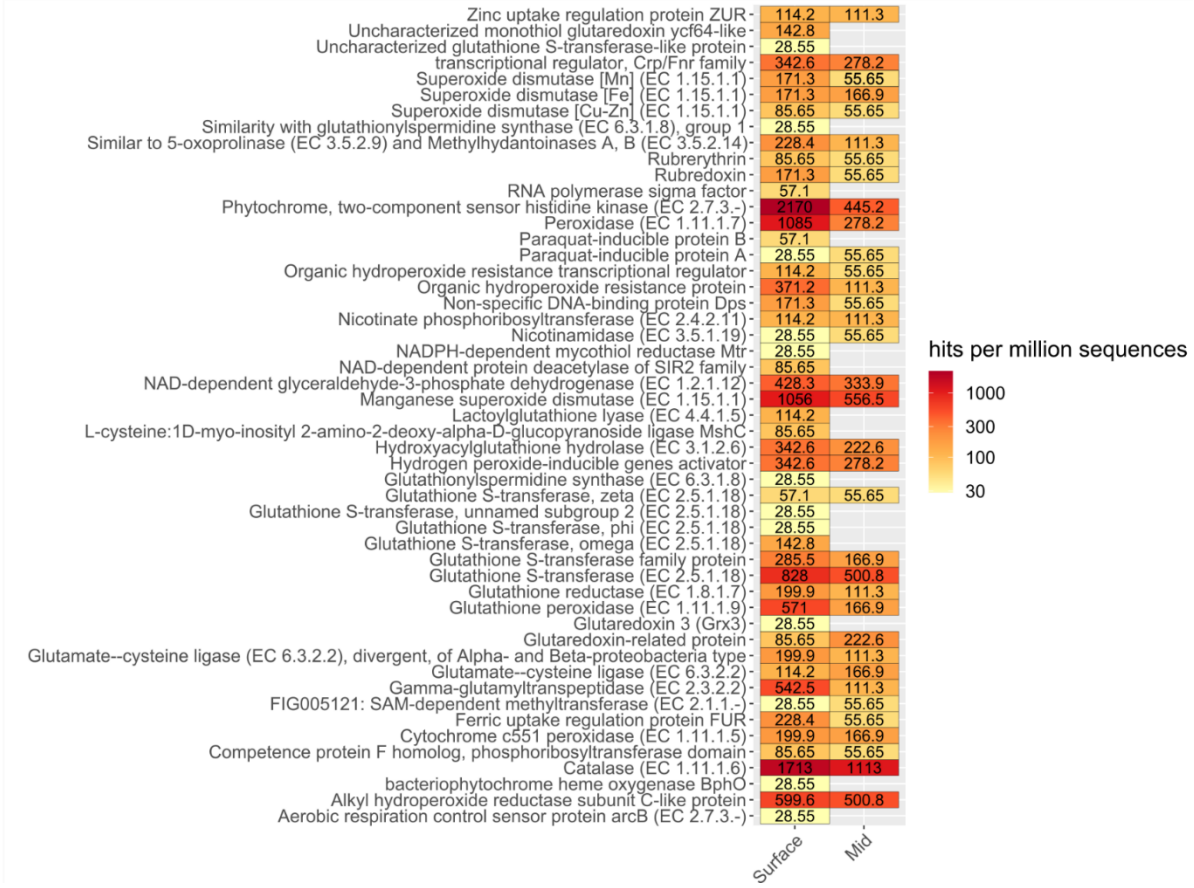


Figure 3-11. Heat map of oxidative transcripts for Surface and Mid snowpack samples. Transcripts annotated by SEED subsystem level 4. Oxidative transcripts were higher in the Surface snowpack compared to Mid snowpack.

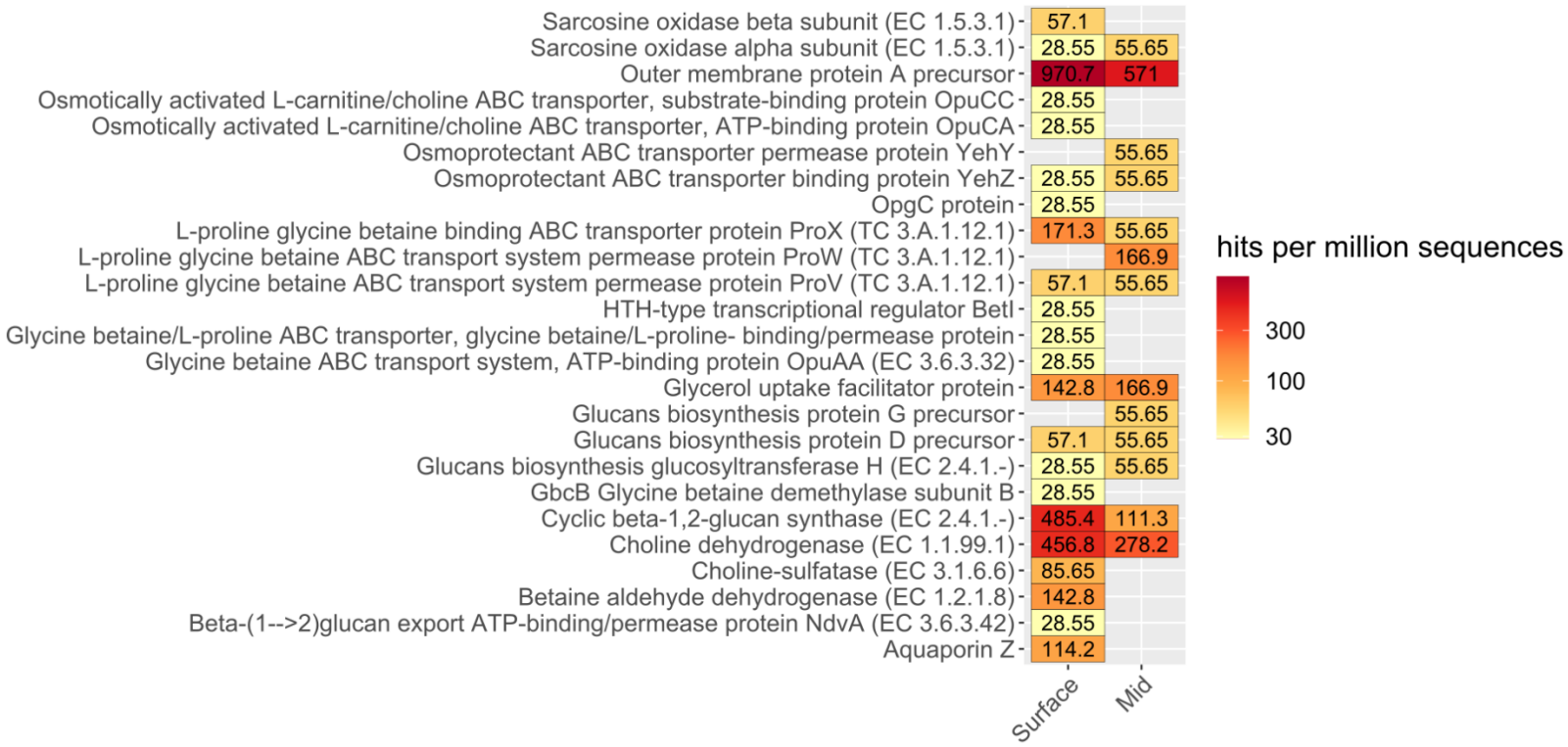


Figure 3-12. Heat map of osmotic transcripts for Surface and Mid snowpack samples. Transcripts annotated by SEED subsystem level 4**.** More osmotic transcripts were observed at the Surface than at the Mid snowpack.

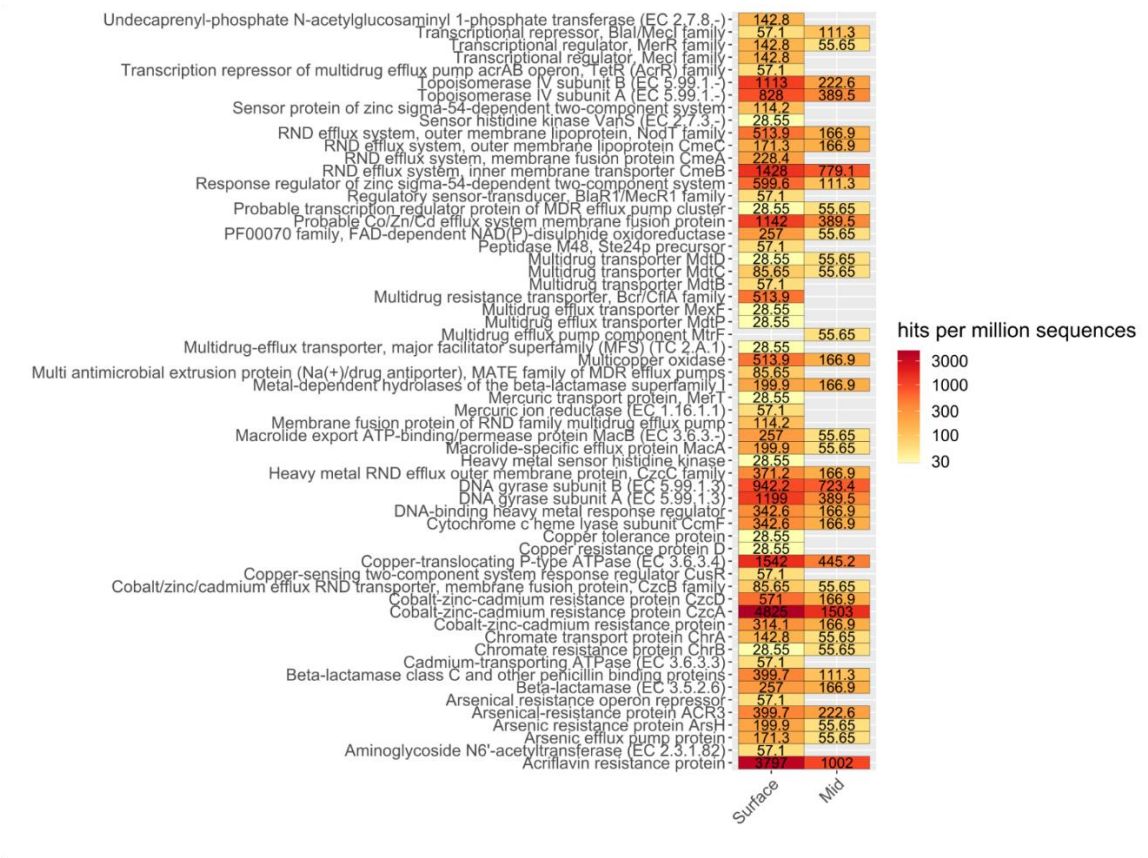


Figure 3-13. Heat map of antibiotic resistance transcripts for Surface and Mid snowpack samples. Transcripts annotated by SEED subsystem level 4. More antibiotic resistance transcripts were observed at the Surface than at the Mid snowpack.

CHAPTER FOUR

DIVERSE PHOTOTROPHIC POTENTIAL AND STRESS TOLERANCES IN AN ANTARCTIC POLYEXTREME ENVIRONMENT

Experiments and analysis were conducted by Caleb Schuler. Samples used for experiments and analysis were collected by Jill Mikucki. Caleb Schuler and Jill Mikucki wrote the manuscript.

Abstract

Hypersaline brines in high latitude polar deserts create a gradient of extreme conditions. Don Juan Pond (DJP) is a near-saturated $CaCl_2$-brine that forms in the Upper Wright Valley of the McMurdo Dry Valleys of Antarctica. This brine is currently considered the second saltiest body of liquid on our planet and forms via the discharge of a confined aquifer. The pond is situated in the proglacial basin of a rock glacier that seasonally generates freshwater melt that supports a discreet microbial mat. Microbial mats are well studied throughout the dry valleys and have been described in stream systems, ice covered lakes, and surface environments. We describe the microbial diversity of this mat and the sediment below it using 16S and 18S rRNA gene amplicon sequencing. The community composition reflected communities more common of hypersaline mats which suggests influence from the high salinity brine of DJP. Genes that encode for stress response to salt, temperature, and light were detected in metagenomes generated from mat and sediments under the mat. Ecologically relevant strains closely related to *Phormidium* (cyanobacteria) and *Chlorellales* (algae) species were enriched from the mat material. These strains could tolerate moderate $CaCl_2$ concentrations, lower temperatures, and shaded light conditions that reflect conditions observed during the austral summer and seasonal transitions at DJP. In comparing mat metagenomes from different environments, we found that the abundance of low light, red light, and blue light

harvesting protein genes were more abundant in polar environments. This analysis indicates that the microbial mat and sediment communities near DJP have the genomic potential to tolerate temperature, light conditions, and salt stressors associated with this region of the dry valleys.

Introduction

The McMurdo Dry Valleys (MDVs) represents a part of the Antarctic continent that is largely ice free (4,800 km^2; Levy, 2012). Due to the low annual precipitation this region is known as one of the driest regions on Earth (< 50 mm water equivalent factor; Fountain *et al*., 2009). The MDVs are subject to strong winds, long periods of light (October through February) when the sun does not set in the austral summer and darkness (March through September) when during the austral winter, accompanied by dramatic fluxes of temperature. For example, the mean annual air temperature at Lake Vanda in the Wright Valley is -19.5°C, but temperatures can reach as high as 10.7°C in the summer and as low as -53.7°C in the winter (Obryk *et al*., 2020). During the summer months there is 24 hours of sunlight with levels of irradiance up to 1,400 μmol m^{-2} s^{-1} (Chrismas *et al*., 2018). Whereas during the winter the only light available would be what is reflected from the moon (theoretical irradiance of .0005 to 0.005 μmol m^{-2} s^{-1}; Raven and Cockell, 2006), as well as a transitional period of twilight between seasons. Soil temperatures remain warmer than the air temperature as soil absorbs and retains heat (Obryk *et al*., 2020). Due to these distinct extreme conditions, the MDVs provides a natural laboratory to study features of polyextreme microbial adaptation and potential astrobiological implications.

Don Juan Pond (DJP) is a closed basin pond located the south fork of the Wright valley of the MDVs (Dugan *et al*., 2022; Toner *et al*., 2017). DJP has been thought to be devoid of life (Smarakin *et al.*, 2010) because of low water activity and high $CaCl_2$ concentrations (40% w/v; Harris and Cartwright 1981). The high concentrations of $CaCl_2$ enables liquid to persist year-round, even when temperatures reach well below zero (Torii *et al*., 1965). The salt concentration and surface area of the pond fluctuations due to evaporation and inputs from the aquifer below (Kato *et al*., 1978; Harris *et al*., 1979; Dickson *et al*., 2016, Dugan et al. 2022). While not directly observed during field campaigns to the pond, these fluctuations may result in the introduction of salts, including $CaCl_2$ to the microbial mat that lies along the rock glacier to the west of the pond. Phototrophs associated with the mat adjacent to DJP (herein referred to as DJP mat) were previously characterized based on morphological characteristics using microscopic techniques (Siegel *et al*., 1979, 1983, 1984). In these original studies, cyanobacteria and algae were described as filamentous Oscillatoria type cells, 'Chlorella-like cells,' Dunaliella and 'gold-yellow tetrads.' Since the 1980s no new reports on this mat or the biology of the pond itself have been published.

Microbial mats and phototrophs in the lakes and streams of the MDVs have been well studied; several surface mats (Sohm *et al*., 2020; Van Horn *et al*., 2016) and lake ice cover mats have been the topic of research for years (e.g. Greco *et al*., 2020; Hawes *et al*., 1999). Work on these mat systems have shown that organisms in mats and ice-

covered lakes tolerate desiccation (Hawes *et al*., 1992) high UV (George *et al*., 2001), low light (Morgan-Kiss *et al*., 2016; Sloughter *et al*., 2018) and low temperatures (Morgan-Kiss *et al*., 2006). A variety of microbial adaptations and mechanisms exist to deal with these stressors such as pigments and mycosporine-like amino acids production to mitigate UV stress (Cockell and Knowland 1999; Mueller *et al*., 2005), phototaxis to spatially migrate in response to light (Garcia-Pichel *et al*., 1994, Mueller *et al*., 2005), and self-shading to protect from high UV and light irradiances (Vinvent *et al*., 1993). When temperatures drop during the winter, other stress responses become important, such as osmolyte (Moore *et al*., 1987, Roser *et al*., 1992) and ice binding protein (IBP) production (Vance *et al*., 2019) that can support activity in subzero temperatures. In cases where water becomes unavailable, desiccation tolerance provided by orange carotenoid pigments (OCP) and helical carotenoid pigments (HCP) likely play a large role in survival (Yang *et al*., 2019; Melnicki *et al*., 2016). Desiccation tolerance, along with spore and cyst formation are typically identified as the key mechanism for phototrophs to survive overwinter in Antarctica (Tashyreva and Elster 2016; Holzinger and Karsten 2013; Šabacká and Elster 2006). However, if phototrophs were to remain active during the low light conditions common during seasonal transition, and perhaps into the winter, they would need adaptations that enable them to use low light irradiances.

During the polar winter, once the sun has set for the season, the only light available would be the low irradiance, red-shifted light from the moon (Ciocca and Wang 2013). Thus, in addition to the stress of winter freezing, distinct light harvesting proteins

would also be needed if phototrophs were to remain active. Examples for dealing with low light have been explored in other systems. These studies identified important adaptations such as allophycocyanin proteins adaptations for low light photoacclimation (LoLiP) and far-red light photoacclimation (FaRLiP; Gan and Bryant 2015; Gan *et al*., 2014; Olsen *et al*., 2015; Chen *et al*., 2019). Organisms that possess these antenna proteins are capable of utilizing light at wavelengths longer than 700nm (Gan and Bryant 2015). Other light harvesting mechanisms that benefit cells during low light conditions are varieties of bacteriochlorophylls (BCHL) that absorb light in the far-red and at very low levels of irradiance (0.00075 μmol m^{-2} s^{-1}; Manske *et al*., 2005). The ability to utilize these wavelengths would be beneficial in sustaining phototrophy throughout the year as high light shifts to low light, but also would enable phototrophs to reside deeper within, or under, the microbial mat to protect them from inhibitory high light irradiances during the summer

In this study we analyzed a microbial mat, and the sediment below it, via amplicon and metagenomic sequencing. A stress database was curated to identify the presence of genes that would aid organisms in tolerating polyextreme conditions, i.e., salinity, temperature, and light. We corroborated the findings of mat community structure originally observed in earlier studies of the DJP mat (Siegel *et al*., 1979, 1983, 1984) with 16S and18S rRNA gene amplicon sequencing. Community composition, in combination with the metagenomic analysis, suggests that cells within the mat can tolerate some level of salt from the adjacent hypersaline pond (DJP). We enriched for

phototrophic organisms from the DJP mat and subjected them to light and shaded environments, temperatures (4°C, 10°C and 20°C), and elevated $CaCl_2$ concentrations (0M and 0.25M $CaCl_2$). These enrichments exhibited $CaCl_2$ tolerance under a range of conditions. Collectively these data describe a community composition and metabolic potential that may support the function of phototrophic activity amidst the polyextremes of DJP and we further confirmed portions of this genetic potential in our cultures.

Methods

Sample Site and Sample Collection

The DJP mat (S77.56, E161.17) was located at the western edge of the DJP pond at the eastern terminus of a rock glacier in the MDVs of Antarctica (Figure4-1; all figures and tables are located in the appendix). The mat spans ~500 m^2 and is ~5 mm thick. The mat is inconspicuous with black/orange pigmentation which is surrounded by rocks and pebbles (Figure. 4-1, C-E). Samples were collected on 5 Dec 2018 using an individually wrapped sterile scoopula (Sterileware), with pieces of mat placed into sterile whirl-pak bags (Nasco). Once the mat was removed, sediment immediately below the mat was collected in the same way with new sterile scoopulas. Both samples were stored in a cooler during transport back to the McMurdo Station Cray Labs (~5 hours) where materials transferred to -80°C and shipped to the University of Tennessee Knoxville on dry ice and subsequently stored at -40°C until processed for DNA extraction and culturing.

Nucleic acid extraction and sequencing

Mat and sediment material (0.5 g each) were thawed and homogenized for DNA extraction using Qiagen DNeasy kit according to manufacturer's protocol with a modified bead beating step that consisted of 45 seconds at 6.6 m/s, followed by 30 seconds of rest, and an additional 45 seconds at 6.6 m/s, using the MBio fastprep24 bead beater. The extracted nucleic acid from the mat and sediment samples were sent to Novogene Corporation Inc. (Sacramento CA) for 16S and18S rRNA gene amplicon sequencing via Illumina platform PE250. V4 primers 515F and 806R were used for 16S rRNA gene sequencing (GTGCCAGCMGCCGCGGTAA, GGACTACHVGGGTWTCTAAT) and V9 primers 1380F and 1510R were used for 18S rRNA gene sequencing (CCTGCCHTTTGTACACAC, CCTTCYGCAGGTTCACCTAC).

Extracted nucleic acid from the environmental sample of mat material was prepared for metagenomic sequencing using the Nanopore field sequencing kit (SQK-LRK001) and sequenced on the Oxford Nanopore Technologies Minion (Jain *et al*., 2015) using a R9.4.1 flow cell, following manufacturers protocol. This process was completed an additional two times, with washing the flow cell between each sequencing effort using the Flow Cell Wash Kit (EXP-WSH003), following the manufacturers 'storage protocol.' In addition, a fourth nanopore sequencing effort was performed using the Rapid Sequencing Kit (SQK-RAD004), following the manufacturers protocol.

Extracted mat and sediment nucleic acid were also sent to Novogene Corporation Inc. (Sacramento CA) for metagenomic sequencing using the Illumina platform PE150.

Amplicon and metagenomic pipeline

Amplicon sequence data, both 16S and 18S rRNA amplicon sequences were processed using DADA2 pipeline v1.16 (Callahan *et al*., 2016) following default parameters using the SILVA reference database v1.38 (Quast *et al*., 2012). Further analysis was performed with phyloseq v 1.22.3 (McMurdie and Holmes 2013), and figures were made with GGPlot2 v3.3.2 (Wickham 2016) using R (v4.0.3). The top amplicon sequence variants (ASVs) that resulted in 'NA' classification were further analyzed via BLAST (Altschul *et al*., 1990) using NCBI's non-redundant database (Pruitt *et al*., 2007) to assign taxonomy.

Raw nanopore sequence data was quality filtered and cleaned using default parameters of Oxford Nanopore Technologies Guppy v3.4.4. The nanopore reads were then trimmed, with adaptors and low-quality reads were removed with Trimmomatic v0.39 (Bolger *et al*., 2014). Resulting sequences were than assembled with the Illumina reads. A hybrid assembly (mat samples only) was generated using SPAdes 3.11.0 (Nurk *et al*., 2013, Antipov *et al*., 2015) using the '–meta' flag. Raw reads were than mapped back to the assembly using Bowtie2 (Langmead and Salzberg 2012), Samtools (Li *et al*., 2009) and Anvio v5.5 (Eren *et al*., 2015) was used to make the bam sequence alignment files. Depth file and binning were completed using MetaBAT 2.12.1(Kang *et al*., 2015)

with default parameters. Bin quality was assessed using CheckM (Parks *et al*., 2015) and taxonomically classified locally using and GTDB-Tk v1.1.0 (Chaumiel *et al*., 2019) via KBASE (Arkin *et al*., 2018). Further annotation of specific bins was performed by GhostKoala (Kanehisa *et al*., 2016), and the basic local alignment search tool, BLAST (Altschul *et al*., 1990) against local databases made with proteins and genes of interest, described below. Lastly, annotation and counts of presence of primary energy metabolisms were characterized using MG-RAST KEGG Orthology (KO) outputs (Meyer *et al*., 2008; Kaneshisa and Goto 2000). This same pipeline, was used to map, assemble, bin, and annotate the sediment metagenome, however no nanopore sequences were used for the sediment assembly.

Local BLAST databases were curated to survey sequence data for the presence of specific low light and far red-light photosynthesis genes using organisms that possess these pathways exclusively (Gann and Bryant 2015). The low light allophycocyanin (LoLiP) database was generated using genes from *Gloeocapsa* sp. PCC 7428, *Xenococcus* sp. PCC 7305 and *Leptolyngbya* sp. PCC 6406. *Halomicronema hongdechloris* C2206, *Leptolyngbya* sp. JSC-1, and *Calothrix* sp. PCC 7507 were used to generate a far-red light photoacclimation (FaRLiP) and allophycocyanin database. The necessary proteins and sequences were identified using sequence annotations from Chen *et al*. (2019). Multiple cyanobacteria species were used in these databases to avoid potential database bias due to species specific proteins causing false positive hits. To investigate the presence rhodopsin and bacteriochlorophyll further BLAST databases

were curated to encompass the full range of rhodopsin and bacteriochlorophyll. Full sequence and databases can be found in supplemental material along with corresponding accession numbers (Appendix file no. 1).

A database containing stress genes was generated to assess the presence of genes involved in tolerance to elevated salt concentrations, cold to freezing temperatures, desiccation, and low and high light tolerances. These proteins and genes were pulled from several organisms with a focus on phototrophic organisms. Phototaxis (Cph1 and 2 genes; Rockwell and Lagarias 2006; Fiedler *et al*., 2005), high light inducible proteins (Hlia and CAB/ELIP/HLIP gene family; Komenda and Sobotka 2016), scytonemin proteins (ScyA though ScyF genes; Soule *et al*., 2009), desiccation tolerance genes (OCP and HCP1 through HCP9 genes; (Solinmskiy *et al*., 2019), mycosporine-like amino acids (MysA though MySD genes; Miyamoto *et al*., 2014), UV-B photoreceptor (Tillbrook *et al*., 2016), IBP (DUF3494, IBP1-11 and IBP0 genes; Raymond 2014; Raymond *et al*., 2007), and salt tolerance (cyclophilin, spermidine synthase, protein disulfide isomerase, F-box protein Skip 5 and GG synthase genes; Chen *et al*., 2007; Liu *et al*., 2015; Marin *et al*., 1998). Hits to the database were identified as orthologs if the e-values were $< 1x10^{-10}$ and the percent identities were > 40% (Pearson 2014). In cases where query sequences resulted in multiple hits, the query sequence that resulted in the lowest e-value and highest percent identity was selected as the best result. The full databases can be found in supplemental material.

The gene hits for metagenomes were further annotated using the protocol described by Pound *et al*. (2020). Top BLAST hit sequences were extracted (Gann *et al*., 2019) and ran against the NCBI non-redundant database using Diamond (Buchfink *et al*., 2015) to identify the taxonomic origin of the sequences and further classify hits as belonging to phototrophic or non-phototrophic organisms. A cross environmental metagenome comparison was conducted to compare the relative abundance of light harvesting genes (allophycocyanin, phycocyanin, phycoerythrin, FaRLiP/LoLiP, rhodopsin and BCHL genes). The above curated databases generated in this study were used for the comparison with other environmental metagenomes. Top hits were selected as previously described. Furthermore, the top hit results for each gene were visually inspected to ensure no query sequence was counted twice during our analysis. The environmental metagenomes were selected based on the following criteria: they were mats from polyextreme environments and those environments had extreme stressors (light, temp, and salinity) similar to those at DJP. Published metagenomes used for this analysis can be found in Table 4-1.

Cultures and Enrichments

Raw mat material was thawed and placed in 250 ml autoclaved Erlenmeyer flasks containing BG-11 media with sterile sand (ethanol rinsed and autoclaved), to mimic the natural matrix the DJP mat grows on. Cultures were grown at room temp (~20°C) and at ~15 µmol m^{-2} s^{-1} irradiance. A variety of morphologies and pigments were observed, and discrete pigmented biomass was selected for further isolation and transferred to fresh flasks containing BG-11 (Figure. 4-2). Biomass was selected from specific areas of

cultures flasks, i.e., bottom of flask under the sand, for collection into fresh BG-11 media (Figure. 4-3, A &B). Cultures were grown over a period of 6 to 12 months and when sufficient biomass was observed, samples were extracted for 16S and 18S rRNA gene analysis following the DNA extraction and analysis methods described above. Cultures identified via sequencing were transferred into 5 ml culture tubes with 2 ml of BG-11, for challenge experiments. Starting biomass of the cultures were normalized to start near the limit of detection the Turner Trilogy Fluorometer (product no. 998-7210) chlorophyll-a module (~ 100 RFUs). Cultures were all grown in triplicate (biological replicates) in each combination of light, salt, and temperature under the following conditions: shaded (0.5 µmol m^{-2} s^{-1} irradiance), light (50 µmol m^{-2} s^{-1}irradiance), $CaCl_2$ concentrations (0M $CaCl_2$ and 0.25M $CaCl_2$) and temperature (4°C, 10°C, and 20°C). Each culture was grown the same distance from the light source; irradiance for the shaded treatment was reduced by layering screening around the cultures. A pilot study (data not shown) indicated growth of phototrophic cultures in $CaCl_2$ concentrations up to 0.25M but not higher, thus setting the upper limit of $CaCl_2$ for the experiments. Temperature and light irradiance were monitored throughout the entirety of the experiments using temperature loggers and a LI-COR LI-250A light meter with LI-190R quantum sensor. Chlorophyll-a measurements were taken daily (minimum n=3 for each condition) to track culture growth over 31 days, excluding weekends. Controls for each condition with no cyanobacteria or algae inoculant were incubated and monitored with treatments throughout the entirety of each experiment to ensure no condition, or combination of conditions caused false positive chlorophyll readings.

Results

Community Composition

A total of 82,785,356 quality filtered Illumina reads and 21,661 quality filtered nanopore reads were used to construct a final DJP mat metagenome which contained 3,047,584 contigs and 1,508,891,192 bases with an average contig length of 495 bases. The quality filtered metagenome for the sediment beneath the mat was constructed of 4,179,546 contigs and 1,742,152,463 bases with an average contig length of 416 bases. Post processing and QC of mat amplicon sequence data resulted in 123,043 16S rRNA gene sequences and 198,514 18S rRNA gene sequences. Sediment amplicon sequencing resulted in 142,163 16S rRNA gene sequences and 200,339 18S rRNA gene sequences. Enrichment culture amplicon sequencing resulted in 83,357 16S rRNA gene sequences and 125,061 18S rRNA gene sequences for the *Phormidium* culture, and 107,169 16S rRNA gene sequences and 153,788 18S rRNA gene sequences for the *Chlorellales* culture. Culture results are detailed below.

The 16S rRNA gene ASVs detected in the DJP mat were comprised of 23 phyla with the top 5 most abundant phyla related to Cyanobacteria (24.5%), Bacteriodota (18.7%), Proteobacteria (18%), Bacteria not assigned by the DADA2 workflow (NA_Bacteria; 14.4%) and Chloroflexi (12.4%). The remaining phyla (18 total) made up 12% of the total ASVs (Figure. 4-4, A). The mat was dominated by two genera that made up 26% of all genera (Figure. 4-4 B), NA_Bacteria (16S-ASV-8; 14.4% of all genera) and *Leptolyngbyaceae LB3-76* (12.6% of all genera). The 16S-ASV-8 ASV was

identified to be most similar to ‘Uncultured bacteria clone UOXB-e03’ (via BLAST) which was associated with the Upper Onyx River, an ephemeral desert stream within the Wright Valley of the MDVs (Zeglin *et al*., 2011). The next most abundant ASVs belonged to *Tychonema CCAP* 1459-11B (6.5%), *Candidatus Chloroploca* (5.8%), NA_Cytophagales (16S-ASV-13; 5.1%) and NA_SBR1031 A4b (16S-ASV-38; 4.1%). The 16S-ASV-13 ASV was identified via BLAST and was most similar to ‘Uncultured bacterium clone 643’ from biofilms of river floodplains (Peipoch *et* al., 2015). The 16S-ASV-38 ASV was most similar to ‘Uncultured bacterium clone 1234’ which is associated with Antarctic mats from King George Island Antarctica (accession no. KX703284).

The sediment directly below the mat was comprised of 33 phyla with the top 5 phyla consisting of Proteobacteria (27.2%), Chloroflexi (15.2%), Bacteriodota (14.3%), Actinobacteriota (12.5%) and Cyanobacteria (6.1%). The other 28 phyla made up 24.7% of the ASVs (Figure. 4-4, A). The sediment was not dominated by any single genera, the most abundant genera was *Candidatus Chloroploca* (5.6%), followed by *Chryseolinea* (4.5%), NA_SBR1031 A4b (ASV-36; 3 %), *Pseudofulvimonas* (2.3%), and NA_Ardenticatenaceae (16S-ASV-26; 2.2%, Figure. 4-4, B). The 16S-ASV-26 was identified via BLAST as being most similar to ‘Uncultured bacterium clone 1A-E9FB4,’ a clone from microbial communities associated with quartz rocks in Miers Valley Antarctica (Khan *et al*., 2011).

The 18S rRNA gene ASVs detected in the mat were comprised of 7 phyla with Opisthokonta (41%), SAR (35.1%), and Archaeplastida (12.4%) making up the majority of the ASVs, and non-assigned (NA), Amoebozoa, Excavata, and Centrohelida comprising the remainder of the ASVs (11.5% combined; Figure 4-5A). The 18S ASV genera for the mat were dominated by NA_Bdelloidea (18S-ASV-2; 34.2%), Oxytrichidae (22.2%), uncultured_eukaryote_Ulvophyceae (18S-ASV-6; 12.3%) and NA_Eukaryota (18S-ASV-9 majority of ASVs; 7.8%; Figure 4-5 B).

The sediment had a similar Eukaryotic phyla composition to that of the mat, SAR (37.1%), Opisthokonta (30.5%), and Archaeplastida (15.9%) making up the majority of the phyla ASVs, with not assigned (NA), Amoebozoa, Excavata, Centrohelida, and Incertae sedis totaling out the remainder of the ASVs (16.4% combined; Figure 4-5 A). The sediment 18S genera composition was also similar to that of the mat and consisted of Oxytrichidae (21.6%), NA_Bdelloidea (18S-ASV-2; 18.4%), uncultured_eukaryote_Ulvophyceae (18S-ASV-6; 15.5%) and NA_Eukaryota (18S-ASV-9 majority of ASVs; 10.5%; Figure. 4-5 B). The 18S-ASV-2 was most similar to as *Rotaria tardigrada* (accession number KF561105) and *Adineta vaga* (accession number KF561095.1; both 100% identity. 100% query cover, and $2x10^{-65}$ e-value). The 18S-ASV-6 was most similar to *Cf. Chlorothrix sp. NN-4-1-M*, green algae from highly saline potash piles (accession number MT991537; Sommer *et al*., 2020). Lastly, 18S-ASV-9 was most similar to *Chlorococcum microstigmatum* (accession number MT425946) via BLAST.

Recovery of phototrophic classified metagenomic assembled genomes (MAGs)

Binning of metagenomic reads from the DJP mat resulted in the recovery of 84 metagenomic assembled genomes (MAGs), of which 20 were >90% completion with < 10% redundancy and considered high quality. Of these 20 high quality MAGs, 6 were taxonomically classified as organisms known for phototrophy. Out of the remaining 64 MAGs, 7 quality bins were classified as organisms associated with phototrophy and were identified as good quality MAGs (>70% completeness with <10% redundancy). MAG cut offs for high quality and good quality were selected by following previous guidelines by Parks *et al*., 2015. These 13 phototrophic MAGs were comprised of Chloroflexi (7 MAGs), Rhodobacteraceae (2 MAGs), and Cyanobacteria (4 MAGs; Appendix table no. 5). Binning of metagenomic reads from the sediment resulted in the recovery of 55 MAGs, of which 10 were >90% completion with <10% redundancy and considered high quality. Of these 10 high quality MAGs, 4 were taxonomically classified as phototrophic organisms. Out of the remaining 45 MAGs, 4 quality MAGs were identified as photosynthetic organism, these MAGs were >70% complete and <10% redundancy. The 8 MAGS from the sediment that were classified as organisms that perform phototrophy, were Chloroflexi (4 MAGs), Rhodobacteraceae (1 MAG), and Cyanobacteria (3 MAGs; Appendix table no. 6). Out of the total 139 MAGs from both data sets 45 were unique (taxonomical classification was only found in either the mat or sediment data set), 18 MAGs from the sediment and 27 from the mat. None of the MAG classifications (via GTBD) were similar the 16S rRNA identification of the *Phormidium* culture.

Light harvesting gene abundances

Metagenomes from the DJP mat sediment had 881 and 663 hits respectively to light harvesting protein genes. When normalized to the metagenome size (hits per million genes) the mat had 289.1 hits per million genes and the sediment had 158.9 hits per million genes (Figure. 4-6). Direct comparison of LoLiP and FaRLiP ortholog genes in the assembled metagenome of the mat resulted in a lower abundance of LoLiP specific genes (apcD, apcB) with 30 hits, when compared to the same allophycocyanin ortholog genes for FaRLiP, 42 hits. Similarly, the sediment metagenome had more FaRLiP (31) genes than LoLiP (28). Both the mat and sediment had less allophycocyanin (60 mat hits and 43 sediment hits), than phycocyanin (97 mat hits and 88 sediment hits), and phycoerythrin (60 mat hits and 57 sediment hits). In total the mat had 289 antenna protein hits and the sediment had 247 hits. The mat and sediment both had less rhodopsin hits (166 mat hits and 124 sediment hits) than any other group of light harvesting genes. Whereas bacteriochlorophyll was the most abundant of all light harvesting gene groups (BCHL; 426 mat hits and 292 sediment hits). Rhodopsin abundances were broken down into four categories, blue-light (23 mat hits; 11 sediment hits), xanthorhodopsin (115 mat hits; 101 sediment hits), green-light (27 mat hits; 7 sediment hits), the DJP mat had 1 hit to the Halobacterium brp gene. BCHL genes were separated into categories of type, BCHL A through G. BCHL A (79 mat hits; 115 sediment hits) and B (236 mat hits; 96 sediment hits) were the most abundant BCHLs. BCHL C was the next most abundant for both normal BCHL C (43 mat hits; 30 sediment hits) and BCHL C low light specific (6 mat hits; 12 sediment hits). There were no BCHL D hits for either the mat or sediment,

and BCHL E (8 mat hits; 3 sediment hits), BCHL F (13 mat hits; 5 sediment hits) and BCHL G (41 mat hits; 31 sediment hits) comprised the rest of the BCHL genes detected.

Assembled metagenomes from Arctic, Antarctic, hypersaline and hot spring environments (total of 11 of metagenomes) were queried for the photoantenna proteins, rhodopsin, and BCHL using our databases to compare relative abundances of these genes between locales. Samples from polar regions had a significantly higher abundance of FaRLiP genes compared to non-polar environments (t-test, $p = 0.003$; Figure. 4-7, A), with Antarctic sites not being significantly different from Arctic sites, but significantly different from the polyextreme hot spring and hypersaline sites (Anova, $p = 0.0075$; Figure. 4-7, B). More genes that code for phycocyanin proteins were found in hot spring environments (total relative % abundance of light harvesting genes; Anova, $p = 0.00012$) and for normalized data sets (hits per million genes; Anova, $p = 0.039$). Polar Regions also had significantly higher abundances of blue-light rhodopsin (% relative abundance of rhodopsin genes; t-test, $p = 0.0043$, Figure. 4-7, C) and significantly higher hits per million genes compared to nonpolar regions (t-test, $p = 0.0082$). Furthermore, green-light rhodopsins were also significantly higher in polar environments, hits per million genes (t-test, $p = 0.031$), but not when compared at a relative percent abundance of all rhodopsin genes in each metagenome. No other significant differences were identified from the rhodopsin analysis. There were significantly more BCHL B genes in the polar environment samples than non-polar (relative % abundance BCHL genes in each metagenome; t-test, $p = 0.0041$), however no significant difference was observed when

analyzed as hits per million genes in each metagenome (Figure. 4-7 D). There were significantly more BCHL C gene hits (relative % percent abundance of total BCHL genes) in hot spring samples compared to all other samples (Anova, $p=3.3x10^{-5}$), and hits per million gene hits in each metagenome (Anova, p=0.013).

Total metagenome stress database hits

A total of 2,166 hits were identified in the stress database for the mat (711 hits per million genes), and 2,603 hits for the sediment (623 hits per million genes). Both samples contained ice-binding protein genes (mat = 382 hits, sediment =407 hits). These hits mostly belonged to non-phototrophic organisms (99% mat hits and 97.5% sediment hits; Figure. 4-8). Scytonemin proteins A through D were primarily found in non-phototrophic organisms, 224 of the total hits 230 in the mat (97.4% hits) and 324 hits of the 245 hits in sediment (93.9% hits). Mycosporine-like amino acids gene hits (1,021 total mat hits, 1,298 total sediment hits) belonged to a variety of phototrophic organisms however the majority of hits belonged to non-phototrophic organisms (837 mat hits at 82% of all MAA and 1,040 sediment hits at 80.1% of all MAA; Figure. 4-8). Only one specific UV-B photoreceptor protein was in our database and this gene yielded 45 hits in the mat and 54 in the sediment, again non-phototrophic organisms made up the majority of the hits (40 mat hits at 88.9% and 46 sediment hits at 85.2%). High light inducible proteins genes were only found in phototrophic organisms (43 total hits in mat and 23 total hits in the sediment). There was a total of 49 desiccation tolerance genes in the mat and 36 in the sediment, all of which hit to phototrophic organisms. Lastly, salt tolerance genes were

mostly found in non-phototrophic organisms, a total of 396 hits in the mat (362 non-phototrophic made up 91.4% of the hits) and 440 total hits in the sediment with 374 hits belonging to non-phototrophic organisms (85% of salt tolerance hits).

Phototroph enrichments

Mat material grown in BG-11 resulted in several morphologies (Figure 4-2) including green pigmented enrichments (which included algae and cyanobacteria) that grew at the base of the sand, rather than colonizing the surface of the sand. These areas of the cultures were targeted for further isolation (Figure. 4-3). Cultures were non-axenic and amplicon sequencing was used to identify the primary organism in each culture. The culture amplicon sequences were processed using the same DADA2 and SILVA pipeline as the environmental samples, resulting in 100% match between ASVs shared across cultures and environmental samples. Thus, the ASVs identified in the cultures were 100% match to the environmental sample ASVs that shared the same genus/species classification. ASVs from these cultures revealed the primary phototrophic organisms as *Phormidium* sp. CYN64 (41.1% of this cultures 16S ASVs and 98.7% of the cultures cyanobacteria ASVs, Figure. 4-3, C & E). The second enrichment was classified as *Chlorellales* sp. LH10HG2094 (99.9% of this cultures 18S ASVs, Figure. 4-3, D & F). These cultures are herein referred to by their lab strain identifier (the culture with sequence identity closest to *Phormidium* sp. CYN64 culture is referred to as lab strain DJPM_C1 and the culture with sequence identity closest to *Chlorellales* sp. LH10HG2094 culture is referred to as lab strain DJPM_E1). ASVs identified as

Phormidium sp. CYN64 made up 0.4% of all ASVs in the DJP mat and 1.2% of the cyanobacteria ASVs. Whereas *Phormidium* sp. CYN64 accounted for 1.2% of all ASVs in the sediment and 24.9% of the cyanobacteria ASVs in the sediment. ASVs identified as *Chlorellales* sp. LH10HG2094 comprised of less than 0.01% of all ASVs (mat = 0.007%, sediment = 0.005%) and less than 0.06% of Achaeplastida ASVs for the mat (0.05%) and the sediment (0.03%).

DJPM_C1 grew to its highest concentrations of CHLa at 20°C temperature in a shaded environment (0.5 µmol m^{-2} s^{-1}irradiance) with no added $CaCl_2$. DJPM_C1 also tolerated $CaCl_2$ (0.25M), but only when grown in shade below 20°C; DJPM_C1 did not have sustained growth at 50 µmol m^{-2} s^{-1} irradiance with 0.25M of $CaCl_2$. DJPM_C1 culture tolerated both light conditions in all temperatures (4°C, 10°C, and 20°C) but grew to higher CHLa concentrations when shaded. Eukaryotic algal strain DJPM_E1 grew to its highest concentration at 20°C in 50 µmol m^{-2} s^{1} irradiance with no $CaCl_2$. DJPM_E1 did not tolerate 4°C with 50 µmol m^{-2} s^{-1} irradiance (with and without $CaCl_2$) or 10°C with 50 µmol m^{-2} s^{-1} irradiance plus the addition of 0.25M $CaCl_2$. Only when grown at 4°C did DJPM_E1 prefer (grew to higher concentrations than the other conditions at 4°C) $CaCl_2$ and shade. However much lower growth was observed compared to same treatments at 20°C. (Tables 4-5, 4-6; Figures 4-9, 4-10, & 4-11).

Discussion

Comparison of community composition to other studies

Historical microscopy studies conducted by Siegel *et al*. (1979) described a dense mat that consisted primarily of *Oscillatoria* and *Gloeocapsa* types of cyanobacteria, and eukaryotes the included Chlorella and Tardigrada (Siegel *et al*., 1979). A high abundance of the *Leptolyngbya* genera (51% of all cyanobacteria ASVs) and *Tychonema* genera (26% of all cyanobacteria ASVs) were observed in our amplicon data. Both genera are morphologically similar to filamentous cyanobacteria observed by Siegel *et al*. (1979). We also observed eukaryotic sequences including, tardigrades and several eukaryotic algae that were consistent with what Siegel *et al.* (1979) described. Furthermore, we observed similar morphologies as reported by Siegel *et al.* (1979) in our enrichment cultures (Figure. 4-2). Collectively these data suggest the microbial community observed in the mat may be stable and has persisted for at least 50 years.

The DJP mat community observed in this study is similar in composition to that of other mats in Antarctica as the most abundant phototrophic organisms were filamentous and predominately Oscillatoria. However, the lack of Nostoc sets the DJP mat apart from other mats observed in the MDVs (Taton *et al*., 2003; Tytgat *et al*., 2014; Van Horn *et al*., 2016). Studies of Antarctic mats report high abundance of Nostoc, including members of the *Pseudanabaenaceae* genera in black colored mats (Van Horn *et al*., 2016), however, no *Pseudanabaenaceae* ASVs were detected in the DJP mat. The DJP mat community was more similar to MDV stream sediments sampled in Van Horn *et*

al., (2016) in which the cyanobacteria in the samples comprised ~26 % of the abundance and were not dominated by any single genera. The phototrophic community detected in the DJP mat was also similar to the Guerrero Negro hypersaline mat with the predominant genera members of *Microcoleus*, *Oscillatoria*, *Lyngbya*, *Gloeocapsa*, and *Phormidium*, (Preito-Barajas *et al*., 2018). However, the majority of the phototrophs in Guerrero Negro were Chloroflexi with a notable presence of Nostoc (Ley *et al*., 2006). Nostoc is typically found in fresh water and terrestrial systems, with the exception of Calothrix, and are often the primary nitrogen fixing organisms in these microbial mats (Stal 2002). In the DJP mat, *Leptolyngbya* rather than Nostoc genera was the most abundant known nitrogen fixer. A possible explanation for the lack of Nostoc in the DJP mat is due to potential influence from the DJP brine. Species of Nostoc, such as *N. commune*, cannot tolerate NaCl over 0.2M, and shut down photosynthesis in efforts to survive (Sakamoto *et al*., 2009; Sand-Jensen and Jespersen 2012). Thus, the proximity to the hypersaline DJP brine may influence selective pressures on the mat community. Although we did not find any reports on Nostoc $CaCl_2$ tolerance.

The sediment directly below the DJP mat differed from the mat proper as it was not dominated by any single genus, and furthermore Chloroflexi, rather than Cyanobacteria, accounted for the majority of phototrophic associated ASVs. The most abundant bacteria genera in the sediment are common in a range of diverse environments. For example, representatives of the most abundant sediment genera are typically found in soil (*Chryseolinea;* De Corato 2020) but have also been found in basic soils around soda

lakes and within hypersaline mats (*Candidatus Chloroploca;* Gorlenko *et al*., 2014); these genera are also not uncommon in hypolithic polar environments (*NA_ Ardenticatenaceae; Khan* et al., 2011), and some members have been described as polar psychrophiles (*Polaromonas*; Gawor *et al*., 2016). The cyanobacteria of the sediment were similar to those within the DJP mat, the genus *LB3-76* of the Leptolyngbyaceae family accounted for 25% of the cyanobacteria sediment ASVs, and *Phormidium* sp. *CYN64* accounted for another 24%. The *Phormidium* sp. *CYN64* ASVs were complete matches to the ASV of our cyanobacteria in culture (DJPM_C1). The eukaryotic community composition of the sediment contained a high abundance of rotifers (Bdelloidea, *Rotaira* and *Adenita*) and tardigrades (*Oxytrichidae*) common to Antarctica (Sommers *et* al., 2019; Velasco-Castrillón *et a.,* 2018*;* Kagoshima *et al*., 2013). The prominent algae from the sediment were *Chlorothrix,* which have been found in other hypersaline environments (Sommer et al., 2020). While the hydrology of the pond remains poorly documented, detailed observations during the 60s and 70s (Torii & Ossaka1965; Torii *et* al., 1977; Kato *et al*., 1978) and previous observations using time-lapse photography (Dickson *et al*., 2016) show pond level fluctuations with the overall surface area of the pond expanding and contracting on seasonal time scales. Thus, both historic observations and the observed community structure that is dominated by genera common to other hypersaline environments, supports the notion that the hypersaline brine of DJP may interact with the mat.

MAGs recovered from the metagenomic data provided further insight into the diversity of phototrophic organisms found within the mat. These MAGs are referred to at the highest taxonomical identification provided by Genome Database Taxonomy (GTDB-Tk v1.1.0; Chaumiel *et al*., 2019). Several of the phototrophic MAGs are commonly found in environments that have similar conditions to DJP. For example, DJP MAGs were identified as related to organisms commonly found in marine environments such as, Elainallaceae family cyanobacteria (DJP mat MAG 9), *Microcoleus* genus (mat MAG 7), and an Anaerolineae class chloroflexi (DJP mat MAG 11; Waterworth *et al*., 2019). One MAG (DJP mat MAG 75) was classified as *Trabizicola*, which is common in freshwater environments (Tarhiz *et al*., 2013). MAGs were also classified as organisms commonly found in cryosphere environments for example, DJP mat MAG 27 (classified as *P. priestleyi*), and DJP mat MAG 1, a Letptolyngbyaceae family cyanobacteria which are found in arctic cryoconite holes and in the MDVs (Chrismas *et al*., 2016). The original description of the DJP mat indicated the presence of precipitated calcium carbonate the expected portion of saturated $CaCl_{2,}$ and 327,000 ppm total salts (32.7% of the total dissolved material) within the mat (Seigel et al., 1979). The presence of ASVs and MAGs common to marine systems, though are NaCl salts, also indicates that mat populations may be able to tolerate higher solute concentrations. The DJP mat is in direct contact with the freshwater melt channels of the rock glacier thus the presence of common freshwater organisms is not surprising. However, the numerous salt-tolerant species suggests a possible, if sporadic interaction with the hypersaline DJP brine.

Ecologically Relevant Cultures

Our *Phormidium* culture (DJPM_C1) had 100% sequence (ASV) identity to *Phormidium* sp. CYN64 present in both the mat (0.4% relative abundance of the DJP mat) and sediment (1.2% relative abundance of the sediment); this ASV was 23.4% more abundant in the sediment than of the mat. *Phormidium* are found different environments, from hot springs (Sadettin & Dönmez 2006), marine systems (Williamson *et al*., 2002), alkaline soda lakes (Ataeian *et al*., 2021), to toxic benthic mats in riverbeds (Heath *et al.*, 2016). *Phormidium* sp. CYN64 specifically, was first identified in shallow melt-water ponds in the Pyramid Trough located in Southern Victoria Land, Antarctica (NCBI accession number JQ687330; Jungblut *et al*., 2012) and has since been found in other cold environments such as Svalbard soil crusts (Pushkareva et al., 2015), cold deserts in mid latitude regions (Khomutovska *et al*., 2020), and Antarctic mats (Martineau *et al.*, 2013; Strunecký *et al*., 2010). Furthermore, some species of *Phormidium* are known for chromatic adaptation in response to red light in dark environments such as caves (Montechiaro and Giordano 2006) and in permafrost (Vishnivetskaya *et* al., 2005). In the laboratory, DJPM_C1 grew to higher concentrations in shaded environments and when in shaded environments DJPM_C1 showed higher tolerance for $CaCl_2$, suggesting that DJPM_C may prefer lower-light environments or a synergistic effect with light and salt tolerance.

The ASV that matched DJPM_E1 made up a small percent abundance in both the DJP mat and sediment (< 0.007% abundance in both samples). This culture had 100%

sequence identity (ASV) to our enrichment and matched *Chlorellales* sp. LH10HG2094, which was originally isolated from grassland soil in Denmark (Hodač *et al*., 2016). Members of the Chlorellales order are found in a wide range of habitats from polar environments (Fernandes *et al*., 2019) to tropical and temperate environments (Hodač, *et al.*, 2016). Species similar to the DJPM_E1 culture, such as *Nannochloris*, are common in permafrost ecosystems, from Siberia to Antarctica (Vishnivetskaya, 2009; Vishnivetskaya et al., 2020). Furthermore, members of the *Chlorella* genus have been shown to grow in dark conditions (Vishnivetskaya *et* al., 2005). At lower temperatures, DJPM_E1 grew in BG-11 with 0.25M $CaCl_2$, but only when shaded (0.5 µmol m^{-2} s^{-1} irradiance) and not in direct light (50 µmol m^{-2} s^{-1} irradiance). Further work to identify the mechanisms that enable tolerances under low light conditions needs to be further explored, however the work presented here suggests some phototrophs from the DJP mat and sediment have some tolerance for $CaCl_2$, low light, and low temperatures. Under laboratory conditions the cultures showed a preference for low light environments and in some cases $CaCl_2$. Tolerating and potentially preferring these conditions would be beneficial in the DJP environment.

Dry Valley Conditions and Adaptations

Ice binding proteins (IBPs) are a common mechanism to protect cells from freeze damage in cryosphere environments. Some of these proteins can also depress the freezing point of solvents thus enabling water to remain liquid in subzero temperatures (Davies 2014; Białkowska *et al*., 2020). Both phototrophic and non-phototrophic organisms in the DJP mat and sediment possessed IBPs genes, however the majority of IBPs belonged to

non-phototrophic members of the community. Whether secreted into the environment or anchored, IBPs have an impact on the local microenvironment (Vance *et al*., 2019). For example, IBPs produced by bacteria can physically bind to ice and recruit photosynthetic organisms, and create a symbiotic relationship (Guo *et al*., 2017). IBPs also can increase freeze tolerance in environments by limiting ice recrystallization (Raymond and Fristen 2001). The majority of our mat and sediment IBPs belonged to non-phototrophic community. This suggests a potential cooperation in which organisms that do not produce their own IBPs depend on others to produce them (Raymond 2015).

The presence of salt tolerance genes associated the metagenomes further suggest interactions between the DJP salts and the mat may occur. Genes associated with salt tolerance were the second most abundant group of genes (from our database) found in our metagenomes. The sediment had a total of 440 salt tolerance genes and the mat had a total of 396 gene hits. We observed hits for cyclophilin which has been shown to enhance salt tolerance in *Chlamydomonas* (Lee *et al*., 2017). As well as glucosylglycerol and spermidine synthases which have been shown to be important for salt tolerance, albeit NaCl, in cyanobacteria and algae (Klähn and Hagermann 2011; Liu *et al*., 2015). Studies have shown cyanobacteria can tolerate perchlorates and 1mM $CaCl_2$ (Billi *et* al., 2021; Singh *et al*., 2016). However, our cultures grew at concentrations as high as 0.25M $CaCl_2$. The cyanobacteria strains used for these experiments (Billi *et* al., 2021; Singh *et al*., 2016) were isolated from freshwater sources and not naturally from environments exposed to $CaCl_2$. The tolerance of $CaCl_2$ in our cultures as well as the presence of salt

tolerance genes within the environmental metagenomes suggests that the organisms in the DJP mat and sediment have likely encountered salt from DJP and thus have the potential to tolerate it. While in some cases, such as lower temperatures and low light, organisms like DJPM_E1, may prefer an increase in $CaCl_2$ (Figure 4-11).

The winter light environment around the DJP mat is reduced to only moonlight and temperatures can drop from 10°C in the summer to as low as -30°C (Obryk *et al*., 2020). However, less severe are the transitional seasons when the sun begins to set before winter and beings to rise after the winter. Algae have been shown to prefer these lower light events in Antarctica, such as in East Antarctica freshwater lakes (Tanabe *et al*., 2008). Though extreme, the genetic potential of the mat could enable the community to survive, if not remain active during low light to no light periods. For example, phototaxis genes would allow for vertical migration to the surface of the mat where light is available, pigments would aid in absorbing as much light as possible and would lower albedo to aid in retaining liquid water. Pigments have been shown to play a large role in light absorption, for example, astaxanthin in snow algae and ice algae not only protect the algae from UV but the pigments also lower the surface albedo. The decrease in albedo results in an increase in snow/ice melt and provides liquid water for bacteria and algae in these environments (Hoham and Remias 2020). Black pigmentation, to include dirty ice and snow, lowers surface albedo even more so than red, green, and orange pigments (Williamson *et al*., 2020; Ganey *et al*., 2017). The black coloring of the DJP mat (Figure. 4-1) may primarily be for protecting/absorbing high light and UV during the summer, but

it may also extend liquid water retention as ambient temperatures cool during seasonal shifts.

In contrast to the dark cold winter, the austral summer in the MDVs experience light irradiances that can reach 1,400 µmol m^{-2} s^{-1} (Bagshaw *et al*., 2016). The phototrophic production during the high irradiance summer is likely enabled by self-shading, pigments, and low light photosynthesis adaptations (Kvíderová *et al*., 2019). For example, motility in response to light enables organisms to self-shade at the bottom of mats, protecting them from such high irradiances (Garcia-Pichel *et al*., 1994). The production of pigments (i.e., scytonemin, astaxanthin and canthaxanthin) and mycosporine-like amino acids, such as those found in our metagenomes, protect organisms from high irradiances and UV (Rehakova *et al*., 2019; Mueller *et al*., 2005). Our data suggests that UV protection provided by mycosporine-like amino acids and scytonemin are likely produced by the non-phototrophic organisms in the DJP mat and sediment.

Microbial mats are typically communities that have a photic layer under the surface which receives community shading from a darker pigmented community at the top of the mat. This structure results in lower light irradiances reaching phototrophs towards the base of the mat (Becraft *et al*, 2015). Phototrophs deep within microbial mats benefit from both low light and far red-light adaptations in order to extend their photosynthetic capacity beyond 700 nm and utilize light wavelengths not absorbed at the mat surface (Gan and Bryant 2015). The majority of the photosynthetic antenna proteins

genes in the DJP mat metagenome were red light absorbing allophycocyanin (45.7% relative abundance to other antenna protein genes) with ~55% belonging to LoLiP or FaRLiP specific genes. However, the most abundant light harvesting protein gene within the mat was BCHL B (26.8% relative abundance to all other light harvesting genes in the database), which absorbs the furthest red light of harvesting proteins (> 1000 nm; Hoogewerf *et al*., 2003). The sediment under the mat had similar results, with allophycocyanin accounting for the majority of the photosynthetic antenna proteins (41.3%); 57.8% of the allophycocyanin genes were LoLiP or FaRLiP specific. Similar to the DJP mat, BCHL B was most abundant light harvesting protein gene in the sediment (14.5%). LoLiP and FaRLiP antenna proteins, as well as BCHL B, would be the most beneficial for organisms that are exposed to long periods of low light. We found there to be significantly more FaRLiP protein genes in metagenomes from polar environments compared to non-polar poly-extreme environments, with no significant difference in allophycocyanin genes. This suggests that latitude and long-term light limitations may play a role in the abundances of the genes that produce these proteins. BCHL is known for absorbing light within the far-red wavelengths (Larkum *et al*., 2018) with BCHL E enabling the use of light irradiances as low as 0.00075 µmol m^{-2} s^{-1} (Manske *et al*., 2005). Our data suggests that BCHL B is more abundant in the DJP mat than the sediment and all other metagenomes surveyed in this study. Furthermore, we found there to be significantly more BCHL B in polar environments than non-polar environments. This suggests that absorbing far-red light may be more beneficial in polar environments where the organisms are exposed to long periods of high light and must remain shaded within

the mat, or long periods of red shifted light. Rhodopsin also plays a role in light harvesting though the wavelengths at which these absorb or typically shorter, from 436 to 690 nm (Govorunova *et al*., 2020; Broser *et al*., 2020). We observed significantly more blue-light rhodopsin genes in the polar environments than non-polar environments. Polar environments in general are exposed to more UV light (Vincent 2000) and blue-light rhodopsin are typically found in water columns and ice due to water/ice's ability to scatter light (Béja *et al*., 2001; Koh *et al*., 2010). The higher abundance of blue-light absorbing rhodopsin in the mat, compared to those found in the other metagenomes searched, may be in response to the increase in UV radiation in due to the ozone hole over Antarctica (Farman *et al*., 1985; Núñez-Pons *et al*., 2018). However, the overlap between UV and blue-light rhodopsin would likely be minimal. Further research into blue light absorbing rhodopsin in Antarctic mats should be conducted to understand the prevalence of these rhodopsin and the uniqueness of these environments.

Conclusion

The first reports on the microbiology of DJP mat were in the late 1970s and early 1980s, but has not been revisited since (Siegel *et al*., 1979; 1983; 1984). We confirmed the original taxonomical description of the DP mat, via 16S and 18S rRNA gene amplicons, metagenomics, and culture dependent methods. We further investigated the mechanisms that would enable organisms of the DJP mat, and sediment beneath it, to tolerate the extreme conditions of the DJP area, i.e., salt fluctuations, temperature and both high and low light irradiances.

We found a similar community to that of the original description and further expanded on these initial observations. Our investigation of the species composition and gene content of the DJP mat suggests that the adjacent hypersaline brine may episodically interact with the DJP mat. Due to the presence of salt tolerant microbes, salt tolerance genes and the lack of Nostoc species, we conclude that the community composition reflects an environment that deals with fluctuations of salinity.

The genetic potential to produce a combination of ice binding proteins, protective pigments, maintain salt tolerances and variety of light harvesting proteins within the DJP mat and sediment metagenomes suggests that resident microbial populations have a variety of adaptations to handle the stress of this particular dry valley niche. The distribution of these genes among phototrophic and non-phototrophic organisms suggests that potential cooperative relationships within the mat and sediment enables survival during extreme conditions. The abundant photosynthetic antenna proteins, bacteriochlorophyll, rhodopsin, and phototaxis genes we detected would be essential for organisms to take advantage of the light fluctuations that occur from the high light Antarctic summer to the low light Antarctic winter. Furthermore, culture-based approaches confirmed $CaCl_2$ tolerance in two phototrophic organisms enriched from the mat. The ecologically relevant cyanobacteria (DJPM_C1) preferred shaded environments over non-shaded environments and tolerated a variety of temperatures down to 4°C. DJP and polar environments are unique polyextreme systems where phototrophic organisms may be adapted to use low light, blue light, and red-light wavelengths more so than mid

latitude polyextreme mats that do not undergo prolonged shifts of high to low light irradiances. Overwinter research and further laboratory culturing experiments should be conducted to investigate the extent at which the genetic potential translates to functional stress response and activity during the extreme conditions of the low light polar winter as well as to further understand the impacts that the extreme conditions of DJP have on the community composition and the relationships within the microbial community.

Acknowledgments

All fieldwork was made possible with logistics from the Antarctic Support Contractor; we are grateful to all members of the ANTAEM Team for assistance with sample collection.

Funding

This work was funded by NSF - Office of Polar Programs (grant # NSF 1643687 and 2148730 to JAM)

Declaration of interest

The authors declare no conflict of interest.

References

Altschul, S. F., Gish, W., Miller, W., Myers, E. W., & Lipman, D. J. (1990). Basic local alignment search tool. *Journal of Molecular Biology, 215*(3), 403–410. https://doi.org/10.1016/S0022-2836(05)80360-2

Antipov, D., Korobeynikov, A., McLean, J. S., & Pevzner, P. A. (2016). hybridSPAdes: An algorithm for hybrid assembly of short and long reads. *Bioinformatics*, *32*(7), 1009–1015. https://doi.org/10.1093/bioinformatics/btv688

Arkin, A. P., Cottingham, R. W., Henry, C. S., Harris, N. L., Stevens, R. L., Maslov, S., Dehal, P., Ware, D., Perez, F., Canon, S., Sneddon, M. W., Henderson, M. L., Riehl, W. J., Murphy-Olson, D., Chan, S. Y., Kamimura, R. T., Kumari, S., Drake, M. M., Brettin, T. S., … Yu, D. (2018). KBase: The United States Department of Energy Systems Biology Knowledgebase. *Nature Biotechnology*, *36*(7), 566–569. https://doi.org/10.1038/nbt.4163

Ataeian, M., Vadlamani, A., Haines, M., Mosier, D., Dong, X., Kleiner, M., ... & Hawley, A. K. (2021). Proteome and strain analysis of cyanobacterium Candidatus "Phormidium alkaliphilum" reveals traits for success in biotechnology. Iscience, 24(12), 103405.

Becraft, E. D., Wood, J. M., Rusch, D. B., Kühl, M., Jensen, S. I., Bryant, D. A., Roberts, D. W., Cohan, F. M., & Ward, D. M. (2015). The molecular dimension of microbial species: 1. Ecological distinctions among, and homogeneity within, putative ecotypes of Synechococcus inhabiting the cyanobacterial mat of Mushroom Spring, Yellowstone National Park. *Frontiers in Microbiology, 6*. https://doi.org/10.3389/fmicb.2015.00590

Béja, O., Spudich, E. N., Spudich, J. L., Leclerc, M., & DeLong, E. F. (2001). Proteorhodopsin phototrophy in the ocean. *Nature*, *411*(6839), 786-789.

Białkowska, A., Majewska, E., Olczak, A., & Twarda-Clapa, A. (2020). Ice binding proteins: Diverse biological roles and applications in different types of industry. Biomolecules, 10(2), 274.

Billi, D., Fernandez, B. G., Fagliarone, C., Chiavarini, S., & Rothschild, L. J. (2021). Exploiting a perchlorate-tolerant desert cyanobacterium to support bacterial growth for in situ resource utilization on Mars. International Journal of Astrobiology, 20(1), 29-35.

Broser, M., Spreen, A., Konold, P. E., Peter, E., Adam, S., Borin, V., ... & Hegemann, P. (2020). NeoR, a near-infrared absorbing rhodopsin. *Nature communications*, *11*(1), 1-10.

Buchfink, B., Xie, C., & Huson, D. H. (2015). Fast and sensitive protein alignment using DIAMOND. *Nature Methods*, *12*(1), 59–60. https://doi.org/10.1038/nmeth.3176

Capece, M. C., Clark, E., Saleh, J. K., Halford, D., Heinl, N., Hoskins, S., & Rothschild, L. J. (2013). Polyextremophiles and the Constraints for Terrestrial Habitability. In J. Seckbach, A. Oren, & H. Stan-Lotter (Eds.), *Polyextremophiles: Life Under Multiple Forms of Stress* (pp. 3–59). Springer Netherlands. https://doi.org/10.1007/978-94-007-6488-0_1

Castenholz, R. W., & Garcia-Pichel, F. (2012). Cyanobacterial Responses to UV Radiation. In B. A. Whitton (Ed.), *Ecology of Cyanobacteria II: Their Diversity in*

Space and Time (pp. 481–499). Springer Netherlands. https://doi.org/10.1007/978-94-007-3855-3_19

Chaumeil, P.-A., Mussig, A. J., Hugenholtz, P., & Parks, D. H. (2020). GTDB-Tk: A toolkit to classify genomes with the Genome Taxonomy Database. *Bioinformatics*, *36*(6), 1925–1927. https://doi.org/10.1093/bioinformatics/btz848

Chen, A.-P., Wang, G.-L., Qu, Z.-L., Lu, C.-X., Liu, N., Wang, F., & Xia, G.-X. (2007). Ectopic expression of ThCYP1, a stress-responsive cyclophilin gene from Thellungiella halophila, confers salt tolerance in fission yeast and tobacco cells. *Plant Cell Reports*, *26*(2), 237–245. https://doi.org/10.1007/s00299-006-0238-y

Chen, M., Hernandez-Prieto, M. A., Loughlin, P. C., Li, Y., & Willows, R. D. (2019). Genome and proteome of the chlorophyll f-producing cyanobacterium Halomicronema hongdechloris: Adaptative proteomic shifts under different light conditions. *BMC Genomics*, *20*(1), 207. https://doi.org/10.1186/s12864-019-5587-3

Chrismas, N. A. M., Anesio, A. M., & Sánchez-Baracaldo, P. (2015). Multiple adaptations to polar and alpine environments within cyanobacteria: A phylogenomic and Bayesian approach. *Frontiers in Microbiology*, *6*. https://doi.org/10.3389/fmicb.2015.01070

Chrismas, N. A. M., Barker, G., Anesio, A. M., & Sánchez-Baracaldo, P. (2016). Genomic mechanisms for cold tolerance and production of exopolysaccharides in the Arctic cyanobacterium Phormidesmis priestleyi BC1401. *BMC Genomics*, *17*(1), 533. https://doi.org/10.1186/s12864-016-2846-4

Chrismas, N. A. M., Williamson, C. J., Yallop, M. L., Anesio, A. M., & Sánchez-Baracaldo, P. (2018). Photoecology of the Antarctic cyanobacterium Leptolyngbya sp. BC1307 brought to light through community analysis, comparative genomics and in vitro photophysiology. *Molecular Ecology*, *27*(24), 5279–5293. https://doi.org/10.1111/mec.14953

Ciocca, M., & Wang, J. (2013). By the light of the silvery Moon: Fact and fiction. *Physics Education*, *48*(3), 360–367. https://doi.org/10.1088/0031-9120/48/3/360

Cockell, C. S., Kaltenegger, L., & Raven, J. A. (2009). Cryptic Photosynthesis—Extrasolar Planetary Oxygen Without a Surface Biological Signature. *Astrobiology*, *9*(7), 623–636. https://doi.org/10.1089/ast.2008.0273

Davies, P. L. (2014). Ice-binding proteins: a remarkable diversity of structures for stopping and starting ice growth. Trends in biochemical sciences, 39(11), 548-555.

De Corato, U. (2020). Soil microbiota manipulation and its role in suppressing soil-borne plant pathogens in organic farming systems under the light of microbiome-assisted strategies. Chemical and Biological Technologies in Agriculture, 7(1), 1-26.

Delesky, E. A., Thomas, P. E., Charrier, M., Cameron, J. C., & Srubar, W. V. (2021). Effect of pH on the activity of ice-binding protein from Marinomonas primoryensis. Extremophiles, 25(1), 1-13.

Dugan, H.A., Doran, P.T., Grombacher, D., Auken, E., Bording, T., Foged, N., Foley, N., Mikucki, J., Virginia, R.A. and Tulaczyk, S., 2022. Brief communication: The hidden labyrinth: Deep groundwater in Wright Valley, Antarctica. The Cryosphere Discussions, pp.1-8.

Eren, A. M., Esen, Ö. C., Quince, C., Vineis, J. H., Morrison, H. G., Sogin, M. L., & Delmont, T. O. (2015). Anvi'o: An advanced analysis and visualization platform for 'omics data. *PeerJ*, *3*, e1319. https://doi.org/10.7717/peerj.1319

Farman, J. C., Gardiner, B. G., & Shanklin, J. D. (1985). Large losses of total ozone in Antarctica reveal seasonal ClOx/NOx interaction. *Nature*, *315*(6016), 207-210.

Fernandes, M. S., Calsing, L. C., Nascimento, R. C., Santana, H., Morais, P. B., de Capdeville, G., & Brasil, B. S. (2019). Customized cryopreservation protocols for chlorophytes based on cell morphology. Algal Research, 38, 101402.

Fiedler, B., Börner, T., & Wilde, A. (2005). Phototaxis in the Cyanobacterium Synechocystis sp. PCC 6803: Role of Different Photoreceptors. *Photochemistry and Photobiology*, *81*(6), 1481–1488. https://doi.org/10.1562/2005-06-28-RA-592

Gan, F., & Bryant, D. A. (2015). Adaptive and acclimative responses of cyanobacteria to far-red light. *Environmental Microbiology*, *17*(10), 3450–3465. https://doi.org/10.1111/1462-2920.12992

Gan, F., Zhang, S., Rockwell, N. C., Martin, S. S., Lagarias, J. C., & Bryant, D. A. (2014). Extensive remodeling of a cyanobacterial photosynthetic apparatus in far-red light. *Science*, *345*(6202), 1312–1317. https://doi.org/10.1126/science.1256963

Ganey, G. Q., Loso, M. G., Burgess, A. B., & Dial, R. J. (2017). The role of microbes in snowmelt and radiative forcing on an Alaskan icefield. *Nature Geoscience*, *10*(10), 754–759. https://doi.org/10.1038/ngeo3027

Gann, E. R., Pound, H. L., and Wilhelm, S. W. (2019). *Python Script: Extracting Aligned Portion of Viral Hallmark Genes from Blastx*

Sequence. Available: https://github.com/Wilhelmlab/general-scripts/blob/master/Pound2019_Extract_aligned.py

Garcia-Pichel, F., Mechling, M., & Castenholz, R. W. (1994). Diel Migrations of Microorganisms within a Benthic, Hypersaline Mat Community. *Applied and Environmental Microbiology*, *60*(5), 1500–1511.

Gawor, J., Grzesiak, J., Sasin-Kurowska, J., Borsuk, P., Gromadka, R., Górniak, D., ... & Zdanowski, M. K. (2016). Evidence of adaptation, niche separation and microevolution within the genus Polaromonas on Arctic and Antarctic glacial surfaces. Extremophiles, 20(4), 403-413.

Gorlenko, V. M., Bryantseva, I. A., Kalashnikov, A. M., Gaisin, V. A., Sukhacheva, M. V., Gruzdev, D. S., & Kuznetsov, B. B. (2014). Candidatus 'Chloroploca asiatica'gen. nov., sp. nov., a new mesophilic filamentous anoxygenic phototrophic bacterium. Microbiology, 83(6), 838-848.

Govorunova, E. G., Sineshchekov, O. A., Li, H., Wang, Y., Brown, L. S., & Spudich, J. L. (2020). RubyACRs, nonalgal anion channelrhodopsins with highly red-shifted absorption. *Proceedings of the National Academy of Sciences*, *117*(37), 22833-22840.

Greco, C., Andersen, D. T., Hawes, I., Bowles, A. M., Yallop, M. L., Barker, G., & Jungblut, A. D. (2020). Microbial diversity of pinnacle and conical microbial mats in the perennially ice-covered lake Untersee, East Antarctica. Frontiers in Microbiology, 11, 607251.

Guo, S., Stevens, C. A., Vance, T. D. R., Olijve, L. L. C., Graham, L. A., Campbell, R. L., Yazdi, S. R., Escobedo, C., Bar-Dolev, M., Yashunsky, V., Braslavsky, I., Langelaan, D. N., Smith, S. P., Allingham, J. S., Voets, I. K., & Davies, P. L. (2017). Structure of a 1.5-MDa adhesin that binds its Antarctic bacterium to diatoms and ice. *Science Advances*, *3*(8), e1701440. https://doi.org/10.1126/sciadv.1701440

Harris, H. J. H., Cartwright, K., & Torii, T. (1979). Dynamic chemical equilibrium in a polar desert pond: a sensitive index of meteorological cycles. Science, 204(4390), 301-303.

Harris, H. J. H., & Cartwright, K. (1981). Hydrology of the Don Juan Basin, Wright Valley, Antarctica. *Dry Valley drilling project*, *33*, 161-184.

Harrison, J. P., Gheeraert, N., Tsigelnitskiy, D., & Cockell, C. S. (2013). The limits for life under multiple extremes. *Trends in Microbiology*, *21*(4), 204–212. https://doi.org/10.1016/j.tim.2013.01.006

Hawes, I., & Schwarz, A. M. (1999). Photosynthesis in an extreme shade environment: benthic microbial mats from Lake Hoare, a permanently ice-covered Antarctic lake. Journal of Phycology, 35(3), 448-459.

Heath, M., Wood, S. A., Young, R. G., & Ryan, K. G. (2016). The role of nitrogen and phosphorus in regulating Phormidium sp.(cyanobacteria) growth and anatoxin production. FEMS Microbiology Ecology, 92(3), fiw021.

Hodač, L., Hallmann, C., Spitzer, K., Elster, J., Faßhauer, F., Brinkmann, N., ... & Friedl, T. (2016). Widespread green algae Chlorella and Stichococcus exhibit polar-

temperate and tropical-temperate biogeography. FEMS Microbiology Ecology, 92(8).

Hoham, R. W., & Remias, D. (2020). Snow and glacial algae: a review1. Journal of phycology, 56(2), 264-282.

Holzinger, A., & Karsten, U. (2013). Desiccation stress and tolerance in green algae: Consequences for ultrastructure, physiological and molecular mechanisms. *Frontiers in Plant Science*, *4*. https://doi.org/10.3389/fpls.2013.00327

Jain, M., Olsen, H. E., Paten, B., & Akeson, M. (2016). The Oxford Nanopore MinION: delivery of nanopore sequencing to the genomics community. Genome biology, 17(1), 1-11.

Jiang, F. Sun, & X. Zhang (Eds.), *Research in Computational Molecular Biology* (pp. 158–170). Springer. https://doi.org/10.1007/978-3-642-37195-0_13

Jungblut, A.-D., S. A. Wood, I. Hawes, J. Webster-Brown & C. Harris, 2012. The Pyramid Trough Wetland: environment-biota relationships in a newly created protected area. FEMS Microbiology Ecology 82: 356–366.

Kanehisa, M., & Goto, S. (2000). KEGG: Kyoto Encyclopedia of Genes and Genomes. *Nucleic Acids Research*, *28*(1), 27–30.

Kanehisa, M., Sato, Y., & Morishima, K. (2016). BlastKOALA and GhostKOALA: KEGG Tools for Functional Characterization of Genome and Metagenome Sequences. *Journal of Molecular Biology*, *428*(4), 726–731. https://doi.org/10.1016/j.jmb.2015.11.006

Kang, D. D., Froula, J., Egan, R., & Wang, Z. (2015). MetaBAT, an efficient tool for accurately reconstructing single genomes from complex microbial communities. *PeerJ*, *3*. https://doi.org/10.7717/peerj.1165

Kato, K., Torii, T., & Nakai, N. (1978). Dilution and concentration of saline water in Don Juan Pond in 1974.

Khan, N., Tuffin, M., Stafford, W., Cary, C., Lacap, D. C., Pointing, S. B., & Cowan, D. (2011). Hypolithic microbial communities of quartz rocks from Miers Valley, McMurdo dry valleys, Antarctica. Polar biology, 34(11), 1657-1668.

Khomutovska, N., Sandzewicz, M., Łach, Ł., Suska-Malawska, M., Chmielewska, M., Mazur-Marzec, H., ... & Jasser, I. (2020). Limited microcystin, anatoxin and cylindrospermopsin production by cyanobacteria from microbial mats in cold deserts. Toxins, 12(4), 244.

Kiang, N. Y., Siefert, J., Govindjee, & Blankenship, R. E. (2007, April 3). *Spectral Signatures of Photosynthesis. I. Review of Earth Organisms* (2 Madison Avenue Larchmont, NY 10538 USA) [Research-article]. Https://Home.Liebertpub.Com/Ast; Mary Ann Liebert, Inc. 2 Madison Avenue Larchmont, NY 10538 USA. https://doi.org/10.1089/ast.2006.0105

Kirsch, F., Klähn, S., & Hagemann, M. (2019). Salt-Regulated Accumulation of the Compatible Solutes Sucrose and Glucosylglycerol in Cyanobacteria and Its Biotechnological Potential. *Frontiers in Microbiology*, *10*. https://doi.org/10.3389/fmicb.2019.02139

Klähn, S., & Hagemann, M. (2011). Compatible solute biosynthesis in cyanobacteria. Environmental microbiology, 13(3), 551-562.

Koh, E. Y., Atamna-Ismaeel, N., Martin, A., Cowie, R. O., Beja, O., Davy, S. K., ... & Ryan, K. G. (2010). Proteorhodopsin-bearing bacteria in Antarctic sea ice. *Applied and environmental microbiology*, *76*(17), 5918-5925.

Komenda, J., & Sobotka, R. (2016). Cyanobacterial high-light-inducible proteins—Protectors of chlorophyll–protein synthesis and assembly. *Biochimica et Biophysica Acta (BBA) - Bioenergetics*, *1857*(3), 288–295. https://doi.org/10.1016/j.bbabio.2015.08.011

Koopmans, M. P., Köster, J., Van Kaam-Peters, H. M. E., Kenig, F., Schouten, S., Hartgers, W. A., de Leeuw, J. W., & Sinninghe Damsté, J. S. (1996). Diagenetic and catagenetic products of isorenieratene: Molecular indicators for photic zone anoxia. *Geochimica et Cosmochimica Acta*, *60*(22), 4467–4496. https://doi.org/10.1016/S0016-7037(96)00238-4

Kvíderová, J., Elster, J., & Komárek, J. (2019). Chapter 14—Ecophysiology of Cyanobacteria in the Polar Regions. In A. K. Mishra, D. N. Tiwari, & A. N. Rai (Eds.), *Cyanobacteria* (pp. 277–302). Academic Press. https://doi.org/10.1016/B978-0-12-814667-5.00014-3

Lamprinou, V., Skaraki, K., Kotoulas, G., Anagnostidis, K., Economou-Amilli, A., & Pantazidou, A. (2013). A new species of Phormidium (Cyanobacteria, Oscillatoriales) from three Greek Caves: Morphological and molecular analysis.

Fundamental and Applied Limnology / Archiv f??R Hydrobiologie, *182*(2), 109–116. https://doi.org/10.1127/1863-9135/2013/0323

Langmead, B., & Salzberg, S. L. (2012). Fast gapped-read alignment with Bowtie 2. *Nature Methods*, *9*(4), 357–359. https://doi.org/10.1038/nmeth.1923

Larkum, A. W. D., Ritchie, R. J., & Raven, J. A. (2018). Living off the Sun: chlorophylls, bacteriochlorophylls and rhodopsins. *Photosynthetica*, *56*(1), 11-43.

Lee, H. N., Kim, S. H., Han, Y. J., Im, S., Jeong, W. J., Park, E. J., ... & Choi, D. W. (2017). PsCYP1 of marine red alga Pyropia seriata (Bangiales, Rhodophyta) confers salt and heat tolerance in Chlamydomonas. Journal of Applied Phycology, 29(1), 617-625.

Ley, R. E., Harris, J. K., Wilcox, J., Spear, J. R., Miller, S. R., Bebout, B. M., Maresca, J. A., Bryant, D. A., Sogin, M. L., & Pace, N. R. (2006). Unexpected Diversity and Complexity of the Guerrero Negro Hypersaline Microbial Mat. *Applied and Environmental Microbiology*, *72*(5), 3685–3695. https://doi.org/10.1128/AEM.72.5.3685-3695.2006

Li, H., Handsaker, B., Wysoker, A., Fennell, T., Ruan, J., Homer, N., Marth, G., Abecasis, G., Durbin, R., & 1000 Genome Project Data Processing Subgroup. (2009). The Sequence Alignment/Map format and SAMtools. *Bioinformatics (Oxford, England)*, *25*(16), 2078–2079. https://doi.org/10.1093/bioinformatics/btp352

Liu, J., Zhang, D., & Hong, L. (2015). Isolation, characterization and functional annotation of the salt tolerance genes through screening the high-quality cDNA

library of the halophytic green alga Dunaliella salina (Chlorophyta). *Annals of Microbiology*, *65*(3), 1293–1302. https://doi.org/10.1007/s13213-014-0967-z

Manske, A. K., Glaeser, J., Kuypers, M. M., & Overmann, J. (2005). Physiology and phylogeny of green sulfur bacteria forming a monospecific phototrophic assemblage at a depth of 100 meters in the Black Sea. *Applied and environmental microbiology*, *71*(12), 8049-8060.

Marin, K., Zuther, E., Kerstan, T., Kunert, A., & Hagemann, M. (1998). The ggpS Gene from Synechocystis sp. Strain PCC 6803 Encoding Glucosyl-Glycerol-Phosphate Synthase Is Involved in Osmolyte Synthesis. *Journal of Bacteriology*, *180*(18), 4843–4849.

Martineau, E., Wood, S. A., Miller, M. R., Jungblut, A. D., Hawes, I., Webster-Brown, J., & Packer, M. A. (2013). Characterisation of Antarctic cyanobacteria and comparison with New Zealand strains. Hydrobiologia, 711(1), 139-154.

Melnicki, M. R., Leverenz, R. L., Sutter, M., López-Igual, R., Wilson, A., Pawlowski, E. G., Perreau, F., Kirilovsky, D., & Kerfeld, C. A. (2016). Structure, Diversity, and Evolution of a New Family of Soluble Carotenoid-Binding Proteins in Cyanobacteria. *Molecular Plant*, *9*(10), 1379–1394. https://doi.org/10.1016/j.molp.2016.06.009

Merino, N., Aronson, H. S., Bojanova, D. P., Feyhl-Buska, J., Wong, M. L., Zhang, S., & Giovannelli, D. (2019). Living at the Extremes: Extremophiles and the Limits of Life in a Planetary Context. *Frontiers in Microbiology, 10*. https://doi.org/10.3389/fmicb.2019.00780

Meyer, F., Paarmann, D., D'Souza, M., Olson, R., Glass, E., Kubal, M., Paczian, T., Rodriguez, A., Stevens, R., Wilke, A., Wilkening, J., & Edwards, R. (2008). The metagenomics RAST server – a public resource for the automatic phylogenetic and functional analysis of metagenomes. *BMC Bioinformatics*, *9*(1), 386. https://doi.org/10.1186/1471-2105-9-386

Miyamoto, K. T., Komatsu, M., & Ikeda, H. (2014). Discovery of Gene Cluster for Mycosporine-Like Amino Acid Biosynthesis from Actinomycetales Microorganisms and Production of a Novel Mycosporine-Like Amino Acid by Heterologous Expression. *Applied and Environmental Microbiology*, *80*(16), 5028–5036. https://doi.org/10.1128/AEM.00727-14

Montechiaro, F., & Giordano, M. (2006). Effect of prolonged dark incubation on pigments and photosynthesis of the cave-dwelling cyanobacterium Phormidium autumnale (Oscillatoriales, Cyanobacteria). Phycologia, 45(6), 704–710. https://doi.org/10.2216/06-15.1

Mueller, D. R., Vincent, W. F., Bonilla, S., & Laurion, I. (2005). Extremotrophs, extremophiles and broadband pigmentation strategies in a high arctic ice shelf ecosystem. *FEMS Microbiology Ecology*, *53*(1), 73–87. https://doi.org/10.1016/j.femsec.2004.11.001

Núñez-Pons, L., Avila, C., Romano, G., Verde, C., & Giordano, D. (2018). UV-protective compounds in marine organisms from the Southern Ocean. *Marine drugs*, *16*(9), 336.

Nurk, S., Bankevich, A., Antipov, D., Gurevich, A., Korobeynikov, A., Lapidus, A., Prjibelsky, A., Pyshkin, A., Sirotkin, A., Sirotkin, Y., Stepanauskas, R., McLean, J., Lasken, R., Clingenpeel, S. R., Woyke, T., Tesler, G., Alekseyev, M. A., & Pevzner, P. A. (2013). Assembling Genomes and Mini-metagenomes from Highly Chimeric Reads. In M. Deng, R.

Obryk, M. K., Doran, P. T., Fountain, A. G., Myers, M., & McKay, C. P. (2020). Climate from the McMurdo Dry Valleys, Antarctica, 1986–2017: surface air temperature trends and redefined summer season. Journal of Geophysical Research: Atmospheres, 125(13), e2019JD032180.

Oda, K., Vierock, J., Oishi, S., Rodriguez-Rozada, S., Taniguchi, R., Yamashita, K., Wiegert, J. S., Nishizawa, T., Hegemann, P., & Nureki, O. (2018). Crystal structure of the red light-activated channelrhodopsin Chrimson. *Nature Communications*, *9*(1), 3949. https://doi.org/10.1038/s41467-018-06421-9

O'Leary, N. A., Wright, M. W., Brister, J. R., Ciufo, S., Haddad, D., McVeigh, R., Rajput, B., Robbertse, B., Smith-White, B., Ako-Adjei, D., Astashyn, A., Badretdin, A., Bao, Y., Blinkova, O., Brover, V., Chetvernin, V., Choi, J., Cox, E., Ermolaeva, O., … Pruitt, K. D. (2016). Reference sequence (RefSeq) database at NCBI: Current status, taxonomic expansion, and functional annotation. *Nucleic Acids Research*, *44*(D1), D733-745. https://doi.org/10.1093/nar/gkv1189

Olsen, M. T., Nowack, S., Wood, J. M., Becraft, E. D., LaButti, K., Lipzen, A., Martin, J., Schackwitz, W. S., Rusch, D. B., Cohan, F. M., Bryant, D. A., & Ward, D. M. (2015). The molecular dimension of microbial species: 3. Comparative genomics of

Synechococcus strains with different light responses and in situ diel transcription patterns of associated putative ecotypes in the Mushroom Spring microbial mat. *Frontiers in Microbiology, 6*. https://doi.org/10.3389/fmicb.2015.00604

Parks, D. H., Imelfort, M., Skennerton, C. T., Hugenholtz, P., & Tyson, G. W. (2015). CheckM: Assessing the quality of microbial genomes recovered from isolates, single cells, and metagenomes. *Genome Research*, *25*(7), 1043–1055. https://doi.org/10.1101/gr.186072.114

Peipoch, M., Jones, R., & Valett, H. M. (2015). Spatial patterns in biofilm diversity across hierarchical levels of river-floodplain landscapes. PloS one, 10(12), e0144303.

Pothipongsa, A., Jantaro, S., & Incharoensakdi, A. (2016). Spermidine Synthase is Required for Growth of Synechococcus sp. PCC 7942 Under Osmotic Stress. *Current Microbiology*, *73*(5), 639–645. https://doi.org/10.1007/s00284-016-1107-8

Prieto-Barajas, C. M., Valencia-Cantero, E., & Santoyo, G. (2018). Microbial mat ecosystems: Structure types, functional diversity, and biotechnological application. *Electronic Journal of Biotechnology*, *31*, 48–56. https://doi.org/10.1016/j.ejbt.2017.11.001

Pruitt, K. D., Tatusova, T., & Maglott, D. R. (2007). NCBI reference sequences (RefSeq): a curated non-redundant sequence database of genomes, transcripts and proteins. Nucleic acids research, 35(suppl_1), D61-D65.

Pushkareva, E., Pessi, I. S., Wilmotte, A., & Elster, J. (2015). Cyanobacterial community composition in Arctic soil crusts at different stages of development. FEMS microbiology ecology, 91(12), fiv143.

Raven, J. a., & Cockell, C. s. (2006). Influence on Photosynthesis of Starlight, Moonlight, Planetlight, and Light Pollution (Reflections on Photosynthetically Active Radiation in the Universe). *Astrobiology*, *6*(4), 668–675. https://doi.org/10.1089/ast.2006.6.668

Raymond, J. A., & Fritsen, C. H. (2001). Semipurification and ice recrystallization inhibition activity of ice-active substances associated with Antarctic photosynthetic organisms. Cryobiology, 43(1), 63-70.

Raymond, J. A., Fritsen, C., & Shen, K. (2007). An ice-binding protein from an Antarctic sea ice bacterium. FEMS Microbiology Ecology, 61(2), 214–221. https://doi.org/10.1111/j.1574-6941.2007.00345.x

Raymond, J. A. (2014). The ice-binding proteins of a snow alga, Chloromonas brevispina: Probable acquisition by horizontal gene transfer. *Extremophiles*, *18*(6), 987–994. https://doi.org/10.1007/s00792-014-0668-3

Raymond, J. A. (2016). Dependence on epiphytic bacteria for freezing protection in an Antarctic moss, Bryum argenteum. *Environmental Microbiology Reports*, *8*(1), 14–19. https://doi.org/10.1111/1758-2229.12337

Rehakova, K., Capkova, K., Hrouzek, P., Koblizek, M., & Dolezal, J. (2019). Microbial photosynthetic and photoprotective pigments in Himalayan soils originating from

different elevations and successional stages. *Soil Biology and Biochemistry*, *132*, 153–164. https://doi.org/10.1016/j.soilbio.2019.02.008

Rockwell, N. C., & Lagarias, J. C. (2006). The Structure of Phytochrome: A Picture Is Worth a Thousand Spectra. *The Plant Cell*, *18*(1), 4–14. https://doi.org/10.1105/tpc.105.038513

Šabacká, M., & Elster, J. (2006). Response of Cyanobacteria and Algae from Antarctic Wetland Habitats to Freezing and Desiccation Stress. *Polar Biology*, *30*(1), 31. https://doi.org/10.1007/s00300-006-0156-z

Sadettin, S., & Dönmez, G. (2006). Bioaccumulation of reactive dyes by thermophilic cyanobacteria. Process Biochemistry, 41(4), 836-841.

Sand-Jensen, K., & Jespersen, T. S. (2012). Tolerance of the widespread cyanobacterium Nostoc commune to extreme temperature variations (− 269 to 105 C), pH and salt stress. Oecologia, 169(2), 331-339.

Siegel, B. Z., Mcmurty, G., Siegel, S. M., Chen, J., & Larock, P. (1979). Life in the calcium chloride environment of Don Juan Pond, Antarctica. *Nature*, *280*(5725), 828–829. https://doi.org/10.1038/280828a0

Siegel, B. Z., Siegel, S. M., Chen, J., & LaRock, P. (1983). An extraterrestrial habitat on earth: The algal mat of Don Jaun Pond. *Advances in Space Research*, *3*(8), 39–42. https://doi.org/10.1016/0273-1177(83)90171-0

Siegel, B. Z., Siegel, S. M., Speitel, T., Waber, J., & Stoecker, R. (1984). Brine organisms and the question of habitat-specific adaptation. *Origins of Life*, *14*(1), 757–770. https://doi.org/10.1007/BF00933731

Singh, S., Verma, E., Tiwari, B., & Mishra, A. K. (2016). Exopolysaccharide production in Anabaena sp. PCC 7120 under different CaCl2 regimes. Physiology and Molecular Biology of Plants, 22(4), 557-566.

Slonimskiy, Y. B., Muzzopappa, F., Maksimov, E. G., Wilson, A., Friedrich, T., Kirilovsky, D., & Sluchanko, N. N. (2019). Light-controlled carotenoid transfer between water-soluble proteins related to cyanobacterial photoprotection. *The FEBS Journal*, *286*(10), 1908–1924. https://doi.org/10.1111/febs.14803

Samarkin, V.A., Madigan, M.T., Bowles, M.W., Casciotti, K.L., Priscu, J.C., Mckay, C.P. and Joye, S.B., 2010. Abiotic nitrous oxide emission from the hypersaline Don Juan Pond in Antarctica. Nature Geoscience, 3(5), pp.341-344.

Sohm, J. A., Niederberger, T. D., Parker, A. E., Tirindelli, J., Gunderson, T., Cary, S. C., ... & Carpenter, E. J. (2020). Microbial mats of the McMurdo dry valleys, Antarctica: oases of biological activity in a very cold desert. Frontiers in microbiology, 11, 537960.

Sommer, V., Mikhailyuk, T., Glaser, K., & Karsten, U. (2020). Uncovering unique green algae and cyanobacteria isolated from biocrusts in highly saline potash tailing pile habitats, using an integrative approach. Microorganisms, 8(11), 1667.

Sommers, P., Darcy, J. L., Porazinska, D. L., Gendron, E., Fountain, A. G., Zamora, F., ... & Schmidt, S. K. (2019). Comparison of microbial communities in the sediments and water columns of frozen cryoconite holes in the McMurdo Dry Valleys, Antarctica. Frontiers in microbiology, 65.

Strunecký, O., Elster, J., & Komárek, J. (2010). Phylogenetic relationships between geographically separate Phormidium cyanobacteria: Is there a link between north and south polar regions? Polar Biology, 33(10), 1419–1428. https://doi.org/10.1007/s00300-010-0834-8

Tarhriz, V., Thiel, V., Nematzadeh, G., Hejazi, M. A., Imhoff, J. F., & Hejazi, M. S. (2013). Tabrizicola aquatica gen. Nov. Sp. Nov., a novel alphaproteobacterium isolated from Qurugöl Lake nearby Tabriz city, Iran. *Antonie van Leeuwenhoek*, *104*(6), 1205–1215. https://doi.org/10.1007/s10482-013-0042-y

Tashyreva, D., & Elster, J. (2016). Annual Cycles of Two Cyanobacterial Mat Communities in Hydro-Terrestrial Habitats of the High Arctic. *Microbial Ecology*, *71*(4), 887–900. https://doi.org/10.1007/s00248-016-0732-x

Taton, A., Grubisic, S., Brambilla, E., Wit, R. D., & Wilmotte, A. (2003). Cyanobacterial Diversity in Natural and Artificial Microbial Mats of Lake Fryxell (McMurdo Dry Valleys, Antarctica): A Morphological and Molecular Approach. *Applied and Environmental Microbiology*, *69*(9), 5157–5169. https://doi.org/10.1128/AEM.69.9.5157-5169.2003

Tilbrook, K., Dubois, M., Crocco, C. D., Yin, R., Chappuis, R., Allorent, G., Schmid-Siegert, E., Goldschmidt-Clermont, M., & Ulm, R. (2016). UV-B Perception and Acclimation in Chlamydomonas reinhardtii[OPEN]. *The Plant Cell*, *28*(4), 966–983. https://doi.org/10.1105/tpc.15.00287

Toner, J. D., Catling, D. C., & Sletten, R. S. (2017). The geochemistry of Don Juan Pond: Evidence for a deep groundwater flow system in Wright Valley, Antarctica. Earth and Planetary Science Letters, 474, 190-197.

Torii, T., & Ossaka, J. (1965). Antarcticite: a new mineral, calcium chloride hexahydrate, discovered in Antarctica. Science, 149(3687), 975-977.

Torii, T., Yamagata, N., Ossaka, J., & Murata, S. (1977). Salt balance in the Don Juan basin.

Tytgat, B., Verleyen, E., Obbels, D., Peeters, K., Wever, A. D., D'hondt, S., Meyer, T. D., Criekinge, W. V., Vyverman, W., & Willems, A. (2014). Bacterial Diversity Assessment in Antarctic Terrestrial and Aquatic Microbial Mats: A Comparison between Bidirectional Pyrosequencing and Cultivation. *PLOS ONE*, *9*(6), e97564. https://doi.org/10.1371/journal.pone.0097564

Van Horn, D. J., Wolf, C. R., Colman, D. R., Jiang, X., Kohler, T. J., McKnight, D. M., Stanish, L. F., Yazzie, T., & Takacs-Vesbach, C. D. (2016). Patterns of bacterial biodiversity in the glacial meltwater streams of the McMurdo Dry Valleys, Antarctica. *FEMS Microbiology Ecology*, *92*(10). https://doi.org/10.1093/femsec/fiw148

Vance, T. D. R., Bayer-Giraldi, M., Davies, P. L., & Mangiagalli, M. (2019). Ice-binding proteins and the 'domain of unknown function' 3494 family. *The FEBS Journal*, *286*(5), 855–873. https://doi.org/10.1111/febs.14764

Velasco-Castrillón, A., Hawes, I., & Stevens, M. I. (2018). 100 years on: a re-evaluation of the first discovery of microfauna from Ross Island, Antarctica. Antarctic Science, 30(4), 209-219.

Vigneron, A., Cruaud, P., Mohit, V., Martineau, M.-J., Culley, A. I., Lovejoy, C., & Vincent, W. F. (2018). Multiple Strategies for Light-Harvesting, Photoprotection, and Carbon Flow in High Latitude Microbial Mats. *Frontiers in Microbiology*, *9*. https://doi.org/10.3389/fmicb.2018.02881

Vincent, W. F. (2000). Cyanobacterial dominance in the polar regions. In *The ecology of cyanobacteria* (pp. 321-340). Springer, Dordrecht.

Vishnivetskaya, T. A., Almatari, A. L., Spirina, E. V., Wu, X., Williams, D. E., Pfiffner, S. M., & Rivkina, E. M. (2020). Insights into community of photosynthetic microorganisms from permafrost. FEMS Microbiology Ecology, 96(12), fiaa229.

Vishnivetskaya, T. A. (2009). Viable Cyanobacteria and Green Algae from the Permafrost Darkness. In R. Margesin (Ed.), Permafrost Soils (pp. 73–84). Springer. https://doi.org/10.1007/978-3-540-69371-0_6

Vishnivetskaya, T. A., Erokhina, L. G., Spirina, E. V., Shatilovich, A. V., Vorobyova, E. A., Tsapin, A. I., & Gilichinsky, D. A. (2005). Viable phototrophs: cyanobacteria and green algae from the permafrost darkness (pp. 140-158). Princeton University Press: Princeton, NJ, USA.

Waterworth, S. C., Isemonger, E. W., Rees, E. R., Dorrington, R. A., & Kwan, J. C. (2019). Metabolic specializations within a bacterial community to create living rocks. *BioRxiv*, 818625. https://doi.org/10.1101/818625

Williamson, C. J., Cook, J., Tedstone, A., Yallop, M., McCutcheon, J., Poniecka, E., Campbell, D., Irvine-Fynn, T., McQuaid, J., Tranter, M., Perkins, R., & Anesio, A. (2020). Algal photophysiology drives darkening and melt of the Greenland Ice Sheet. *Proceedings of the National Academy of Sciences*, *117*(11), 5694–5705. https://doi.org/10.1073/pnas.1918412117

Williamson, R. T., Boulanger, A., Vulpanovici, A., Roberts, M. A., & Gerwick, W. H. (2002). Structure and absolute stereochemistry of phormidolide, a new toxic metabolite from the marine cyanobacterium Phormidium sp. The Journal of organic chemistry, 67(23), 7927-7936.

Yang, Y.-W., Yin, Y.-C., Li, Z.-K., Huang, D., Shang, J.-L., Chen, M., & Qiu, B.-S. (2019). Orange and red carotenoid proteins are involved in the adaptation of the terrestrial cyanobacterium Nostoc flagelliforme to desiccation. *Photosynthesis Research*, *140*(1), 103–113. https://doi.org/10.1007/s11120-019-00629-6

Zeglin, L. H., Dahm, C. N., Barrett, J. E., Gooseff, M. N., Fitpatrick, S. K., & Takacs-Vesbach, C. D. (2011). Bacterial community structure along moisture gradients in the parafluvial sediments of two ephemeral desert streams. Microbial ecology, 61(3), 543-556.

Appendix I: Tables and Figures

Table 4-1. Metagenomes used for light harvesting gene comparisons with their JGI or MG-RAST identification number, extreme conditions and location.

Sample	JGI/MGRAST-ID	poly-extreme conditions	latitude	longitude
DJP mat	this study	light/dark/freeze thaw/salt	-77.5619	161.1908
DJP sed	this study	light/dark/freeze thaw/salt	-77.5619	161.1908
Lake Vanda mat	3300022222	light/dark	-77.5281	161.59
Lake Fryxel mat	3300007799	light/dark	-77.605	163.163
Markham Ice Shelf	mgm4445126.3	light/dark/freeze thaw	83.02	-71.31
Ward Hunt Island	3300014966	light/dark/freeze thaw	83.07972	-74.1381
Kuujjuarapik	3300014967	light/dark/freeze thaw	55.27501	-77.7585
Mushroom Spring 1	3300031568	high temp/alkaline	44.5387	-110.798
Mushroom Spring 2	3300002493	high temp/alkaline	44.534	-110.798
Octopus Spring	3300031517	high temp/alkaline	44.5361	-110.797
Tebenquiche	3300012002	salt/alkaline	-23.1385	-68.2472
Little Salt Springs	3300005077	salt	27.07472	-82.2333
Hot Lake WA	3300005141	heliothermal/salt/alkaline	48.97348	-119.476

Table 4-2. DJPM_E1 culture conditions and growth rate measured from highest growth peak during the experiment. Rows are in ordered in decreasing growth rate with highest growth rate at the top of the table (n =3 for each condition). The peak growth was measured regardless of when the growth occurred during the experiment, each condition was performed in triplicate. Peak RFU was the highest RFU that the cultures grew to. Dark grey rows are cultures that after the length of the experiment (31 days) were below media/condition controls. No growth indicates the cultures did not grow from initial inoculation.

DJPM_E1 (Peak growth during experiment)					
Temperature (°C)	Light (µmol $m^{-2} s^{-1}$)	$CaCl_2$ (M)	Peak RFU	Growth rate	Standard error
20	50	0	4,783	3.64E-02	6.80E-03
4	50	0	1,181	1.83E-02	9.41E-03
10	50	0	2,876	1.17E-02	2.29E-03
20	50	0.25	1,876.00	8.35E-03	6.66E-04
10	0.5	0	452.9	4.31E-03	4.29E-04
4	0.5	0.25	1,428	2.68E-03	1.53E-04
10	0.5	0.25	475	2.39E-03	3.03E-04
20	0.5	0	1876	2.35E-03	2.39E-05
4	0.5	0	9,07.4	2.32E-03	5.48E-04
20	0.5	0.25	1,465	2.00E-03	1.16E-04
4	50	0.25	347	No growth	No growth
10	50	0.25	475	No growth	No growth

Table 4-3. DJPM_C1 culture conditions and growth rate measured from highest growth peak during the experiment. Rows are in ordered in decreasing growth rate with highest growth rate at the top of the table (n =3 for each condition). The peak growth was measured regardless of when the growth occurred during the experiment, each condition was performed in triplicate. Peak RFU was the highest RFU that the cultures grew to. Dark grey rows are cultures that after the length of the experiment (31 days) were below media/condition controls.

DJPM_C1 (Peak growth during experiment)					
Temperature (°C)	Light (µmol $m^{-2} s^{-1}$)	$CaCl_2$ (M)	Peak RFU	Growth rate	Standard error
20	0.5	0	777	2.75E-02	6.90E-03
4	50	0.25	159	2.30E-02	7.78E-03
4	0.5	0.25	386	1.81E-02	6.08E-03
20	50	0.25	203	1.78E-02	9.13E-03
10	50	0	82	1.68E-02	3.39E-03
10	50	0.25	78	1.23E-02	1.01E-03
20	0.5	0.25	203	1.19E-02	2.82E-03
4	0.5	0	569	8.51E-03	1.24E-03
20	50	0	222	6.08E-03	1.26E-03
10	0.5	0.25	145	4.89E-03	5.11E-04
4	50	0	233	4.48E-03	2.34E-03
10	0.5	0	237	4.15E-03	4.29E-04

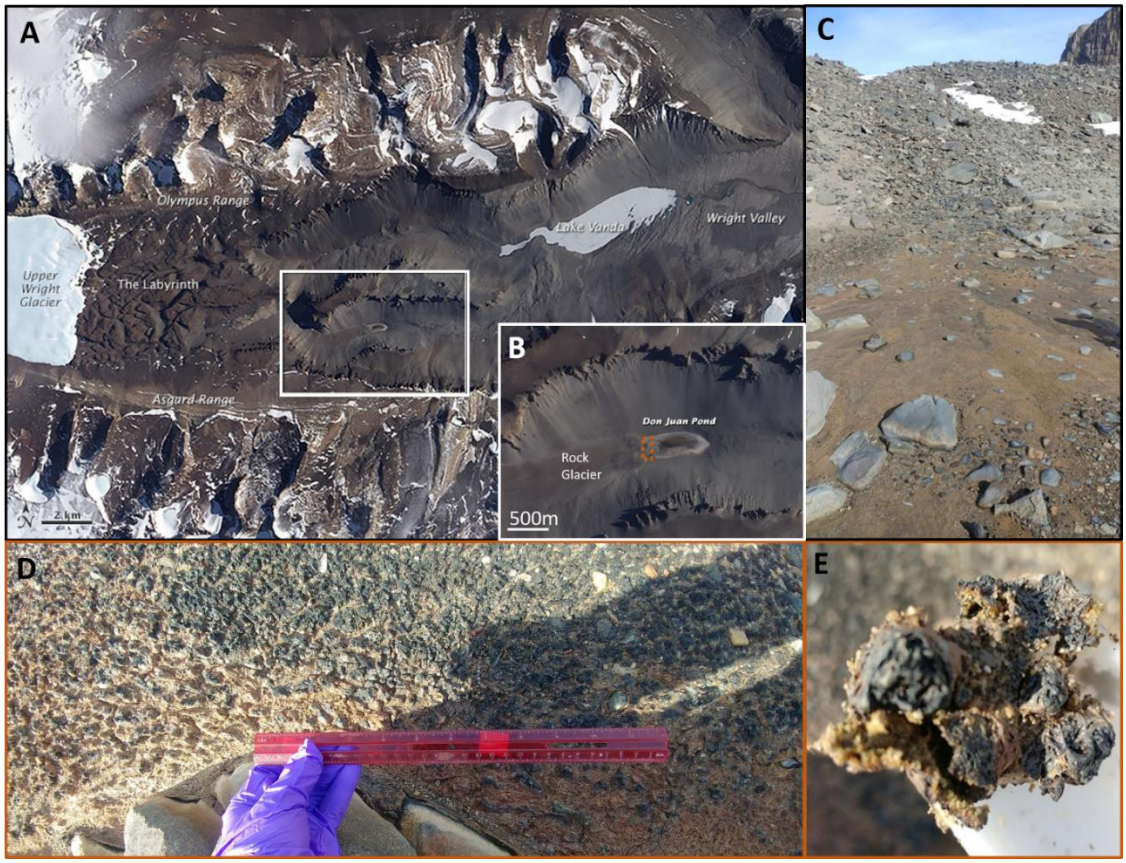


Figure 4-0-1. Sample location for the mat adjacent to Don Juan Pond in the Upper Wright Valley of the McMurdo Dry Valleys. A) Satellite image of the Upper Wright Valley (*NASA Earth Observatory image by Jesse Allen)* box B), closer image of Don Juan Pond and the adjacent rock glacier, orange dotted box represents the location of the mat (*Image credit NASA/JPL-CALTECH)*. The mat is the inconspicuous dirt color as seen when looking towards the rock glacier (C) and appears as a black and orange mix of stones when looking down at the mat (D). (E) At the time of sampling, the orange filamentous mat with small sections of green underneath orange and black layers can be observed.

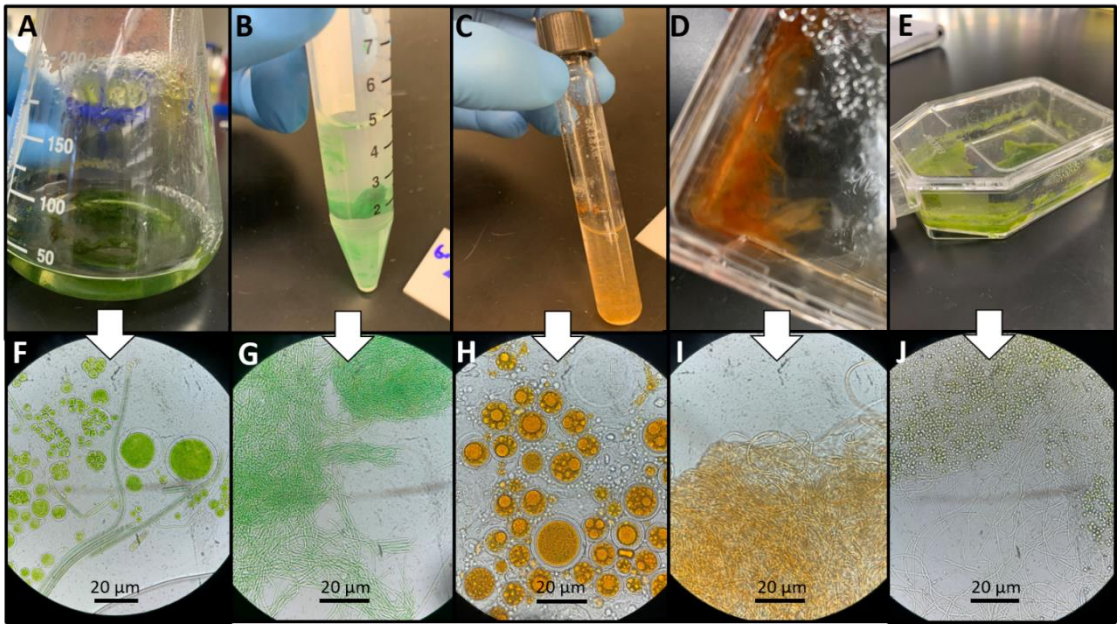


Figure 4-0-2. Variety of cultures from the mat adjacent to Don Juan Pond. (A-E) Examples of cultures from the mat material. (F-J) Microscopy images of the each of the cultures located above the microscopy image. A&F, B&G, C&H, D&I, E&J belong to each other, scale bar in each image is 20 µm. Preliminary identification based on morphology and pigment (A/F) *Dunaliella*-like, (B/G) *Oscillatoria*-like, (C/H) *Dunaliella*-like cysts, (D/I) Unidentified, (E/J) *Oscillatoria*.

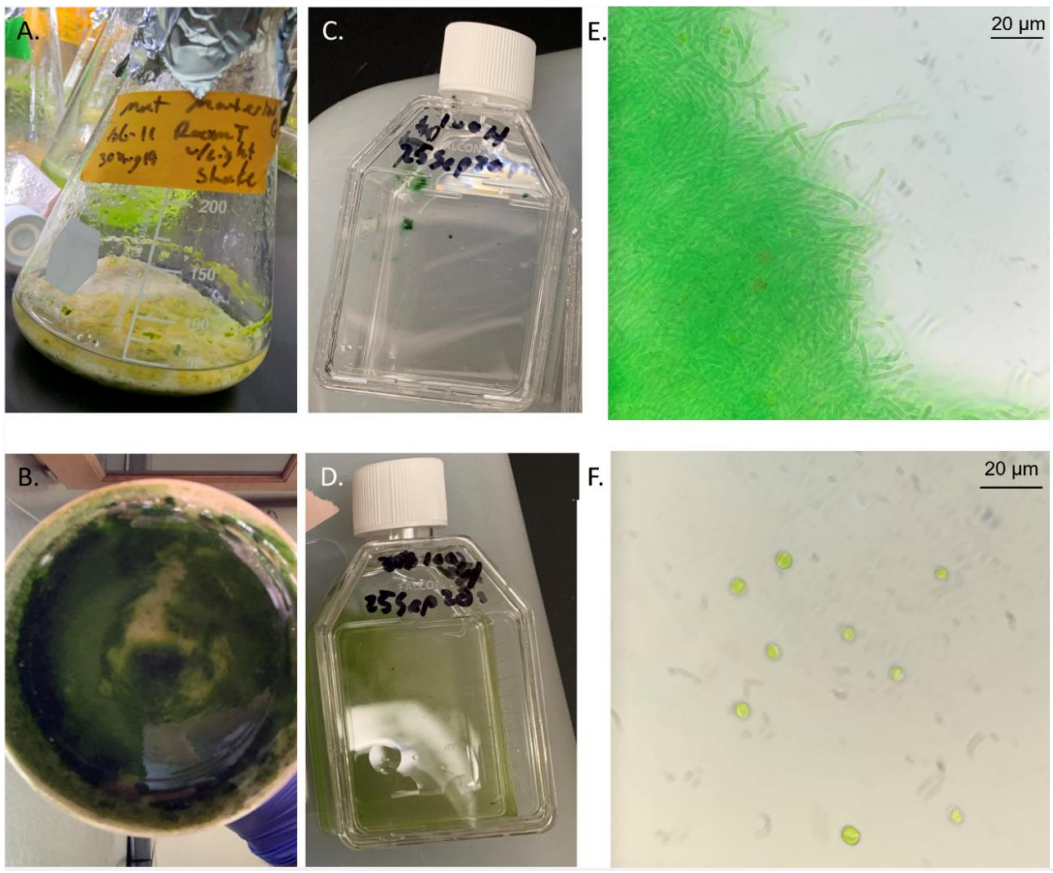
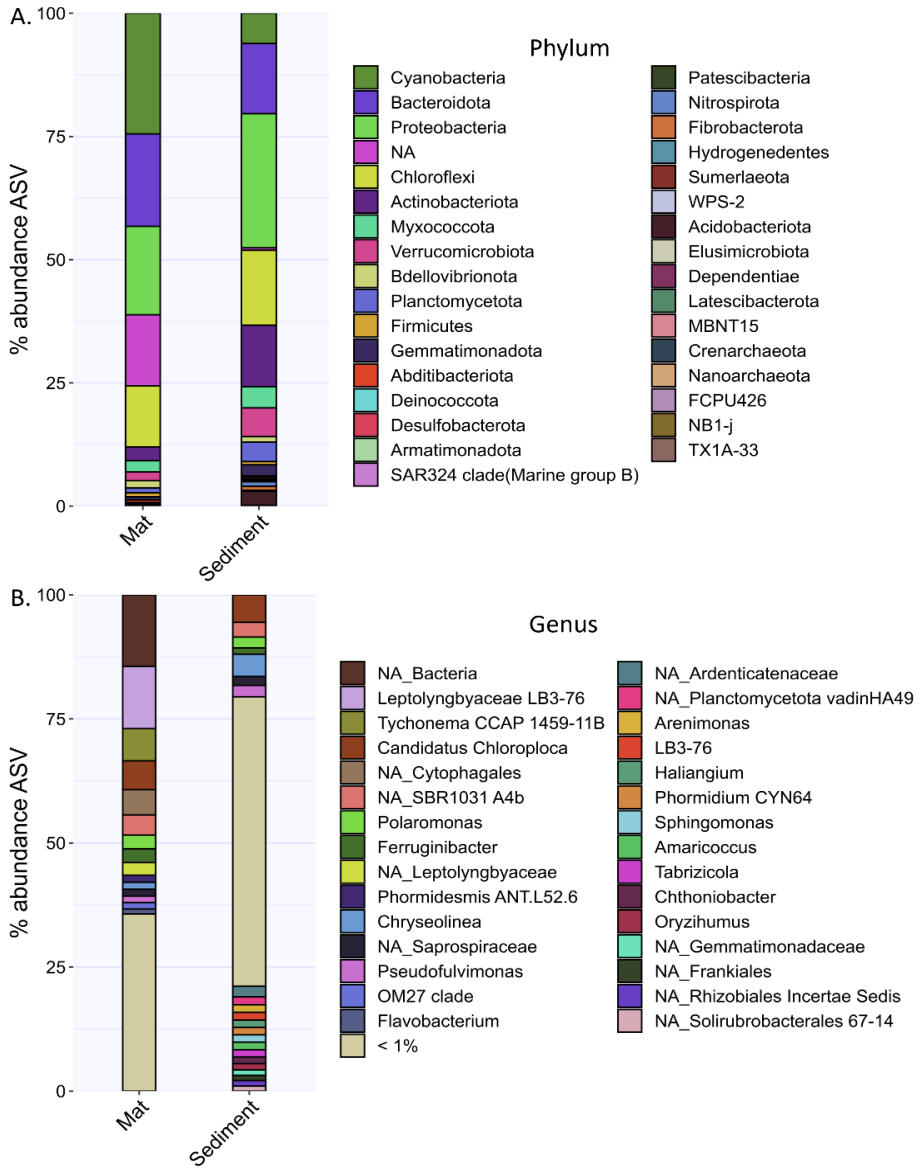


Figure 4-0-3. Cultures isolated from the mat adjacent to Don Juan Pond that were used for light, salt and temperature challenge experiments. A) Side view of flask used to grow raw mat material in BG-11media on autoclaved and ethanol washed sand. B) View of the bottom of the same flask in which subcultures were started from by capturing only what was underneath the sand. C) and D) separate cultures that were further isolated from the flask and grown in a shaded environment (16 µmol m^{-2} s^{-1} irradiance) at room temperature (~20 °C) with BG-11 as the media. E) Microscope image of culture (C) identified as *Phormidium sp.* (DJPM_C1) and F) is a microscopic image of the culture (D), identified as *Chlorellales sp.* (DJPM_E1).

Figure 4-0-4. 16S rRNA ASVs relative abundances for the mat adjacent to Don Juan Pond and the sediment below the mat.

A) Phylum level ASV abundance, DJP Mat and Sediment are similar in composition, the Mat is comprised of more Cyanobacteria and NA (not assigned) reads, whereas the Sediment has greater abundance of Proteobacteria and Actinobacteriota. B) Genus level ASV abundance, < 1% (sequences that individually are less than 1% of the total abundance) make up the majority. The mat and sediment are similar with differences of percent abundance between Cyanobacteria (higher abundance in the mat) and Chloroflexi (higher abundance in sediments) Though cyanobacteria genera are lower abundance for the sediment, *Phormidium CYN64* is observed. This ASV matches that of the DJPM_C1 culture and is the second most abundant cyanobacteria 16S ASV within the sediment behind *LB3-76* (Leptolyngbyaceae).


A.
% abundance ASV
100
75
50
25
0
Mat
Sediment
Phylum
Cyanobacteria
Bacteroidota
Proteobacteria
NA
Chloroflexi
Actinobacteriota
Myxococcota
Verrucomicrobiota
Bdellovibrionota
Planctomycetota
Firmicutes
Gemmatimonadota
Abditibacteriota
Deinococcota
Desulfobacterota
Armatimonadota
SAR324 clade(Marine group B)
Patescibacteria
Nitrospirota
Fibrobacterota
Hydrogenedentes
Sumerlaeota
WPS-2
Acidobacteriota
Elusimicrobiota
Dependentiae
Latescibacterota
MBNT15
Crenarchaeota
Nanoarchaeota
FCPU426
NB1-j
TX1A-33
B.
% abundance ASV
100
75
50
25
0
Mat
Sediment
Genus
NA_Bacteria
Leptolyngbyaceae LB3-76
Tychonema CCAP 1459-11B
Candidatus Chloroploca
NA_Cytophagales
NA_SBR1031 A4b
Polaromonas
Ferruginibacter
NA_Leptolyngbyaceae
Phormidesmis ANT.L52.6
Chryseolinea
NA_Saprospiraceae
Pseudofulvimonas
OM27 clade
Flavobacterium
< 1%
NA_Ardenticatenaceae
NA_Planctomycetota vadinHA49
Arenimonas
LB3-76
Haliangium
Phormidium CYN64
Sphingomonas
Amaricoccus
Tabrizicola
Chthoniobacter
Oryzihumus
NA_Gemmatimonadaceae
NA_Frankiales
NA_Rhizobiales Incertae Sedis
NA_Solirubrobacterales 67-14

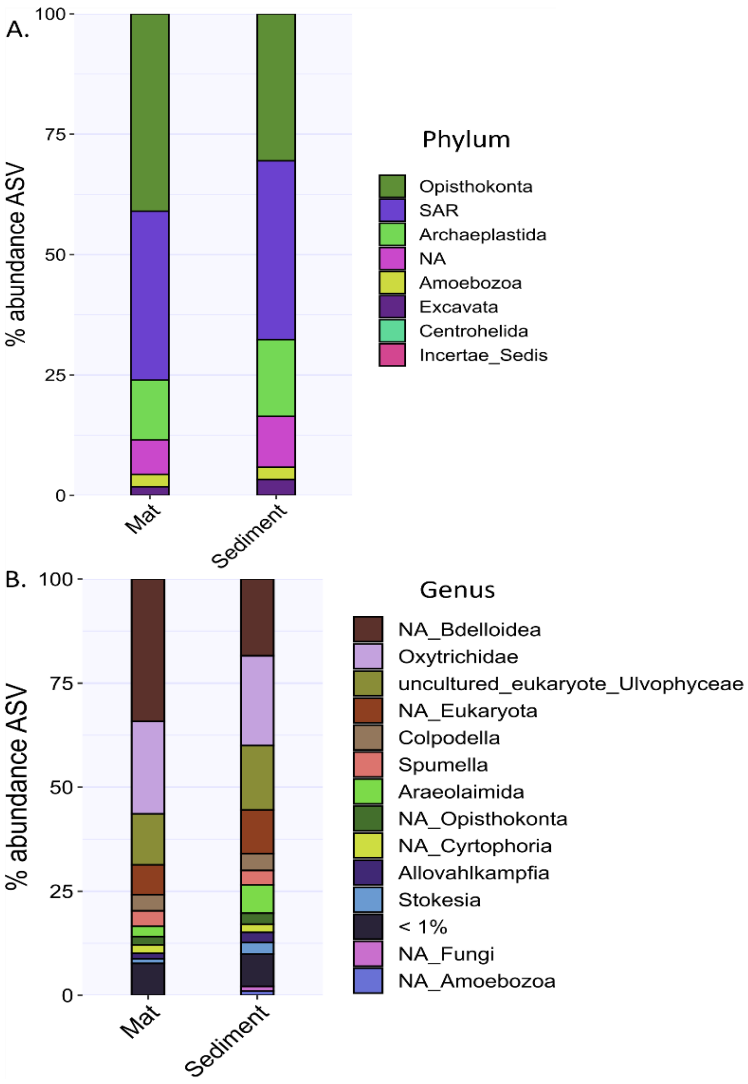


Figure 4-0-5. 18S rRNA ASVs relative abundances for the mat adjacent to Don Juan Pond and the sediment below the mat. A) Phylum level ASV abundance, Mat and Sediment are similar in composition down to the genus level (B). NA genus level identifications are assigned at the highest taxonomical level as assigned by the DADA2 pipeline using the SILVA database. < 1% genus category are comprised of sequences that individually make up less than 1% of the total 18S ASV abundance.

Figure 4-0-6. Metagenome from polyextreme environments comparing light absorbing protein gene abundances.

A) Comparison of the percent abundance of light absorbing phototroph genes grouped together, across microbial mat metagenomes from different polyextreme environments. DJP Mat (this study), DJP Mat-Sed (this study), Fryxell and Vanda are from Antarctic environments. Kuujjuarapik, Marhkam Ice are from arctic environments. Mushroom Spring 1, Octopus Spring and Mushroom Spring 2 are from Yellowstone National Park hot springs. Hot Lake, Little Salt Spring and Tebenquiche are from salty environments. Colors of the genes reflect the light they absorb. Blue-light rhodopsin are more abundant in the mat than any other metagenome in this analysis while the abundance of BCHL B is more abundant in the Antarctic and Arctic samples. B) Same data sets normalized to account for the size difference of each metagenome (hits per million sequences).

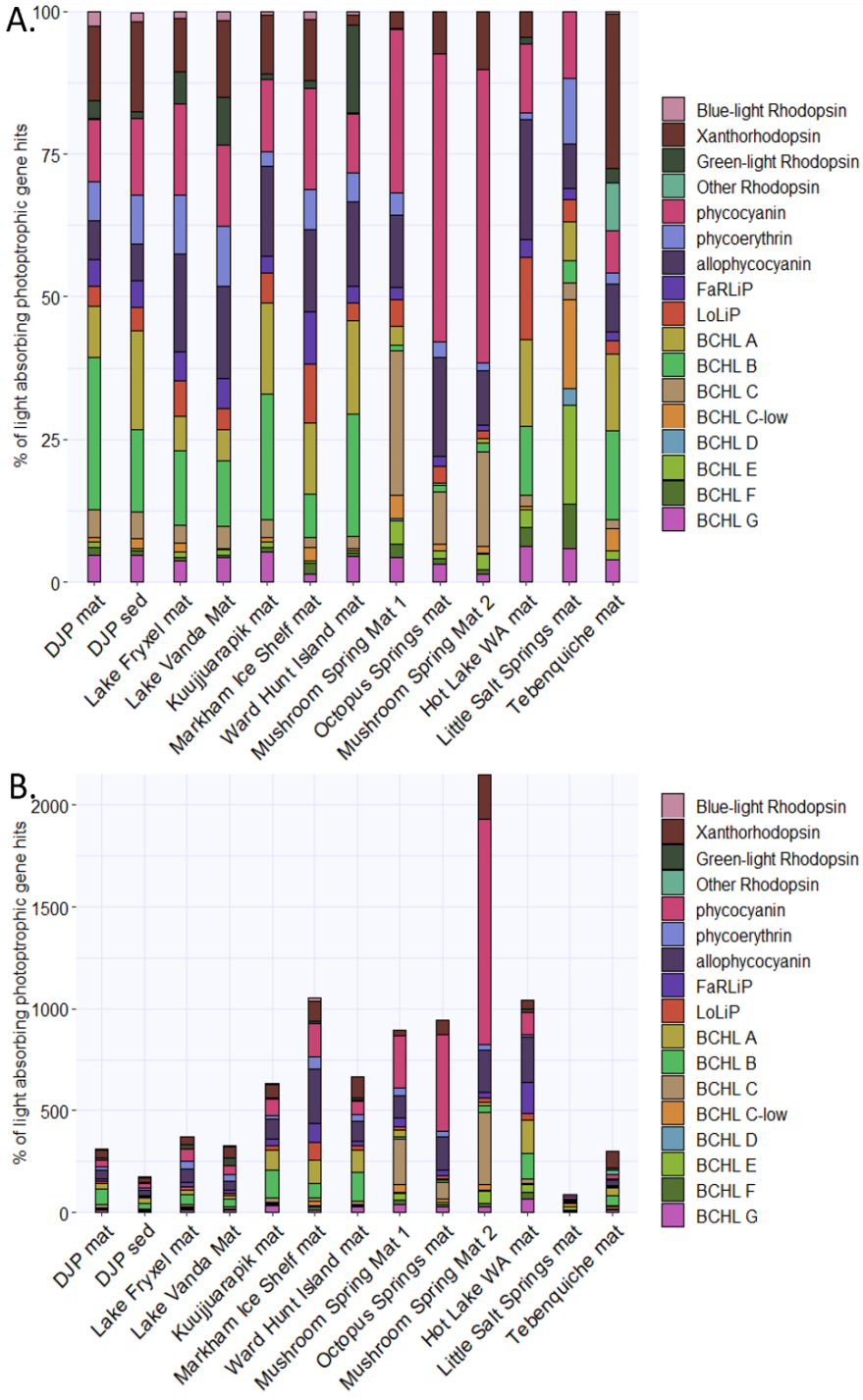
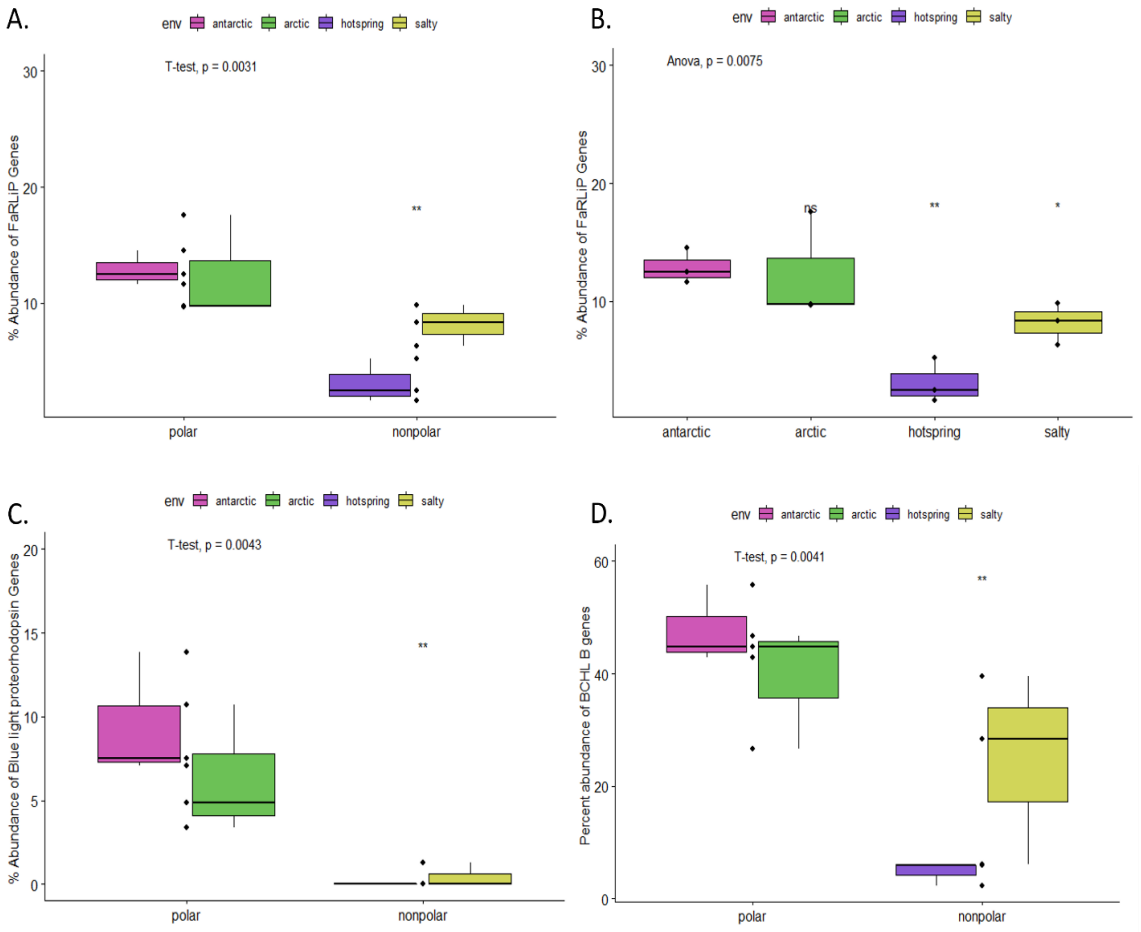

A.
% of light absorbing photoptrophic gene hits
100
75
50
25
0
DJP mat
DJP sed
Lake Fryxel mat
Lake Vanda Mat
Kuujjuarapik mat
Markham Ice Shelf mat
Ward Hunt Island mat
Mushroom Spring Mat 1
Octopus Springs mat
Mushroom Spring Mat 2
Hot Lake WA mat
Little Salt Springs mat
Tebenquiche mat
Blue-light Rhodopsin
Xanthorhodopsin
Green-light Rhodopsin
Other Rhodopsin
phycocyanin
phycoerythrin
allophycocyanin
FaRLiP
LoLiP
BCHL A
BCHL B
BCHL C
BCHL C-low
BCHL D
BCHL E
BCHL F
BCHL G
B,
% of light absorbing photoptrophic gene hits
2000
1500
1000
500
0
DJP mat
DJP sed
Lake Fryxel mat
Lake Vanda Mat
Kuujjuarapik mat
Markham Ice Shelf mat
Ward Hunt Island mat
Mushroom Spring Mat 1
Octopus Springs mat
Mushroom Spring Mat 2
Hot Lake WA mat
Little Salt Springs mat
Tebenquiche mat
Blue-light Rhodopsin
Xanthorhodopsin
Green-light Rhodopsin
Other Rhodopsin
phycocyanin
phycoerythrin
allophycocyanin
FaRLiP
LoLiP
BCHL A
BCHL B
BCHL C
BCHL C-low
BCHL D
BCHL E
BCHL F
BCHL G

Figure 4-0-7. Statistical results of polyextreme metagenome light absorbing protein gene abundances comparisons. Comparison of light harvesting protein genes across metagenomes from other poly extreme environments (Antarctic, Arctic, hot springs and salty environments) grouped by latitude (polar sites or nonpolar sites). (A) There were significantly more FaRLiP genes in polar vs nonpolar environments when viewed as a percent abundance of total light harvesting genes (t-test; $p = 0.0031$), though no significant difference was found between Antarctic sites and Arctic sites (B), there was a significant difference observed between Antarctic and hot springs environments, as well as Antarctic and salty environments (Anova; $p = 0.0075$). (C) There were significantly more blue light rhodopsin genes (t-test; $p = 0.0043$) and BCHL B genes (D) in polar environments compared to nonpolar environments, as a percent abundance of total light harvesting genes within each metagenome (t-test; $p = 0.0041$).


A.
env antarctic arctic hotspring salty
T-test, p = 0.0031
% Abundance of FaRLiP Genes
30
20
10
**
polar
nonpolar
B.
env antarctic arctic hotspring salty
Anova, p = 0.0075
% Abundance of FaRLiP Genes
30
20
10
ns
**
*
antarctic
arctic
hotspring
salty
C.
env antarctic arctic hotspring salty
T-test, p = 0.0043
% Abundance of Blue light proteorhodopsin Genes
20
15
10
5
0
**
polar
nonpolar
D.
env antarctic arctic hotspring salty
T-test, p = 0.0041
Percent abundance of BCHL B genes
60
40
20
0
**
polar
nonpolar

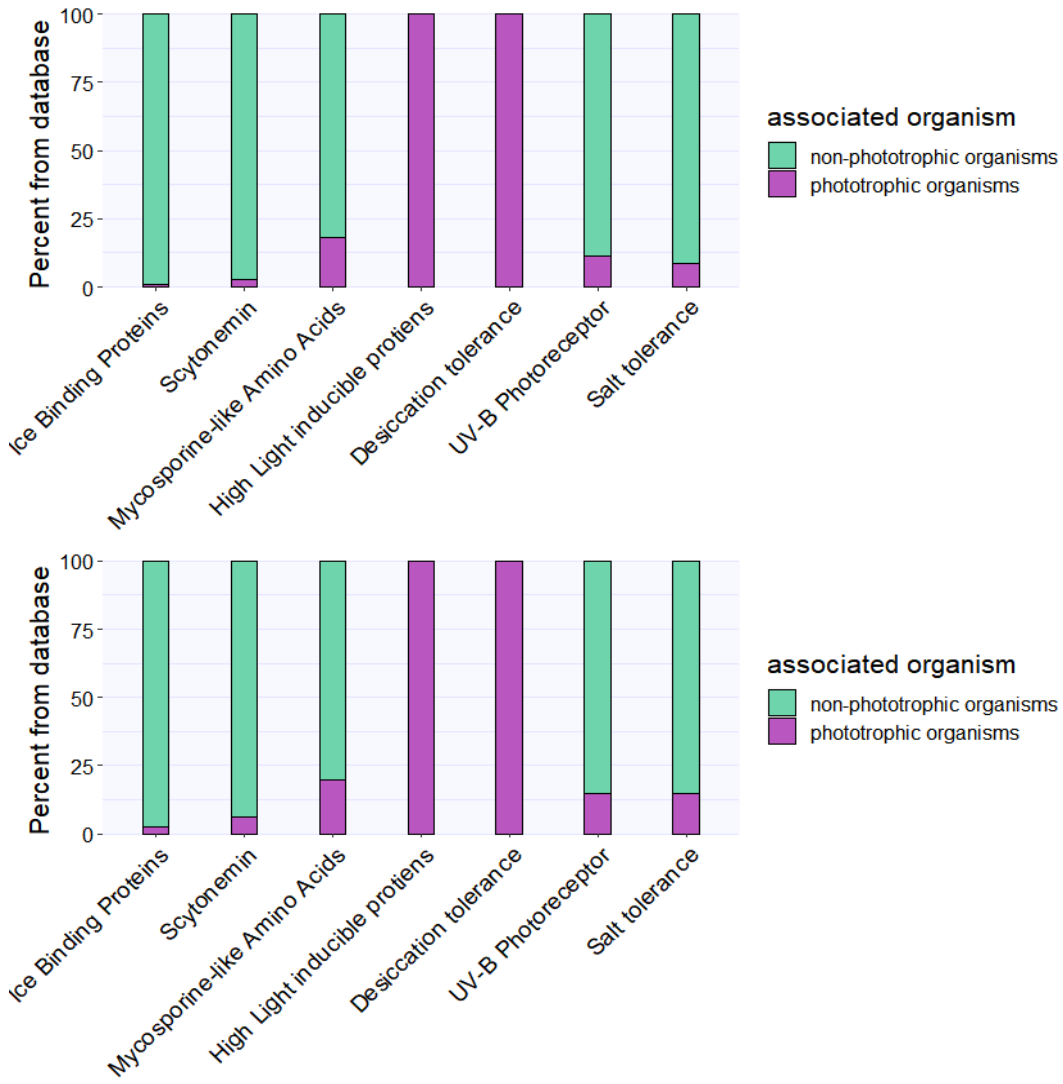


Figure 4-0-8. Stress database results grouped by phototrophic and non-phototrophic organisms of the Mat adjacent to Don Juan Pond and the sediment beneath the mat. Stress database distribution amongst phototrophic and non-phototrophic organisms for the mat (A) and the sediment beneath the mat (B).

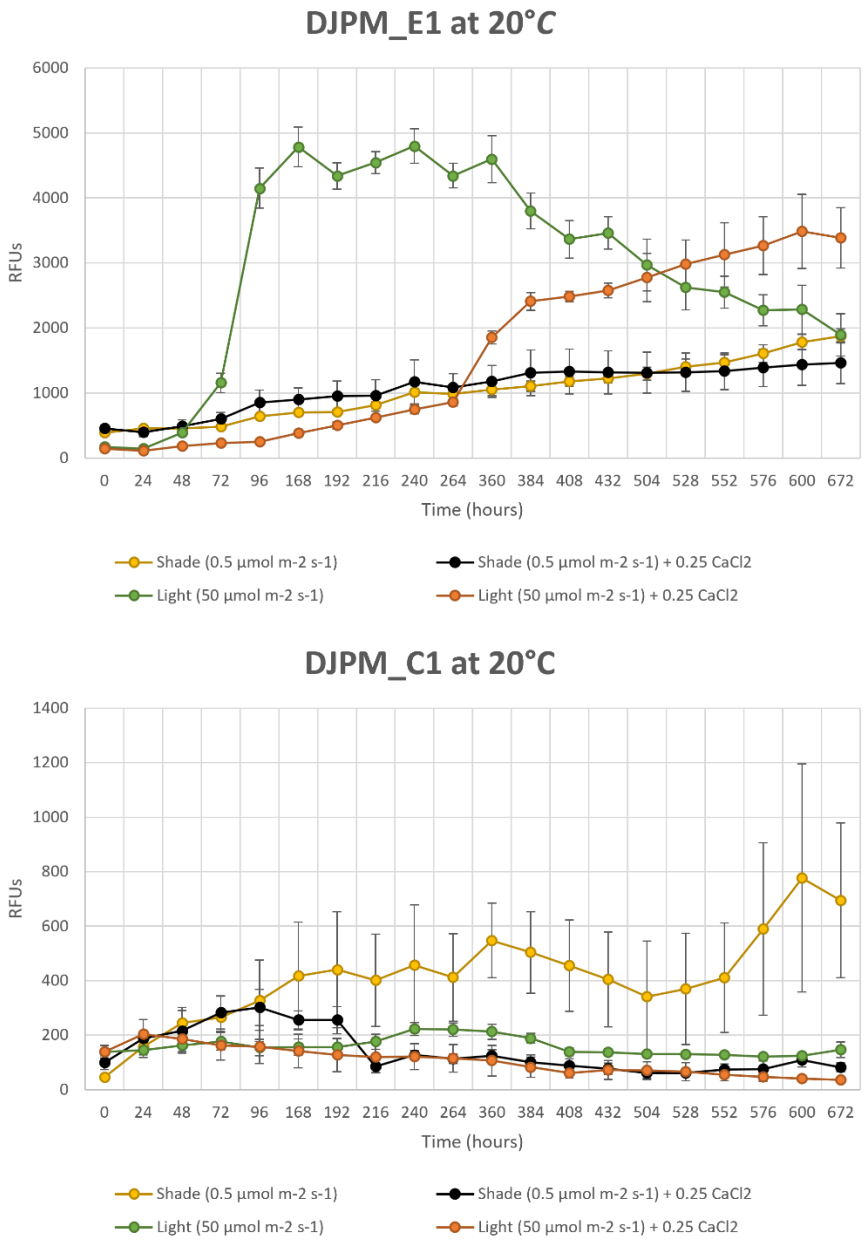


Figure 4-0-9. Growth curves of DJPM_E1 and DJPM_C1 at 20°C, cultures were isolated from the mat adjacent to Don Juan Pond. DJPM_E1 (top) and DJPM_C1 (bottom). Error bars are standard error (n=3) of biological replicates. Shaded environments were exposed to 0.5 µmol m^{-2} s^{-1} irradiance and the light environments were exposed to 50 µmol m^{-2} s^{-1} irradiance.

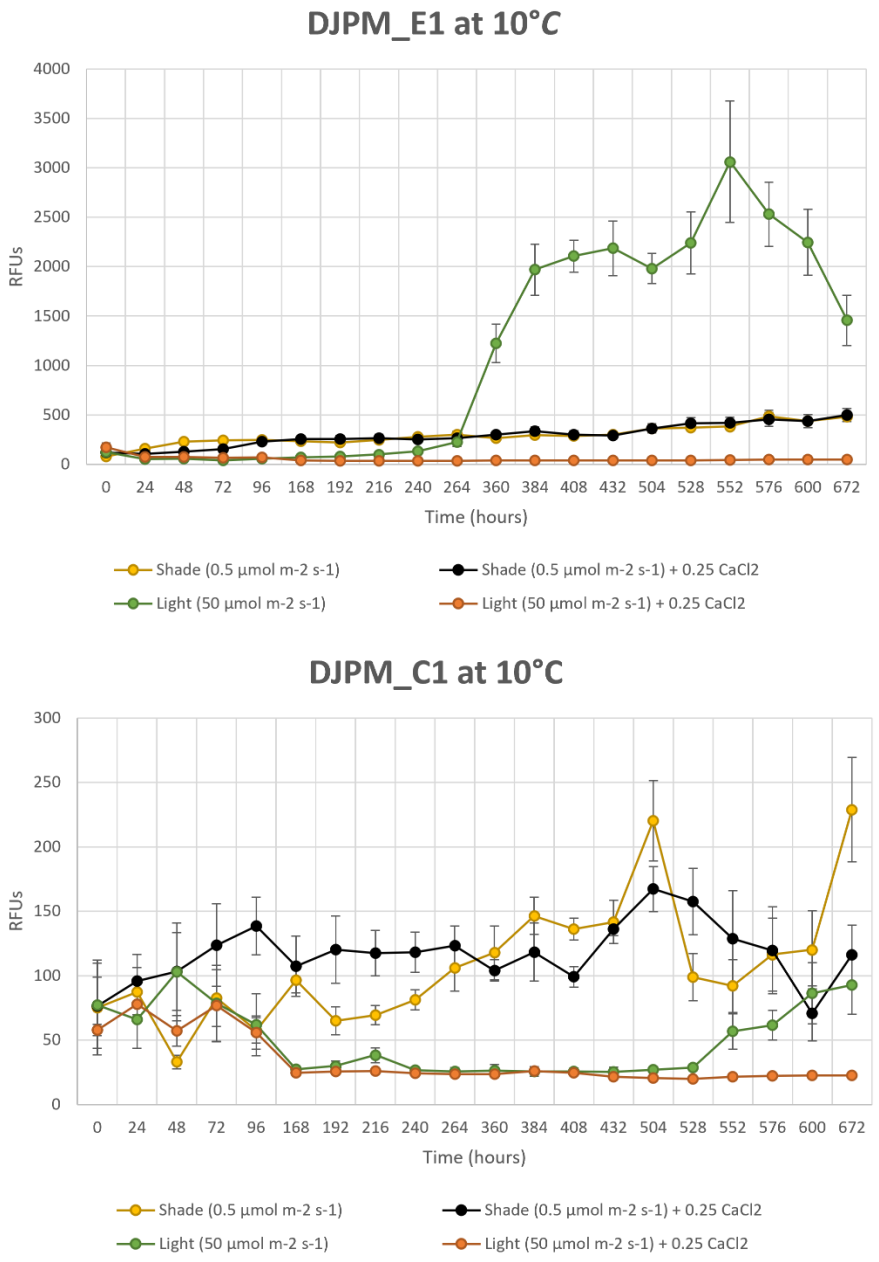


Figure 4-0-10. Growth curves of DJPM_E1 and DJPM_C1 at 10°C, cultures were isolated from the mat adjacent to Don Juan Pond. DJPM_E1 (top) and DJPM_C1 (bottom). Error bars are standard error (n=3) of biological replicates. Shaded environments were exposed to 0.5 µmol m^{-2} s^{-1} irradiance and the light environments were exposed to 50 µmol m^{-2} s^{-1} irradiance

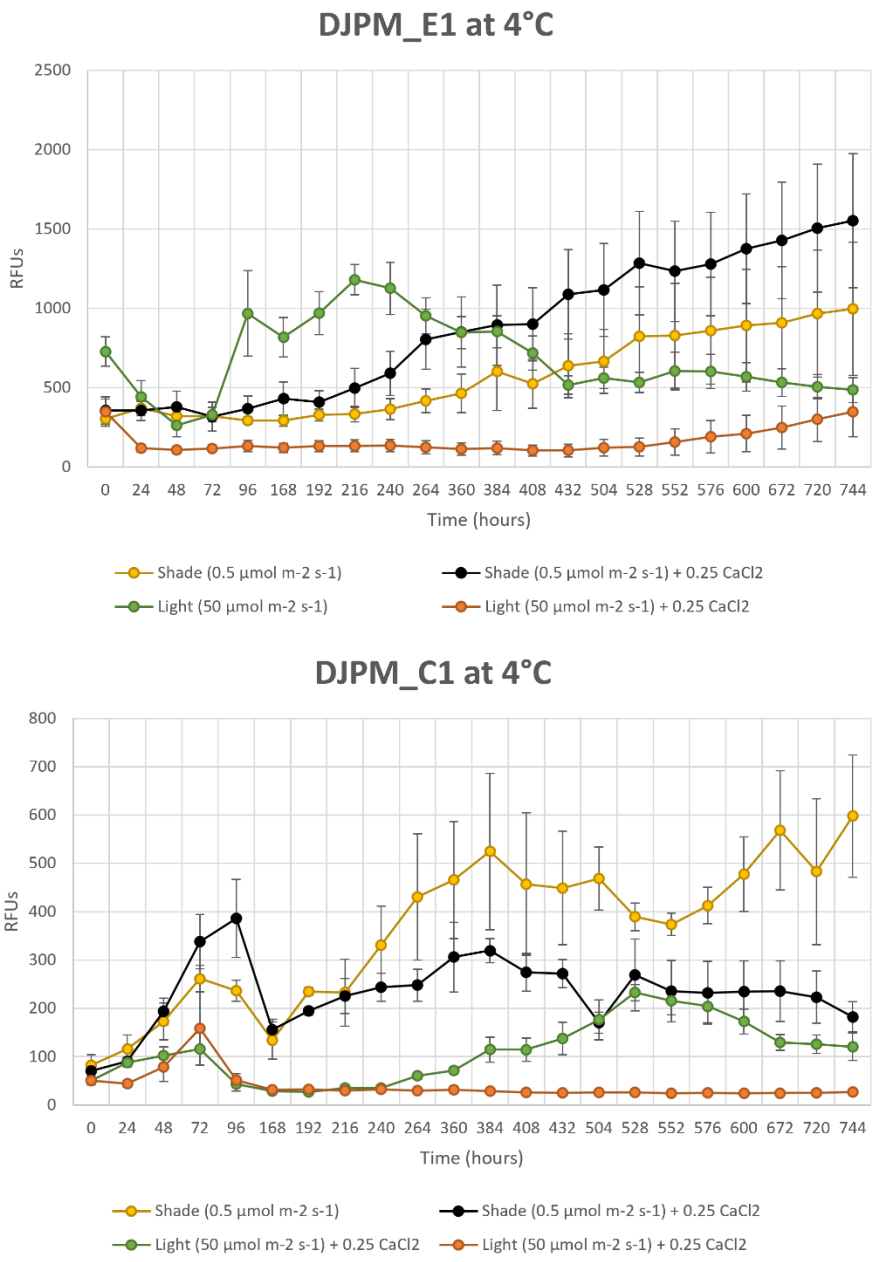


Figure 4-0-11. Growth curves of DJPM_E1 and DJPM_C1 at 4°C, cultures were isolated from the mat adjacent to Don Juan Pond. DJPM_E1 (top) and DJPM_C1 (bottom). Error bars are standard error (n=3) of biological replicates. Shaded environments were exposed to 0.5 µmol m^{-2} s^{-1} irradiance and the light environments were exposed to 50 µmol m^{-2} s^{-1} irradiance

CHAPTER FIVE

CONCLUSION

Polyextremophiles survive at the boundaries of what is considered physically and chemically possible for life. Cryosphere ecosystems provide an important opportunity to investigate polyextremophilic microbial habitats. Many of icy environments are at risk of dramatic change due to global climate warming. Some features may disappear completely before they can be thoroughly investigated. Thus, the investigation and exploration of these environments is urgent.

Because cryospheric systems are often challenging to access, developing methods to study these environments remotely and with novel, logistically minimal tools. Tools that can be cleaned for microbiological sample acquisition and study is essential. Sample integrity is particularly essential for highly sensitive methods such as multi-omics approaches. Interest in the utility of thermal melt probes has increased in the last decade. Thus, there is a need to understand the mechanisms, disturbances, and contamination possible from melting through ice to collect samples. This is a multi-step process from cleaning in the field to understanding sampling and melt behavior *in situ* and finally confirming the integrity of the acquired sample. Chapter 2 of this dissertation demonstrated that field-based cleaning approaches met proposed NASA clean room standards as well as strict Antarctic clean access requirements. We further showed, via novel laboratory ice block experiments, the extent to which melt probes drag ice immured microbes with them as it descends to a target at lower depth. Our results indicated that dragging was minimal and would meet Antarctic Code of Conduct requirements for subglacial environments.

In an alpine glacial system, we showed how the complex snow algae life cycle may play a role in community composition, while providing the first *in situ* observations of multiple life cycles of snow algae within the same depth profile of snowpack (Chapter 3). We further showed, via metatranscriptomics, that both the surface and middle of a snowpack contained actively photosynthesizing microbial communities. These new data support the hypothesis that algae within the snowpack may be more active than algae at the surface. This work provides important information towards understanding 1) the life cycle of snow algae, 2) how the life cycle influences community composition, and 3) if snowpack is actually a larger carbon sink than previously described.

Our investigation of the polyextreme mat adjacent to Don Juan Pond (DJP), one of the saltiest brines on Earth, revealed unique characteristics of the microbial community. Though this mat was first studied in the late 1970s; it had not been characterized using modern molecular, multi-omics approaches. These approaches furthered our understanding of this environment revealing the genetic capacity of microorganism to survive in extreme conditions, as well as deciphering what organisms possess these genes and how these findings compare to other polyextreme environments. The amplicon and metagenomic sequencing data suggest that $CaCl_2$-rich brine of DJP may interact with mat, applying a selective pressure that shapes the community composition. The DJP microbial mat community was more similar to other hypersaline environments, than freshwater environments. The mat metagenome also contained genes

involved in stress responses to the cold temperatures, high light, low light, and salt stress. Light harvesting genes that enable low light and far-red light absorption were abundant, which would be beneficial for transitional periods from the Antarctic summer to winter. Lastly, we cultured an environmentally relevant cyanobacteria from the mat belonging to the genus *Phormidium*. Culture incubations indicated that this strain preferred darker environments and could tolerate 0.25M $CaCl_2$. We also demonstrated that a eukaryotic alga from the mat, *Chlorellales*. can tolerate shaded environments as well as 0.25M $CaCl_2$. These results provide evidence that the DJP mat may interact with the saline pond and soils it lies adjacent to. Further work should be conducted to challenge the limits of the cultured phototrophs and investigate any bacterial relationships that are beneficial to them.

Many challenges exist with cryosphere work. From gaining access to remote locations to performing the work in austere conditions. As the climate continues to change, researching these environments becomes essential as many of the environments are under threat of irrevocable change. These polyextreme systems have unique microorganisms that have adapted to tolerate stresses associated with cryospheric environments. The microorganisms from these environments can provide insight into detecting life off Earth, as well as improving life on Earth with applications in biotechnology.

VITA

Caleb Garry Schuler was born and raised in Dayton Ohio, he moved to Knoxville to pursue a PhD at the University of Tennessee Knoxville. Caleb's path to science was not normal by any means. Upon graduating high school in 2006 Caleb began working at UPS as a preload package handler. Caleb did not want to attend college and decided to enlist in the U.S. Navy in 2007. Caleb gained confidence and found himself working his way up through the enlisted ranks as a Master at Arms while volunteering for a deployment to Iraq in 2009-2010 and several other missions afterwards. While pursuing a military career Caleb continued to work at UPS and found himself promoted to a shift supervisor, while also working part time as a certified personal trainer. During this time, he began school at Sinclair Community College in Dayton Ohio. At Sinclair, Caleb found a love for learning and sought to pursue this love by transferring to the University of Cincinnati to obtain a Bachelor of Science in biology. Always interested in space, Caleb looked for a way to connect biology and space. In this search Caleb discovered the broad field of astrobiology within the realm of microbiology. While working two jobs, he volunteered to work in Dr. Trinity Hamilton's lab where he would produce a first authored paper and while discovering that attending graduate school was a possibility for him. Caleb found a graduate school home at the University of Tennessee in Jill Mikucki's lab. In Knoxville, Caleb discovered what mattered most to him, family. Caleb continues to grow as both a scientist and a father and seeks to continue his scientific career.